

T-3291

P-WAVE ONE-DIMENSIONAL SEISMIC RESPONSE OF A
LINEAR VELOCITY TRANSITION ZONE USING WAVE THEORY

by

JAAFAR MUHAMMAD AL-NEMER

July, 1987

ARTHUR LARSEN LIBRARY
COLORADO SCHOOL of MINES
GOLDEN, COLORADO 80401

ProQuest Number: 10782857

All rights reserved

INFORMATION TO ALL USERS

The quality of this reproduction is dependent upon the quality of the copy submitted.

In the unlikely event that the author did not send a complete manuscript and there are missing pages, these will be noted. Also, if material had to be removed, a note will indicate the deletion.



ProQuest 10782857

Published by ProQuest LLC (2018). Copyright of the Dissertation is held by the Author.

All rights reserved.

This work is protected against unauthorized copying under Title 17, United States Code
Microform Edition © ProQuest LLC.

ProQuest LLC.
789 East Eisenhower Parkway
P.O. Box 1346
Ann Arbor, MI 48106 – 1346

T-3291

A thesis submitted to the Faculty and the Board of Trustees of the Colorado School of Mines in partial fulfillment of the requirements for the degree of [Master of Science (Geophysical Engineering)].

Golden, Colorado

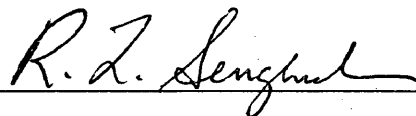
Date July 27, 1987

Signed: _____



JAAFAR MUHAMMAD AL-NEMER

Approved: _____



Professor R. L. Sengbush

Thesis Advisor

Golden, Colorado

Date 7 August 87



Professor P. R. Romig Jr.

Professor of Geophysics

Head of Department

Geophysical Department

ABSTRACT

In seismic work, one needs to know the responses of geological features in order to understand the seismic implications. The one-dimensional wave equation has been used here to obtain the responses of transition zones which have a linear velocity variation as a function of depth. This corresponds to a linear function of the natural logarithm of the velocity with respect to time. The wave equation solution is obtained in the frequency domain using analytical expressions for pressure and particle displacement. Exact reflectivity and transmissivity in the frequency domain were found for a pulse going into the transition zone and going out of the transition zone where adjacent layers have constant velocities. Numerical inversions of those functions show that time responses are related to Bessel functions. An analytical expression for the reflectivity function of an interface between a uniform layer and a transition zone was found to be proportional to the first order Bessel function divided by time. The reflectivity function of an interface between a transition zone and a uniform layer below appears to be related to the Bessel-Neumann function. For a transition zone, the conventional reflectivity is rectangular, which the wave-

theoretic reflectivity approximates, except for a discrepancy in amplitude, if the zone is thin. The amplitude of the reflectivity function is smaller than the conventional result. Numerical work from this thesis has shown that the generation of multiples from a linear velocity transition zone is insignificant.

TABLE OF CONTENTS

ABSTRACT	iii
TABLE OF CONTENTS	v
LIST OF FIGURES	vii
LIST OF TABLES	x
ACKNOWLEDGEMENTS	xi
INTRODUCTION	1
1. STATEMENT OF THE PROBLEM AND BASIC SOLUTIONS	6
Variable Velocity Wave Equation	6
Temporal and spatial separation	6
Pressure and displacement fields	8
Linearly Varying Velocity Layer Basic Solutions	11
Constant Velocity Layer Basic Solutions	18
2. THE MODELS AND ANALYTICAL RESULTS	20
Three Layer Model	24
Formulation and analytical solutions	24
Reflection coefficient	33
Transmission coefficient	34
Four Layer Model	36
Formulation and analytical solutions	36
Reflection coefficient	45
Transmission coefficient	46
3. NUMERICAL IMPLEMENTATION	47
4. NUMERICAL RESULTS	53
A Theoretical Model	53
A Realistic Model	77
Soft Sea Floor Model	87
Hard Sea Floor Model	97

General Discussion Of The Results	107
5. CONCLUSIONS AND RECOMMENDATIONS	114
BIBLIOGRAPHY	116
APPENDIX A: Three Uniform Layers	118
APPENDIX B: Program Listings	119
Program Listings	120

LIST OF FIGURES

FIGURES	CONTENTS	PAGE
2-1	Three-Layer Model	25
2-2	Four-Layer Model	37
3-1	Ricker wavelet	48
3-2	Ricker wavelet spectrum	49
4-1	Theoretical model: Reflection Impulse Response	59
4-2	Theoretical model: Reflection Ricker Response	60
4-3	Theoretical model: Reflection Impulse Response wave theoretic (solid) vs. conventional reflectivity (Dashed)	61
4-4	Theoretical model: Reflection Ricker Response wave theoretic (solid) vs. conventional reflectivity (Dashed)	62
4-5	Theoretical model: Transmission Impulse Response	63
4-6	Theoretical model: Transmission Ricker Response	64
4-7	Theoretical model: Reflection Function R12	65
4-8	Theoretical model: Reflection Function R23	66
4-9	Theoretical model: Transmission Function T12	67
4-10	Theoretical model: Transmission Function T23	68
4-11	Theoretical model: Amplitude spectrum of reflection function R12	69

LIST OF FIGURES

FIGURE	CONTENTS	PAGE
4-12	Theoretical model: Phase spectrum of reflection function R12	70
4-13	Theoretical model: Amplitude spectrum of reflection function R23	71
4-14	Theoretical model: Phase spectrum of reflection function R23	72
4-15	Theoretical model: Amplitude spectrum of reflection Transmission function T12	73
4-16	Theoretical model: Phase spectrum of Transmission function T12	74
4-17	Theoretical model: Amplitude spectrum of Transmission function T23	75
4-18	Theoretical model: Phase spectrum of Transmission function T23	76
4-19	Realistic model: Reflection Impulse Response	80
4-20	Realistic model: Reflection Ricker Response	81
4-21	Realistic model: Reflection Ricker Response wave theoretic (solid) vs. conventional reflectivity (Dashed)	82
4-22	Realistic model: Transmission Impulse Response	83

LIST OF FIGURES

FIGURE	CONTENTS	PAGE
4-23	Realistic model: Transmission Ricker Response	84
4-24	Realistic model: Reflection function R12	85
4-25	Realistic model: Reflection function R23	86
4-26	Soft sea floor model: Reflection Impulse Response	90
4-27	Soft sea floor model: Reflection Ricker Response	91
4-28	Soft sea floor model: Reflection Ricker Response wave theoretic (solid) vs. conventional reflectivity (Dashed)	92
4-29	Soft sea floor model: Transmission Impulse Response ...	93
4-30	Soft sea floor model: Transmission Ricker Response ...	94
4-31	Soft sea floor model: Reflection function R12	95
4-32	Soft sea floor model: Reflection function R23	96
4-33	Hard sea floor model: Reflection Impulse Response	100
4-34	Hard sea floor model: Reflection Ricker Response	101
4-35	Hard sea floor model: Reflection Ricker Response wave theoretic (solid) vs. conventional reflectivity (Dashed)	102
4-36	Hard sea floor model: Transmission Impulse Response ..	103
4-37	Hard sea floor model: Transmission Ricker Response ...	104
4-38	Hard sea floor model: Reflection function R12	105
4-39	Hard sea floor model: Reflection function R23	106

LIST OF TABLES

TABLES	CONTENTS	PAGE
2-1	Parameters Definition	29
4-1	A theoretical model Parameters for basic analytical results	58
4-2	A realistic model Parameters for basic analytic results	79
4-3	Soft sea floor model Parameters for basic analytical results	89
4-4	Hard sea floor model Parameters for basic analytical results	99
4-5	Relation of thickness of Transition zone, velocity gradient, velocity ratio and zeroes of Bessel function arguments	109

ACKNOWLEDGEMENTS

First of all, I thank GOD for everything. I acknowledge the help and support of my country Saudi Arabia through Aramco for this project. This could not have been possible without the generous support received.

Special thanks are due to Dr. Rup K. Kaul, my local supervisor and adviser in absentia. This project would not have been possible without his generous spirit of letting people study and learn, and showing them how to do research and solve problems. He not only provided the idea of this topic when I dropped by his office one day but also encouraging to do scientific analyses. His guidance through this thesis was of very great help in accomplishing the work.

I thank my committee members at Colorado School of Mines for their patience and guidance through my course work in the school. This includes Professor R. L. Sengbush as advisor, who contributed valuable suggestions and advice, Professors F. Hadsel and A. Ibrahim as the other committee members.

Dr. Ahmed Fouda of Training Unit of the Exploration Department in Aramco who provided encouraging support and made things go smoother.

Finally, I reserved this to highlight the special thanks for my family: father (who passed away during my graduate

courses study), mother, brother and sisters for their support and prayer and, last but not the least, to my wife Zahra and the three kids Muhammad, Nassr, Maram who suffered a lot through this trip.

INTRODUCTION

In order to study the seismic response of any stratigraphic feature, one needs to understand the behavior of a seismic pulse incident on the feature. Many examples of such studies can be found in the existing literature. In this thesis, the behavior of linearly varying velocity transition zones has been studied theoretically through the wave equation. Such zones are encountered in a gradual deposition layer such as a water-bottom transition zone and the permafrost in which a linear change in the velocity with depth exists.

Wolf (1937) has apparently been the first who worked on a related problem and defined a transition zone in which the elastic constants are continuous functions of depth and thus the reflection function becomes wave-length dependent. He considered the reflection of harmonic waves from a transition layer. In a subsequent paper, Wolf (1940) discussed the group delay of a wave of a given predominant frequency traveling in a weathered layer which has a linear increase of velocity with depth. A study by Peterson, Fillippone and Coker (1955) accomplished a significant simplification by introducing an approximation for the reflection coefficient in a continuous Earth model. Menzel and Rosenbach (1957)

studied the reflection of a pressure impulse incident on a weathered-layer transition zone through use of Fourier analysis. Berryman, Goupillaud, and Waters (1958) approximated velocity logs by a series of velocity transition zones. They calculated the reflection response of a series of transition layers using an iterative technique. Their solution took into account multiple reflections between layers. A companion paper with Berryman et al (1958) suggests an experimental approach to the study of multiple transition layers by showing that the velocity of longitudinal waves in a nylon rod is a linear function of the temperature in the range of 20° C to 100° C. Menzel and Rosenbach (1958) again show that the shape of the seismic pulse is remarkably influenced by a layer with linearly changing velocity. They used numerical inversion of Laplace transform to obtain the response to a pulse of any shape. Endtz and Hazenbrock (1959) disagreed with Menzel and Rosenbach's (1957) derivation of the particle velocity signal transmitted through a weathered layer which has linearly increasing velocity. Bortfeld (1959) showed that the transition layer can be regarded as the limit of a sequence of constant velocity layer subdivisions. Wuenschel (1960) obtained synthetic seismograms including multiples and transmission coefficients by solving the boundary value

problem for uniform models and for models containing transition layers of variable velocity. Sengbush, Lawrence and McDonal (1961), using a non-mathematical discussion of the reflections from idealized velocity layering, showed that a ramp reflectivity transition zone produces integrated shot pulses at the changes in the slope of the velocity function. Gupta (1965) found exact solutions for normal and oblique incidence of reflected plane waves from a linear transition layer in a liquid medium. Foster (1975) concluded that the transmission effects on a reflected pulse as observed at the surface are unsubstantial in a continuous one-dimensional seismic model. He pointed out the fallacy that sampling creates layers. Gray (1984) found the validity limit of Foster's work, and showed that in some cases transmission losses produce a predictable and non-trivial effect on reflection seismograms. A recent work by Justice and Zuba (1986) considered the effect of a simple transition zone between two half spaces of constant velocity and discusses some characteristic features of the transition zone.

Some of the papers cited use the Peterson et al (1955) conventional convolutional reflectivity model. This model is widely used in seismic exploration. Although the model has the appealing virtue of great simplicity and has value in estimating the primary reflection arrival times, it ignores

the wave theoretical propagation attributes even in the simplest geometries. In the convolutional model, the reflectivity function for an Earth with continuous acoustic impedance is defined as one-half of the derivative of the natural logarithm of the impedance with respect to travel time. This is a plausible extension of the familiar discrete reflection coefficient sequence to the continuous impedance case. It is evident that this way of modeling ignores the intrinsic wave-theoretic attribute that the input wavelet must change in both amplitude and shape as it propagates. Therefore the contribution to the primary reflection wavelet from any point within the model must depend continuously upon the entire past history of the input wavelet up to that point. For simplicity, the conventional model ignores multiples from a continuously varying earth. This concept of modeling achieves its inherent simplicity at the cost of obtaining incorrect amplitudes and shapes in the continuous case.

Although the wave-theoretic response is quite complex in a general acoustic impedance variation, some simpler models can be studied to provide valuable insight. Some workers have done so, as indicated above, and have obtained reasonable results. But their claim of having obtained significant multiples is not substantiated by the work done

here on models containing linear velocity variation as a function of depth. In these models, the reflectivity is found to be significantly different from the reflectivity obtained in the conventional model.

The one-dimensional wave equation is used to solve for the response of a layered Earth in the case of a normally incident plane wave. In the models, the first and the fourth layers are half-spaces with constant velocity, the third layer has constant velocity, and the second is the linearly varying velocity transition layer. The solution is obtained in the frequency domain using analytical expressions for pressure and displacement. The time-domain response is obtained by numerical inversion using the fast Fourier transform.

In this thesis, four models are studied. The first is a theoretical model for analytical purposes, the second is a realistic model typical of Saudi Arabia, and the last two represent soft and hard sea floor models of typical offshore fields in the Arabian Gulf. The wave-theoretic numerical results are compared to the conventional reflectivity modeling results.

1. STATEMENT OF THE PROBLEM AND BASIC SOLUTIONS

Variable Velocity Wave Equation

Under the acoustic model assumption in which all shear conversions are neglected, the dynamic behavior of the Earth is controlled by the scalar wave equation for a typical physical field quantity of interest such as pressure. The wave equation of interest here is the partial differential equation of the form

$$\frac{\partial^2 \psi}{\partial z^2} = \frac{1}{v^2(z)} \frac{\partial^2 \psi}{\partial t^2} , \quad (1-1)$$

in which z is the depth, t is the time, $v(z)$ is the variable velocity in the medium assumed to be a function of the depth only, and ψ is the field quantity of interest such as pressure. Therefore ψ , as a possible solution of (1-1), is a function of z and t .

Temporal and spatial separation: The particular form of (1-1) suggests that the classical method of separation of variables will yield the most general solution to the partial

differential equation. The solution $\psi(z,t)$ is in the form of a product of two functions as

$$\psi(z,t) = F(z) \cdot G(t) \quad , \quad (1-2)$$

in which $F(z)$ is the spatial function of the depth variable z only and $G(t)$ is the temporal function of the time variable t only.

Upon substituting (1-2) in (1-1), performing the required differentiations, and dividing the result by $F \cdot G$, one obtains

$$v^2(z) \frac{F''(z)}{F(z)} = \frac{\ddot{G}(t)}{G(t)} \quad , \quad (1-3)$$

in which the double-prime and the double-dot denotes the second derivatives with respect to z and t , respectively. The left side of (1-3) is a function of z only and the right side is a function of t only. Since the two variables are independent, both sides of (1-3) must equal the same separation constant. Following the conventional notation, the separation constant is denoted as $-\omega^2$, where ω is the temporal radial frequency in radians per second. A pair of separated ordinary differential equations is obtained,

$$v^2 \frac{F''}{F} = -\omega^2 \quad (1-4)$$

for the spatial left side of (1-3) and

$$\frac{\ddot{G}}{G} = -\omega^2 \quad (1-5)$$

for the temporal right side of (1-3).

The explicit basic linearly independent solution pairs for both (1-4) and (1-5) will be discussed appropriately below for our specific purposes.

Pressure and displacement field: In this subsection the field quantity ψ will be related to the physical quantities of interest to us, namely the pressure and the displacement fields.

As stated above, in the acoustic model assumption the conversion of the pressure waves to shear waves is neglected. Therefore the pressure P is defined as the product of the incompressibility K of the medium and the negative divergence (convergence) of the displacement vector U giving

$$P = -K \nabla \cdot U . \quad (1-6)$$

Differentiating both sides of (1-6) twice partially with respect to t and using the point form (per unit volume) of the Newton's law

$$\rho \frac{\partial^2 U}{\partial t^2} = -\nabla P \quad (1-7)$$

in which ρ is the medium mass density gives

$$\frac{\partial^2 P}{\partial t^2} = K \nabla \cdot \left(\frac{\nabla P}{\rho} \right). \quad (1-8)$$

We assume the density ρ to be a space independent constant ρ_0 and define the medium phase velocity $v = \sqrt{K/\rho_0}$, as is customary. Thus (1-8) simplifies to

$$\nabla^2 P = \frac{1}{v^2} \frac{\partial^2 P}{\partial t^2}. \quad (1-9)$$

In this study, we are interested only in the plane wave normal (z -direction) incidence solution (1-9). Since the phase velocity is also assumed to be a function of z only, the pressure equation (1-9) becomes the one-dimensional wave equation

$$\frac{\partial^2 P}{\partial z^2} = \frac{1}{v^2(z)} \frac{\partial^2 P}{\partial t^2} \quad (1-10)$$

in the variables z and t only. The Newton's law in (1-7) simplifies to

$$\frac{\partial^2 U}{\partial t^2} = - \frac{1}{\rho_0} \frac{\partial P}{\partial z} \quad (1-11)$$

Now we identify the wave function $\Psi(z,t)$ introduced in (1-1) above with our pressure $P(z,t)$ since (1-1) and (1-10) are identical equations. In the following, we will use the product form

$$P(z,t) \equiv \Psi(z,t) = F(z) \cdot G(t) \quad (1-12)$$

introduced in (1-2). The resulting separated ordinary equations (1-4) and (1-5), and (1-11) yield explicit solutions for $P(z,t)$ and $U(z,t)$ for the two cases of velocity variation, the linear and the constant, which are of interest to us in this study.

Linearly Varying Velocity Layer Basic Solutions

For a linear velocity variation medium the velocity at any point z is expressed as

$$v(z) = v_s + \beta z \quad (1-13)$$

in which v_s is the starting velocity and β is the velocity gradient. Accordingly, (1-13) above and (1-10), (1-12) and (1-4) in the preceding yield the spatial part of the equation for the linear case,

$$(v_s + \beta z)^2 F'' + \omega^2 F = 0 \quad (1-14)$$

For convenience, we define a new independent variable by

$$\xi = \frac{v_s + \beta z}{v_0} \quad (1-15)$$

in which v_0 is some normalizing reference velocity to render ξ dimensionless. Recalling that the double-prime " in (1-14) is the second derivative with respect to z , after usual algebra using (1-15) in (1-14), it transforms to

$$\xi^2 \frac{d^2 F(\xi)}{d\xi^2} + \left(\frac{\omega}{\beta}\right)^2 F(\xi) = 0 . \quad (1-16)$$

This is a simpler case of Cauchy-Euler equation in the new variable ξ with the first derivative term absent. Assuming a solution of the form $F(\xi) = \xi^m \neq 0$, we obtain the characteristic quadratic equation for m as

$$m^2 - m + \left(\frac{\omega}{\beta}\right)^2 = 0 , \quad (1-17)$$

which has the two solutions

$$m_{1,2} = \frac{1 \pm \sqrt{1 - \left(\frac{2\omega}{\beta}\right)^2}}{2} . \quad (1-18)$$

We note that, for the special case $\omega = 0$, (1-16) simplifies to $\frac{d^2 F}{d\xi^2} = 0$ with the linear solution ξ and the constant solution 1, say, as the pair of linearly independent solutions. Therefore, (1-18) is valid for this special case as well since it yields $m_{1,2} = 1, 0$, which implies $F_{1,2} = \xi, 1$ as needed. Clearly (1-18) yields three cases as the parameter ω ,

the radial frequency, is permitted to vary over $0 \leq \omega \leq \infty$.

These are:

$$\text{Case I: } 0 \leq \omega \leq \frac{\beta}{2}$$

$$m_{1,2} = \frac{1 \pm \sqrt{1 - \left(\frac{2\omega}{\beta}\right)^2}}{2} \equiv \frac{1}{2} (1 \pm \gamma) ,$$

where $\gamma \equiv \left| 1 - (2\omega/\beta)^2 \right|^{\frac{1}{2}}$. The two independent solutions are

$$F_{1,2} = e^{\frac{1}{2}(1-\gamma) \ln \xi}, e^{\frac{1}{2}(1+\gamma) \ln \xi}$$

$$\text{Case II: } \omega = \frac{\beta}{2}$$

$$m_{1,2} = \frac{1}{2}, \frac{1}{2} .$$

In this case the characteristic roots are equal. Therefore the independent solutions of the Cauchy-Euler equation are

$$F_{1,2} = e^{\frac{1}{2} \ln \xi}, (\ln \xi) e^{\frac{1}{2} \ln \xi}$$

Case III: $\frac{\beta}{2} < \omega < \infty$

$$m_{1,2} = \frac{1 \pm i \sqrt{\left(\frac{2\omega}{\beta}\right)^2 - 1}}{2} \equiv \frac{1}{2} (1 \pm i\gamma)$$

where $\gamma \equiv \left| \left(\frac{2\omega}{\beta}\right)^2 - 1 \right|^{\frac{1}{2}}$, exactly as in case I. The two independent solutions are

$$F_{1,2} = e^{\frac{1}{2}(1-i\gamma) \ln \xi}, e^{\frac{1}{2}(1+i\gamma) \ln \xi}$$

For analytical and numerical reasons, it is important to show that the two linearly independent solutions for case II are indeed contained in Cases I and III, and that the solutions in these cases approach the Case II solutions in the limit $\omega \rightarrow \beta/2$.

For this purpose, we rewrite the Case I solution pair in the form

$$\begin{aligned} e^{-\frac{1}{2} \ln \xi} F_{1,2} &\equiv e^{-\frac{\gamma}{2} \ln \xi}, e^{+\frac{\gamma}{2} \ln \xi} \\ &\equiv \cosh \left[\frac{\gamma}{2} \ln \xi \right], \frac{\sinh \left[\left(\frac{\gamma}{2}\right) \ln \xi \right]}{\left(\frac{\gamma}{2}\right)} \end{aligned}$$

which are equivalent linear combinations of each other. The limit $\omega \rightarrow \beta/2$ means $\gamma \rightarrow 0$, in which case

$$\begin{aligned} e^{-\frac{1}{2}\ln\xi} F_{1,2} &\rightarrow 1, \ln\xi \\ F_{1,2} &\rightarrow e^{\frac{1}{2}\ln\xi}, (\ln\xi) e^{\frac{1}{2}\ln\xi} \end{aligned}$$

which are solutions for Case II. Using an exactly analogous procedure starting with the solution for case III, one can readily show that these also behave similarly under the limit $\omega \rightarrow \beta/2$.

Equation (1-10), (1-12), and (1-15) yield the temporal part equation as

$$\ddot{G} + \omega^2 G = 0. \tag{1-22}$$

This is a well-known second order differential equation which has the linearly independent solution pair

$$G_{1,2} = e^{-i\omega t}, e^{+i\omega t} \quad \text{for } \omega > 0. \tag{1-23}$$

The special case $\omega=0$ needs to be dealt with briefly. The solutions are the constant function 1 and the linear function t . Now (1-23) yields the constant 1 directly for $\omega=0$ and we

are not interested in the linear solution t since it is unbounded. Therefore

$$G_{1,2} = e^{-i\omega t}, \quad e^{i\omega t} \quad \text{for } \omega \geq 0,$$

which, we rewrite as

$$G = e^{+i\omega t} \quad \text{for } -\infty < \omega < +\infty \quad (1-24)$$

equivalently to provide completeness of solutions.

The complete basic solution

$$P(\xi, t) = F(\xi) \cdot G(t) \quad (1-25)$$

therefore is, explicitly, for the three cases

$$P(z, t) = \left[C e^{(1-\gamma) \ln \sqrt{\xi}} + D e^{(1+\gamma) \ln \sqrt{\xi}} \right] e^{i\omega t} \quad (1-26)$$

for $|\omega| < \left| \frac{\beta}{2} \right|$

$$= \left[C e^{\ln \sqrt{\xi}} + D \ln \xi e^{\ln \sqrt{\xi}} \right] e^{i\omega t} \quad (1-27)$$

for $|\omega| = \left| \frac{\beta}{2} \right|$

$$= \left[C e^{(1-i\gamma) \ln \sqrt{\xi}} + D e^{(1+i\gamma) \ln \sqrt{\xi}} \right] e^{i\omega t} \quad (1-28)$$

for $|\omega| > \left| \frac{\beta}{2} \right|$.

Constant Velocity Layer Basic Solutions

For a constant velocity medium the velocity at any point z is fixed and expressed by

$$v(z) = c, \quad (1-29)$$

and, as in (1-4) , we will have

$$\frac{F''}{F} = -\frac{\omega^2}{c} = -k^2, \quad (1-30)$$

where k is the wave number. So (1-29) and (1-10), (1-12) and (1-30) give the spatial part equation for the constant case as

$$\frac{d^2F}{dz^2} + k^2F = 0. \quad (1-31)$$

The independent solutions for (1-31) are well known to be

$$F_{1,2} = e^{-ikz}, \quad e^{ikz}, \quad (1-32)$$

for the spatial part.

The temporal part equation for a constant velocity medium is exactly the same as for the linearly variable velocity medium discussed above in (1-22) through (1-25).

The complete basic solution, therefore is

$$\begin{aligned} P(z,t) &= F(z) \cdot G(t) \\ &= Ae^{i(\omega t - kz)} + Be^{i(\omega t + kz)} \end{aligned} \tag{1-33}$$

for $-\infty < \omega < +\infty$.

2. THE MODELS AND ANALYTICAL RESULTS

In this thesis, a three-layer model and a four-layer model will be studied to understand the effect of a transition velocity zone embedded appropriately in the two models. We wish to study the overall reflection and transmission coefficients for the two cases, using the analytical model solutions which will be developed below.

We need to have the relationship between the pressure and the displacement. These are obtained by using (1-11) in (1-33) and (1-26) through (1-28) to get the displacement fields in the constant velocity case and in the linearly variable velocity case.

To derive the relationship between P and U , we generalize the basic solution by summing (integrating) over the whole frequency range $-\infty < \omega < +\infty$ to yield

$$\begin{aligned}
 P(z, t) &= \int_{-\infty}^{\infty} d\omega \left[A e^{i(\omega t - kz)} + B e^{i(\omega t + kz)} \right] \\
 &= \int_{-\infty}^{\infty} d\omega \bar{P}(z, \omega) e^{i\omega t} , \qquad (2-1)
 \end{aligned}$$

which also satisfies the pressure partial differential equation. Similarly, the displacement field is

$$U(z, t) = \int_{-\infty}^{\infty} d\omega \bar{U}(z, \omega) e^{i\omega t} . \quad (2-2)$$

From (2-1) and (2-2), we have

$$-\frac{1}{\rho_0} \frac{\partial P}{\partial z} = -\frac{1}{\rho_0} \int_{-\infty}^{\infty} d\omega \frac{\partial \bar{P}}{\partial z} e^{i\omega t} \quad (2-3)$$

and

$$\frac{\partial^2 U}{\partial t^2} = \int_{-\infty}^{\infty} d\omega (-\omega^2) \bar{U}(z, \omega) e^{i\omega t} . \quad (2-4)$$

By (1-11)

$$\int_{-\infty}^{\infty} d\omega (-\omega^2) \bar{U}(z, \omega) = -\frac{1}{\rho_0} \int_{-\infty}^{\infty} d\omega \frac{\partial \bar{P}(z, \omega)}{\partial z} , \quad (2-5)$$

which yields the relationship between the displacement and the pressure in the frequency domain upon equating the integrands of the two Fourier transforms. Thus we have

$$\bar{U}(z, \omega) = \frac{1}{\rho_0 \omega^2} \frac{\partial \bar{P}(z, \omega)}{\partial z} \quad (2-6)$$

where the limit does exist when $\omega = 0$.

We use (2-6) to find expressions for a constant velocity (uniform) layer and a linearly varying velocity (transition) layer with its three cases as follows.

The displacement expression in the uniform layer is

$$\bar{U}(z, \omega) = -\frac{ik}{\rho_0 \omega^2} A e^{-ikz} + \frac{ik}{\rho_0 \omega^2} B e^{ikz} \quad (2-7)$$

whereas for the three cases of the transition layer they are

Case I:

$$\bar{U}(z, \omega) = \frac{\beta}{2v(z)\rho_0 \omega^2} \left[(1-\gamma) C e^{(1-\gamma) \ln \sqrt{\xi}} + (1+\gamma) e^{(1+\gamma) \ln \sqrt{\xi}} \right], \quad (2-8)$$

Case II:

$$\bar{U}(z, \omega) = \frac{\beta}{\rho_0 \omega^2} \left[C e^{-\ln \sqrt{4v_0 v(z)}} + D \left(1 + \ln \sqrt{\xi} \right) \times e^{-\ln \sqrt{v_0 v(z)}} \right], \quad (2-9)$$

and Case III:

$$\bar{u}(z, \omega) = \frac{\beta}{2v(z)\rho_0\omega^2} \left[(1-i\gamma) \text{Ce}^{(1-i\gamma)\ln\sqrt{\xi}} + (1+i\gamma) \text{De}^{(1+i\gamma)\ln\sqrt{\xi}} \right]. \quad (2-10)$$

Three-Layer Model

Studying the behavior of a constant velocity layer above a linearly varying velocity layer is rather meaningless for practical purposes. We need to study the effect of a transition zone embedded in an otherwise discrete sequence of constant velocity layers. Therefore, we start with the simplest case of a transition zone embedded between two constant velocity half spaces. Thus, with a fixed constant density assumed for the whole system, the responses we calculate would be due to the presence of the transition layer.

Formulation and analytical solution: This is a study of the three-layer case just defined as a boundary value problem. We assume an infinite plane wave pressure pulse propagating downward in the positive z -direction and, therefore, normally incident on interval 2 from interval 1, figure 2-1. The usual continuity conditions on the pressure and the displacement will be enforced across each of the two interfaces to yield the reflected pulse in interval 1, the total pulse in interval 2, and the transmitted pulse in interval 3.

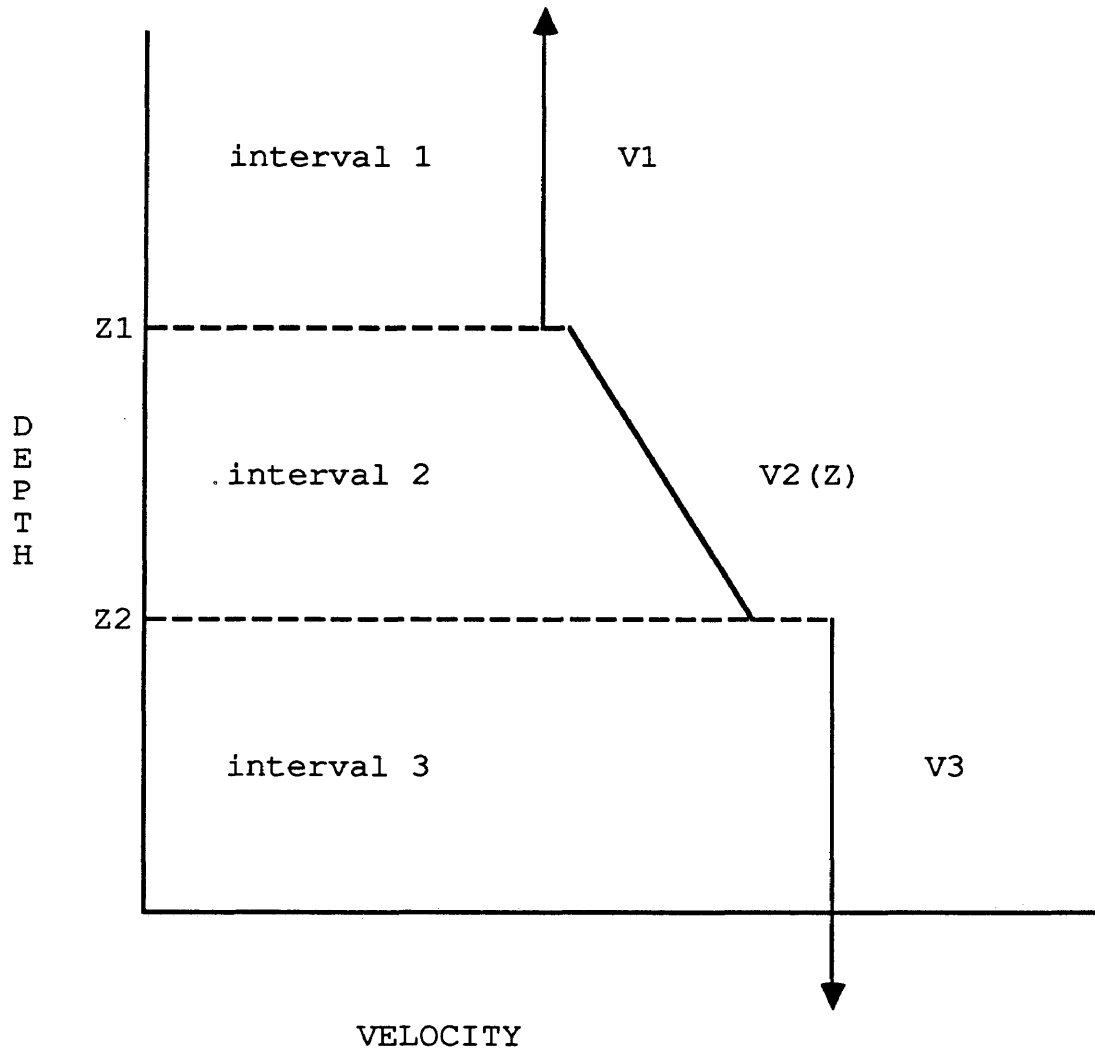


Figure 2-1: Three-layer model.

The required boundary conditions are

$$\bar{P}_1(z_1, \omega) = \bar{P}_2(z_1, \omega), \quad \bar{U}_1(z_1, \omega) = \bar{U}_2(z_1, \omega) \quad \text{at } z=z_1$$

and

$$\bar{P}_2(z_2, \omega) = \bar{P}_3(z_2, \omega), \quad \bar{U}_2(z_2, \omega) = \bar{U}_3(z_2, \omega) \quad \text{at } z=z_2 .$$

The equations which describe the behavior of a pulse in such a system with the transition zone as interval 2, are:

Case I:

$$Ae^{-ik_1z_1} + Be^{ik_1z_1} = Ce^{(1-\gamma)\ln\sqrt{\frac{v_s}{v_0}}} + De^{(1+\gamma)\ln\sqrt{\frac{v_s}{v_0}}} ,$$

$$-ik_1Ae^{-ik_1z_1} + ik_1Be^{ik_1z_1} = \frac{\beta(1-\gamma)}{2v_s} Ce^{(1-\gamma)\ln\sqrt{\frac{v_s}{v_0}}}$$

$$+ \frac{\beta(1+\gamma)}{2v_s} De^{(1+\gamma)\ln\sqrt{\frac{v_s}{v_0}}} ,$$

$$Ce^{(1-\gamma)\ln\sqrt{\frac{v_f}{v_0}}} + De^{(1+\gamma)\ln\sqrt{\frac{v_f}{v_0}}} = Ee^{-ik_3z_2} ,$$

$$\frac{\beta(1-\gamma)}{2v_f} Ce^{(1-\gamma)\ln\sqrt{\frac{v_f}{v_0}}} + \frac{\beta(1+\gamma)}{2v_f} De^{(1+\gamma)\ln\sqrt{\frac{v_f}{v_0}}} = -ik_3 Ee^{-ik_3z_2}$$

(2-11)

Case II:

$$\begin{aligned}
 Ae^{-ik_1z_1} + Be^{ik_1z_1} &= C\sqrt{\frac{v_s}{v_0}} + D\ln\left(\frac{v_s}{v_0}\right) \cdot \sqrt{\frac{v_s}{v_0}}, \\
 -ik_1Ae^{-ik_1z_1} + ik_1Be^{ik_1z_1} &= \frac{C\beta}{2v_s} \sqrt{\frac{v_s}{v_0}} + \frac{D\beta}{v_s} \left(1 + \ln\sqrt{\frac{v_s}{v_0}}\right) \\
 &\quad \times \sqrt{\frac{v_s}{v_0}}, \\
 C\sqrt{\frac{v_f}{v_0}} + D\ln\left(\frac{v_f}{v_0}\right) \cdot \sqrt{\frac{v_f}{v_0}} &= Ee^{-ik_3z_2}, \\
 \frac{C\beta}{2v_f} \sqrt{\frac{v_f}{v_0}} + \frac{D\beta}{v_f} \left(1 + \ln\sqrt{\frac{v_f}{v_0}}\right) \sqrt{\frac{v_f}{v_0}} &= -ik_3Ee^{-ik_3z_2} \quad (2-12)
 \end{aligned}$$

Case III:

$$\begin{aligned}
 Ae^{-ik_1z_1} + Be^{ik_1z_1} &= Ce^{(1-i\gamma)\ln\sqrt{\frac{v_s}{v_0}}} + De^{(1+i\gamma)\ln\sqrt{\frac{v_s}{v_0}}}, \\
 -ik_1Ae^{-ik_1z_1} + ik_1Be^{ik_1z_1} &= \frac{\beta(1-i\gamma)}{2v_s} Ce^{(1-i\gamma)\ln\sqrt{\frac{v_s}{v_0}}} \\
 &\quad + \frac{\beta(1+i\gamma)}{2v_s} De^{(1+i\gamma)\ln\sqrt{\frac{v_s}{v_0}}}, \\
 Ce^{(1-i\gamma)\ln\sqrt{\frac{v_f}{v_0}}} + De^{(1+i\gamma)\ln\sqrt{\frac{v_f}{v_0}}} &= Ee^{-ik_3z_2}, \\
 \frac{\beta(1-i\gamma)}{2v_f} Ce^{(1-i\gamma)\ln\sqrt{\frac{v_f}{v_0}}} + \frac{\beta(1+i\gamma)}{2v_f} e^{(1+i\gamma)\ln\sqrt{\frac{v_f}{v_0}}} &= -ik_3Ee^{-ik_3z_2} \quad (2-13)
 \end{aligned}$$

In these: A is the incident pressure pulse amplitude in first layer 1,

B is the complete upward radiation in layer 1,

C is the complete downward radiation in layer 2,

D is the complete upward radiation in layer 2,

and finally,

E is the complete downward radiation in layer 3.

The purpose here is to solve those equations analytically for the reflected pulse from the second layer into the first and the transmitted pulse out of the second layer into the third. The solution is obtained simply by inverting the coefficient matrix of the set of equations after some detailed algebra for each case. For convenience in notation, we make the definitions shown below in table 2-1.

Table 2-1
(Parameters Definition)

	Case I	Case II	Case III
k_{2s}	$\frac{i(1-\gamma)\beta}{2v_s}$	$\frac{i\beta}{2v_s}$	$\frac{(i+\gamma)\beta}{2v_s}$
\tilde{k}_{2s}	$\frac{-i(1+\gamma)\beta}{2v_s}$	$-\frac{i\beta}{v_s} \left(\frac{1}{\ln\sqrt{\frac{v_s}{v_0}}} + 1 \right)$	$\frac{-(i-\gamma)\beta}{2v_s}$
k_{2f}	$\frac{-i(1+\gamma)\beta}{2v_f}$	$-\frac{i\beta}{v_f} \left(\frac{1}{\ln\sqrt{\frac{v_f}{v_0}}} + 1 \right)$	$\frac{-(i-\gamma)\beta}{2v_f}$
\tilde{k}_{2f}	$\frac{i(1-\gamma)\beta}{2v_f}$	$\frac{i\beta}{2v_f}$	$\frac{(i+\gamma)\beta}{2v_f}$
\emptyset	$(1 + \gamma) \ln \sqrt{\frac{v_f}{v_s}}$	$\ln \left[\sqrt{\frac{v_f}{v_s}} \frac{\ln\left(\frac{v_f}{v_0}\right)}{\ln\left(\frac{v_s}{v_0}\right)} \right]$	$(1+i\gamma) \ln \sqrt{\frac{v_f}{v_s}}$
\emptyset	$(1 - \gamma) \ln \sqrt{\frac{v_f}{v_s}}$	$\ln \sqrt{\frac{v_f}{v_s}}$	$(1-i\gamma) \ln \sqrt{\frac{v_f}{v_s}}$
$k_i = \tilde{k}_i = \frac{\omega}{v_i}$ for $i = 1, 2, 3$ and 4 for the above cases			

With these definitions, the required analytical results are

$$Be^{ik_1z_1} = \left[\frac{k_1 - k_{2s}}{k_1 + k_{2s}} + \frac{(\tilde{k}_{2f} - k_3) \left(\frac{2k_1}{k_1 + k_{2s}} \right) (\tilde{k}_{2s} + k_{2s})}{e^{\emptyset - \tilde{\emptyset}} + \left(\frac{\tilde{k}_{2f} - k_3}{k_{2f} + k_3} \right) \left(\frac{k_1 - \tilde{k}_{2s}}{k_1 + k_{2s}} \right)} \right] Ae^{-ik_1z_1} \tag{2-14}$$

for the reflected pulse into layer 1, and

$$Ee^{-ik_3z_2} = \frac{\left(\frac{\bar{k}_{2s} + k_{2s}}{k_1 + k_{2s}}\right) \left(\frac{2k_3}{k_{2f} + k_3}\right)}{e^{\vartheta - \bar{\vartheta}} + \left(\frac{\bar{k}_{2f} - k_3}{k_{2f} + k_3}\right) \left(\frac{k_1 - \bar{k}_{2s}}{k_1 + k_{2s}}\right)} Ae^{-ik_1z_1 + \vartheta} \quad (2-15)$$

for the transmitted pulse into layer 3.

We now wish to show that the same results as above can be obtained in a different way based upon an interpretation of mechanical systems from Hauser (1966).

We assume that the total reflected pulse from an interface is a resultant of the reflected part of the incident pulse on interface from above and the transmitted part of whatever is incident on the interface from below. Further, the total transmitted pulse at an interface is the resultant of the reflected part of the pulse transmitted below and the transmitted part incident from below. Each constituent part of any pulse above is the pulse scaled by some function. This function is the crucial part of the interpretation in which the reflected scaling function is named the reflection function for that interface between the two defined media. Similar interpretation applies to the definition of the scaling function for the transmission

function. From the development above, we define the following sets of equations for the three cases:

Case I:

$$\begin{aligned}
 B e^{ik_1 z_1} &= R_{12} A e^{-ik_1 z_1} + T_{21} D e^{(1+\gamma) \ln \sqrt{\frac{v_s}{v_0}}}, \\
 C e^{(1-\gamma) \ln \sqrt{\frac{v_s}{v_0}}} &= T_{12} A e^{-ik_1 z_1} + R_{21} D e^{(1+\gamma) \ln \sqrt{\frac{v_s}{v_0}}}, \\
 D e^{(1+\gamma) \ln \sqrt{\frac{v_f}{v_0}}} &= R_{23} C e^{(1-\gamma) \ln \sqrt{\frac{v_f}{v_0}}}, \\
 E e^{-ik_3 z_2} &= T_{23} C e^{(1-\gamma) \ln \sqrt{\frac{v_f}{v_0}}}
 \end{aligned} \tag{2-16}$$

Case II:

$$\begin{aligned}
 B e^{ik_1 z_1} &= R_{12} A e^{-ik_1 z_1} + T_{21} D \ln \frac{v_s}{v_0} \cdot \sqrt{\frac{v_s}{v_0}}, \\
 C \sqrt{\frac{v_s}{v_0}} &= T_{12} A e^{-ik_1 z_1} + R_{21} D \ln \frac{v_s}{v_0} \cdot \sqrt{\frac{v_s}{v_0}}, \\
 D \ln \frac{v_f}{v_0} \cdot \sqrt{\frac{v_f}{v_0}} &= R_{23} C \sqrt{\frac{v_f}{v_0}}, \\
 E e^{-ik_3 z_2} &= T_{23} C \sqrt{\frac{v_f}{v_0}}
 \end{aligned} \tag{2-17}$$

Case III:

$$\begin{aligned}
 Be^{ik_1z_1} &= R_{12}Ae^{-ik_1z_1} + T_{21}De^{(1+i\gamma)\ln\sqrt{\frac{v_s}{v_0}}}, \\
 Ce^{(1-i\gamma)\ln\sqrt{\frac{v_s}{v_0}}} &= T_{12}Ae^{-ik_1z_1} + R_{21}De^{(1+i\gamma)\ln\sqrt{\frac{v_s}{v_0}}}, \\
 De^{(1+i\gamma)\ln\sqrt{\frac{v_f}{v_0}}} &= R_{23}Ce^{(1-i\gamma)\ln\sqrt{\frac{v_f}{v_0}}}, \\
 Ee^{-ik_3z_2} &= T_{23}Ce^{(1-i\gamma)\ln\sqrt{\frac{v_f}{v_0}}}. \tag{2-18}
 \end{aligned}$$

By using the definitions in table 2-1, the solutions for the reflected and transmitted pulses, which are valid for all three cases above, are given by:

The Reflected Pulse:

$$Be^{-ik_1z_1} = \left[R_{12} + \frac{R_{23}T_{21}T_{12}}{e^{\varnothing-\bar{\varnothing}} - R_{21}R_{23}} \right] Ae^{-ik_1z_1} \tag{2-19}$$

The Transmitted Pulse:

$$Ee^{-ik_3z_2} = \left[\frac{T_{12}T_{23}}{e^{\varnothing-\bar{\varnothing}} - R_{21}R_{23}} \right] Ae^{-ik_1z_1+\varnothing} \tag{2-20}$$

where

T_{ij} = transmission factor for a pulse incident in layer i and transmitted into adjacent layer j .

and

R_{ij} = reflection factor for a pulse incident in layer i
and reflected at interface between layers i and j .

Reflection Coefficient: The reflection of an acoustic wave from an abrupt impedance contrast is, of course, well known. In terms of the propagation constants k_i and k_j and velocities v_i and v_j across an interface, the reflection coefficient is

$$r_{ij} = \frac{k_i - k_j}{k_i + k_j} = \frac{v_j - v_i}{v_j + v_i} . \quad (2-21)$$

The question here is how one may generalize this definition when a linearly varying velocity layer is involved. This can be handled by the second approach suggested above in which the scale factor is really a function. Thus we find that we need to define

$$R_{12} = \frac{k_1 - k_{2s}}{k_1 + k_{2s}} , \quad R_{21} = \frac{\bar{k}_{2s} - k_1}{k_{2s} + k_1} , \quad (2-22)$$

and

$$R_{23} = \frac{\tilde{k}_{2f} - k_3}{k_{2f} + k_3}, \quad (2-23)$$

where K_1 , K_{2s} , \tilde{k}_{2s} , \tilde{k}_{2f} , and K_3 are defined in table 2-1 and the tilde (\sim) operation indicates the particular way the quantity is defined in relation to the same quantity without the tilde. In certain cases (in Case III, for example) it denotes pure complex-conjugation, but in others it does not. Here, R_{12} is the reflectivity function at the interface between a discrete layer and a transition zone and R_{23} is the reflectivity function at the interface between a transition layer and a uniform layer as in our three layer model.

Transmission Coefficient: Again, using the definitions above, the transmission coefficient is

$$T_{ij} = \frac{2k_j}{k_i + k_j} = \frac{2v_i}{v_i + v_j} \quad (2-24)$$

for the uniform layer case. Using arguments similar to above for generalization to a linearly varying velocity layer in which the scale factor is a function, and the needed definitions are

$$T_{12} = \frac{\tilde{k}_{2s} + k_{2s}}{k_1 + k_{2s}}, \quad T_{21} = \frac{2k_1}{k_{2s} + k_1}, \quad (2-25)$$

and

$$T_{23} = \frac{2k_3}{k_{2f} + k_3} . \quad (2-26)$$

Here T_{12} is the transmission function at the interface between a uniform layer and a transition zone and T_{23} is the transmission function at the interface between a transition layer and a uniform layer as in our three-layer model.

For a parallel result in a case of three uniform layers, see Appendix A.

Four Layer Model

The main objective of this thesis is to study the theoretical response to a primary wave from and through a linear velocity transition layer. Therefore in this section the transition zone is studied from within a total of four layers. Again, with a fixed assumed constant density, we study the response of the four layer system in the presence of the transition layer.

Formulation and analytical solution: This is a study of a four layer case defined as a boundary value problem. We assume an infinite plane wave pressure pulse propagating downwards in the positive z -direction and, therefore, normally incident on interval 2 from interval 1, figure 2-2. The usual continuity will be enforced across each of the two interfaces to yield the reflected pulse in interval 1, the total pulse in intervals 2 and 3, and the transmitted pulse in interval 4.

The required boundary conditions are

$$\bar{P}_1(z_1, \omega) = \bar{P}_2(z_1, \omega), \quad \bar{U}_1(z_1, \omega) = \bar{U}_2(z_1, \omega) \quad \text{at } z = z_1,$$

$$\bar{P}_2(z_2, \omega) = \bar{P}_3(z_2, \omega), \quad \bar{U}_2(z_2, \omega) = \bar{U}_3(z_2, \omega) \quad \text{at } z = z_2,$$

and

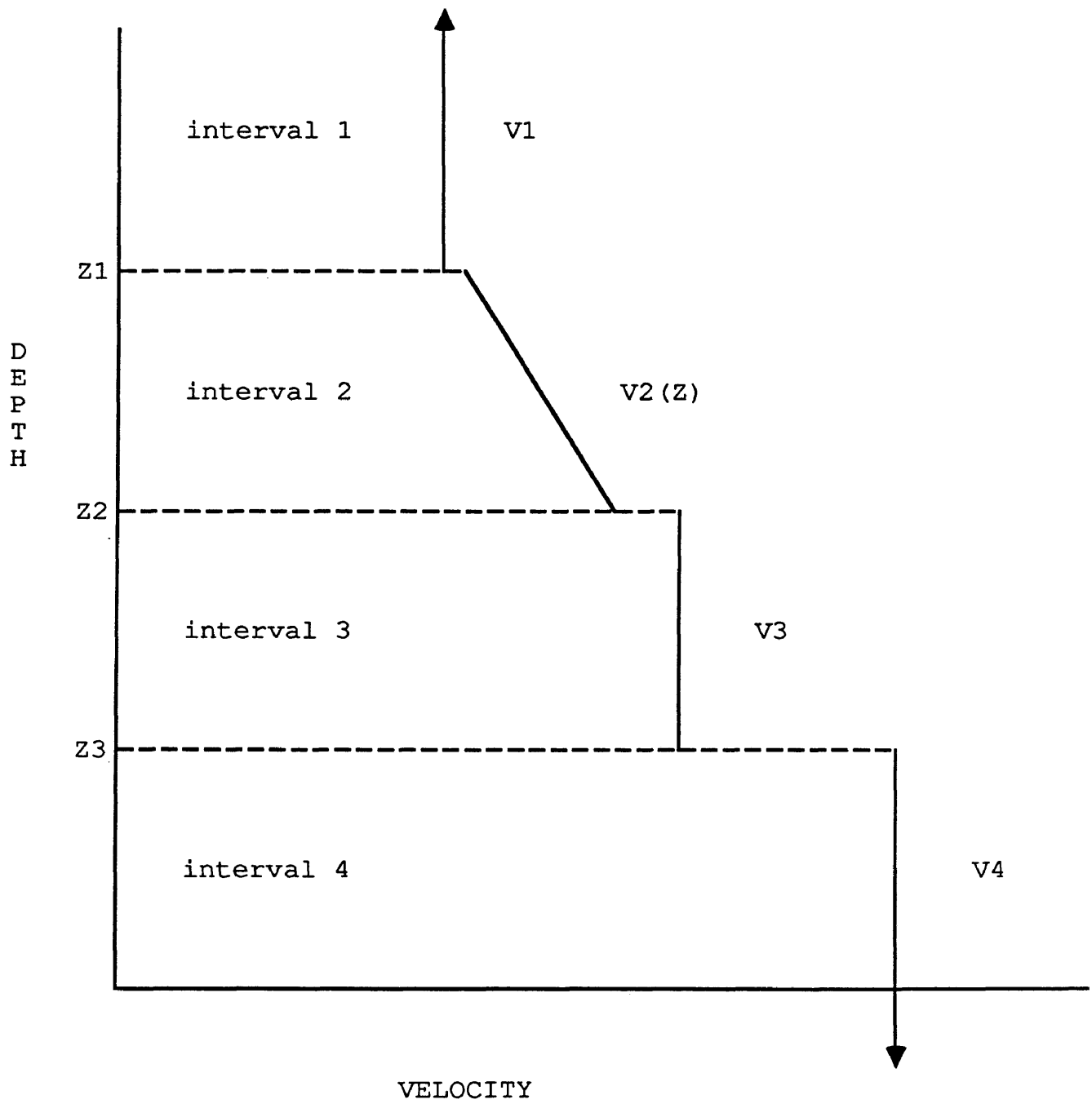


Figure 2-2: Four-layer model.

$$\bar{P}_3(z_3, \omega) = \bar{P}_4(z_3, \omega), \quad \bar{U}_3(z_3, \omega) = \bar{U}_4(z_3, \omega) \quad \text{at } z = z_3 .$$

The equations which describe the behavior of a pulse in such a system with the transition zone as interval 2, are:

Case I:

$$Ae^{-ik_1z_1} + Be^{ik_1z_1} = Ce^{(1-\gamma)\ln\sqrt{\frac{v_s}{v_0}}} + De^{(1+\gamma)\ln\sqrt{\frac{v_s}{v_0}}} ,$$

$$-ik_1Ae^{-ik_1z_1} + ik_1Be^{ik_1z_1} = \frac{\beta(1-\gamma)}{2v_s} Ce^{(1-\gamma)\ln\sqrt{\frac{v_s}{v_0}}}$$

$$+ \frac{\beta(1+\gamma)}{2v_s} De^{(1+\gamma)\ln\sqrt{\frac{v_s}{v_0}}} ,$$

$$Ce^{(1-\gamma)\ln\sqrt{\frac{v_f}{v_0}}} + De^{(1+\gamma)\ln\sqrt{\frac{v_f}{v_0}}} = Ee^{-ik_3z_2} + Fe^{ik_3z_2} ,$$

$$\frac{\beta(1-\gamma)}{2v_f} Ce^{(1-\gamma)\ln\sqrt{\frac{v_f}{v_0}}} + \frac{\beta(1+\gamma)}{2v_f} De^{(1+\gamma)\ln\sqrt{\frac{v_f}{v_0}}} = -ik_3Ee^{-ik_3z_2}$$

$$+ ik_3Fe^{ik_3z_2} ,$$

$$Ee^{-ik_3z_3} + Fe^{ik_3z_3} = Ge^{-ik_4z_3} ,$$

$$-ik_3Ee^{-ik_3z_3} + ik_3Fe^{ik_3z_3} = -ik_4Ge^{-ik_4z_3} . \quad (2-27)$$

Case II:

$$Ae^{-ik_1z_1} + Be^{ik_1z_1} = C\sqrt{\frac{v_s}{v_0}} + D\ln\left(\frac{v_s}{v_0}\right) \cdot \sqrt{\frac{v_s}{v_0}} ,$$

$$-ik_1 A e^{-ik_1 z_1} + ik_1 B e^{ik_1 z_1} = \frac{C\beta}{2v_s} \sqrt{\frac{v_s}{v_0}} + \frac{D\beta}{v_s} \left(1 + \ln \sqrt{\frac{v_s}{v_0}}\right) \times \sqrt{\frac{v_s}{v_0}},$$

$$C \sqrt{\frac{v_f}{v_0}} + D \ln\left(\frac{v_f}{v_0}\right) \cdot \sqrt{\frac{v_f}{v_0}} = E e^{-ik_3 z_2} + F e^{ik_3 z_2},$$

$$\frac{C\beta}{2v_f} \sqrt{\frac{v_f}{v_0}} + \frac{D\beta}{v_f} \left(1 + \ln \sqrt{\frac{v_f}{v_0}}\right) \sqrt{\frac{v_f}{v_0}} = -ik_3 E e^{-ik_3 z_2} + ik_3 F e^{ik_3 z_2},$$

$$E e^{-ik_3 z_3} + F e^{ik_3 z_3} = G e^{-ik_4 z_3},$$

$$-ik_3 E e^{-ik_3 z_3} + ik_3 F e^{ik_3 z_3} = -ik_4 G e^{-ik_4 z_3}. \quad (2-28)$$

Case III:

$$A e^{-ik_1 z_1} + B e^{ik_1 z_1} = C e^{(1-i\gamma) \ln \sqrt{\frac{v_s}{v_0}}} + D e^{(1+i\gamma) \ln \sqrt{\frac{v_s}{v_0}}},$$

$$-ik_1 A e^{-ik_1 z_1} + ik_1 B e^{ik_1 z_1} = \frac{\beta(1-i\gamma)}{2v_s} C e^{(1-i\gamma) \ln \sqrt{\frac{v_s}{v_0}}} + \frac{\beta(1+i\gamma)}{2v_s} D e^{(1+i\gamma) \ln \sqrt{\frac{v_s}{v_0}}},$$

$$C e^{(1-i\gamma) \ln \sqrt{\frac{v_f}{v_0}}} + D e^{(1+i\gamma) \ln \sqrt{\frac{v_f}{v_0}}} = E e^{-ik_3 z_2} + F e^{ik_3 z_2},$$

$$\frac{\beta(1-i\gamma)}{2v_f} C e^{(1-i\gamma) \ln \sqrt{\frac{v_f}{v_0}}} + \frac{\beta(1+i\gamma)}{2v_f} D e^{(1+i\gamma) \ln \sqrt{\frac{v_f}{v_0}}} = -ik_3 E e^{-ik_3 z_2} + ik_3 F e^{ik_3 z_2},$$

$$E e^{-ik_3 z_3} + F e^{ik_3 z_3} = G e^{-ik_4 z_3},$$

$$-ik_3Ee^{-ik_3z_3} + ik_3Fe^{ik_3z_3} = -ik_4Ge^{-ik_4z_3} \quad (2-29)$$

In these: A is the incident pressure pulse amplitude in layer 1,
B is the complete upward radiation in layer 1,
C is the complete downward radiation in layer 2,
D is the complete upward radiation in layer 2,
E is the complete downward radiation in layer 3,
F is the complete upward radiation in layer 3,
and finally,

G is the transmitted pulse amplitude in layer 4.

The purpose here is to solve these equations analytically for the reflected pulse from the second and third layer into the first layer and the transmitted pulse out of the second and third layer into the fourth. The solution is obtained simply by inverting the coefficient matrix of the set of equations after some detailed algebra for each case. Here the convenient notation introduced in table 2-1 continues to hold as before. We obtain the required analytical results as

$$\begin{aligned}
B e^{i k_1 z_1} = & \left[\frac{k_1 - k_{2s}}{k_1 + k_{2s}} + \frac{\left(\frac{2k_1}{k_1 + k_{2s}} \right) \left(\frac{\bar{k}_{2s} + k_{2s}}{k_1 + k_{2s}} \right) \left\{ \left(\frac{\bar{k}_{2f} - k_3}{k_{2f} + k_3} \right) \right.}{e^{\vartheta - \bar{\vartheta} + i 2 k_3 (z_3 - z_2)} - \left(\frac{k_3 - k_4}{k_3 + k_4} \right) \left(\frac{k_3 - k_{2f}}{k_3 + k_{2f}} \right)} \right. \\
& \frac{e^{-i 2 k_3 (z_3 - z_2)} - \left(\frac{\bar{k}_{2f} - k_3}{k_{2f} + k_3} \right) \left(\frac{k_3 - k_4}{k_3 + k_4} \right) \left(\frac{k_3 - k_{2f}}{k_3 + k_{2f}} \right) + \left(\frac{\bar{k}_{2f} + k_{2f}}{k_{2f} + k_3} \right)}{e^{\vartheta - \bar{\vartheta}} - \left(\frac{\bar{k}_{2s} - k_1}{k_{2s} + k_1} \right) \left\{ \left(\frac{\bar{k}_{2f} - k_3}{k_{2f} + k_3} \right) e^{i 2 k_3 (z_3 - z_2)} - \left(\frac{\bar{k}_{2f} - k_3}{k_{2f} + k_3} \right) \right.} \\
& \left. \left. \frac{\left(\frac{k_3 - k_4}{k_3 + k_4} \right) \left(\frac{2k_3}{k_{2f} + k_3} \right) \right\}}{\left(\frac{k_3 - k_4}{k_3 + k_4} \right) \left(\frac{k_3 - k_{2f}}{k_3 + k_{2f}} \right) + \left(\frac{\bar{k}_{2f} + k_{2f}}{k_3 + k_{2f}} \right) \left(\frac{k_3 - k_4}{k_3 + k_4} \right) \left(\frac{2k_3}{k_{2f} + k_3} \right) \right\} \right] \\
& \times A e^{-i k_1 z_1} \tag{2-30}
\end{aligned}$$

for the reflected pulse into layer 1, and

$$\begin{aligned}
G e^{-i k_4 z_3} = & \left[\frac{\left(\frac{\bar{k}_{2s} + k_{2s}}{k_1 + k_{2s}} \right) \left(\frac{2k_3}{k_{2f} + k_3} \right) \left(\frac{2k_4}{k_3 + k_4} \right) e^{\vartheta + i k_3 (z_3 - z_2)}}{e^{\vartheta - \bar{\vartheta} + i 2 k_3 (z_3 - z_2)} - \left(\frac{k_3 - k_4}{k_3 + k_4} \right) \left(\frac{k_3 - k_{2f}}{k_3 + k_{2f}} \right)} \right. \\
& \frac{e^{\vartheta - \bar{\vartheta}} - \left(\frac{\bar{k}_{2s} - k_1}{k_{2s} + k_1} \right) \left\{ \left(\frac{\bar{k}_{2f} - k_3}{k_{2f} + k_3} \right) e^{i 2 k_3 (z_3 - z_2)} - \left(\frac{\bar{k}_{2f} - k_3}{k_{2f} + k_3} \right) \right.}{\left. \left. \left(\frac{k_3 - k_4}{k_3 + k_4} \right) \left(\frac{k_3 - k_{2f}}{k_3 + k_{2f}} \right) + \left(\frac{\bar{k}_{2f} + k_{2f}}{k_3 + k_{2f}} \right) \left(\frac{k_3 - k_4}{k_3 + k_4} \right) \left(\frac{2k_3}{k_{2f} + k_3} \right) \right\}} \right] \\
& \times A e^{-i k_1 z_1} \tag{2-31}
\end{aligned}$$

for the transmitted pulse into layer 4.

Now we wish to show that these results can be obtained using the approach based upon the same special interpretation described in the previous three-layer model. To reiterate, we assume that the total reflected pulse from an interface is the resultant of the reflected part of the incident pulse on the interface from above and the transmitted part of whatever is incident on the interface from below. Further, the total transmitted pulse at an interface is the resultant of the reflected part of the pulse transmitted below and the transmitted part incident from below. Each constituent part of any pulse above is the pulse scaled by some function which will be named either reflection function or transmission function for the interface between each of the consecutive four layers. Using this approach, we define the following equations:

Case I:

$$Be^{ik_1z_1} = R_{12}Ae^{-ik_1z_1} + T_{21}De^{(1+\gamma)\ln\sqrt{\frac{v_s}{v_0}}},$$

$$Ce^{(1-\gamma)\ln\sqrt{\frac{v_s}{v_0}}} = T_{12}Ae^{-ik_1z_1} + R_{21}De^{(1+\gamma)\ln\sqrt{\frac{v_s}{v_0}}},$$

$$De^{(1+\gamma)\ln\sqrt{\frac{v_f}{v_0}}} = R_{23}Ce^{(1-\gamma)\ln\sqrt{\frac{v_f}{v_0}}} + T_{32}Fe^{ik_3z_2},$$

$$\begin{aligned}
Ee^{-ik_3z_2} &= T_{23}Ce^{(1-\gamma)\ln\sqrt{\frac{v_f}{v_0}}} + R_{32}Fe^{ik_3z_2}, \\
Fe^{ik_3z_3} &= R_{34}Ee^{-ik_3z_3}, \\
Ge^{-ik_4z_3} &= T_{34}Ee^{-ik_3z_3}
\end{aligned} \tag{2-32}$$

Case II:

$$\begin{aligned}
Be^{ik_1z_1} &= R_{12}Ae^{-ik_1z_1} + T_{21}D\ln\frac{v_s}{v_0} \cdot \sqrt{\frac{v_s}{v_0}}, \\
C\sqrt{\frac{v_s}{v_0}} &= T_{12}Ae^{-ik_1z_1} + R_{21}D\ln\frac{v_s}{v_0} \cdot \sqrt{\frac{v_s}{v_0}}, \\
D\ln\frac{v_f}{v_0} \cdot \sqrt{\frac{v_f}{v_0}} &= R_{23}C\sqrt{\frac{v_f}{v_0}} + T_{32}Fe^{ik_3z_2}, \\
Ee^{-ik_3z_2} &= T_{23}C\sqrt{\frac{v_f}{v_0}} + R_{32}Fe^{ik_3z_2}, \\
Fe^{ik_3z_3} &= R_{34}Ee^{-ik_3z_3}, \\
Ge^{-ik_4z_3} &= T_{34}Ee^{-ik_3z_3},
\end{aligned} \tag{2-33}$$

Case III:

$$\begin{aligned}
Be^{ik_1z_1} &= R_{12}Ae^{-ik_1z_1} + T_{21}De^{(1+i\gamma)\ln\sqrt{\frac{v_s}{v_0}}}, \\
Ce^{(1-i\gamma)\ln\sqrt{\frac{v_s}{v_0}}} &= T_{12}Ae^{-ik_1z_1} + R_{21}De^{(1+i\gamma)\ln\sqrt{\frac{v_s}{v_0}}},
\end{aligned}$$

$$D e^{(1+i\gamma) \ln \sqrt{\frac{v_f}{v_0}}} = R_{23} C e^{(1-i\gamma) \ln \sqrt{\frac{v_f}{v_0}}} + T_{32} F e^{ik_3 z_2} ,$$

$$E e^{-ik_3 z_2} = T_{23} C e^{(1-i\gamma) \ln \sqrt{\frac{v_f}{v_0}}} + R_{32} F e^{ik_3 z_2} ,$$

$$F e^{ik_3 z_3} = R_{34} E e^{-ik_3 z_3} ,$$

$$G e^{-ik_4 z_3} = T_{34} E e^{-ik_3 z_3} , \quad (2-34)$$

Making use of the definitions in table 2-1, the solutions from this approach, valid for the three cases, are given by

The Reflected Pulse:

$$B e^{ik_1 z_1} = \left[R_{12} + \frac{T_{21} T_{12} (R_{23} e^{i2k_3(z_3-z_2)} - R_{23} R_{34} R_{32} + T_{32} R_{34} T_{23})}{e^{\sigma-\tilde{\sigma}} + i2k_3(z_3-z_2) - R_{34} R_{32} e^{\sigma-\tilde{\sigma}}} \right] \cdot A e^{-ik_1 z_1}$$

(2-35)

and

The Transmitted Pulse:

$$Ge^{-ik_4z_3} = \left[\frac{T_{12}T_{23}T_{34}e^{\vartheta + ik_3(z_3-z_2)}}{e^{\vartheta-\tilde{\vartheta}} + i2k_3(z_3-z_2) - R_{34}R_{32}e^{\vartheta-\tilde{\vartheta}}} \right. \\ \left. \dots \frac{1}{R_{21} (R_{23}e^{i2k_3(z_3-z_2)} - R_{23}R_{34}R_{32} + T_{32}R_{34}T_{23})} \right] \cdot Ae^{-ik_1z_1} \quad (2-36)$$

where

T_{ij} = transmission factor

and

R_{ij} = reflected factor.

Reflection Coefficient: We have already discussed the reflection coefficient of acoustic waves from an abrupt impedance contrast and from a linearly varying velocity transition zone in the previous three layer-model. In the four-layer model we need to use the same definitions (2-22) (2-23) in addition to the following

$$R_{32} = \frac{k_3 - k_{2f}}{k_3 + k_{2f}} \quad (2-37)$$

and

$$R_{34} = \frac{k_3 - k_4}{k_3 + k_4} \quad (2-38)$$

where the notation, again is exactly as shown in table 2-1. Here R_{32} is the reflectivity function at the interface between the uniform layer 3 and the transition zone 2 and R_{34} is the reflectivity factor at the interface between the discrete layer 3 and the discrete layer 4.

Transmission Coefficient: Whatever has been said about the reflection coefficient above can also be applied to the transmission coefficient for the four-layer model. We need to use the definitions (2-25) and (2-26) and the following

$$T_{32} = \frac{\bar{k}_{2f} + k_{2f}}{k_3 + k_{2f}} \quad (2-39)$$

and

$$T_{34} = \frac{2k_4}{k_3 + k_4} \quad (2-40)$$

Here T_{32} is the transmissivity function at the interface between the transition zone 2 and the discrete layer 3 and T_{34} is the transmissivity function between the uniform layer 3 and the uniform layer 4 as in our four-layer model.

3. NUMERICAL IMPLEMENTATION

In the previous chapter we have obtained analytical expressions for the reflected and transmitted response in the frequency domain. These relations are the basis for obtaining the corresponding responses in the time domain. Thus we can predict the synthetic seismograms for any model containing a transition zone. For this purpose we implemented a series of subroutines in Fortran 77 on the Vax-11 in order to evaluate numerically the time responses of the reflected and transmitted pulses from the three and the four layer models for which we developed the analytical expressions.

So far we have been using a monofrequency incident wave of the type $A(\omega)e^{i\omega t}$. This allows us to evaluate the responses using any other type of incident time function via Fourier synthesis. We implemented the numerical calculation of responses using an impulsive time source and an artificially time-limited form of the well-known Ricker wavelet source. The Ricker wavelet source pulse used in our implementation is shown in figures 3-1 and 3-2. The expressions are

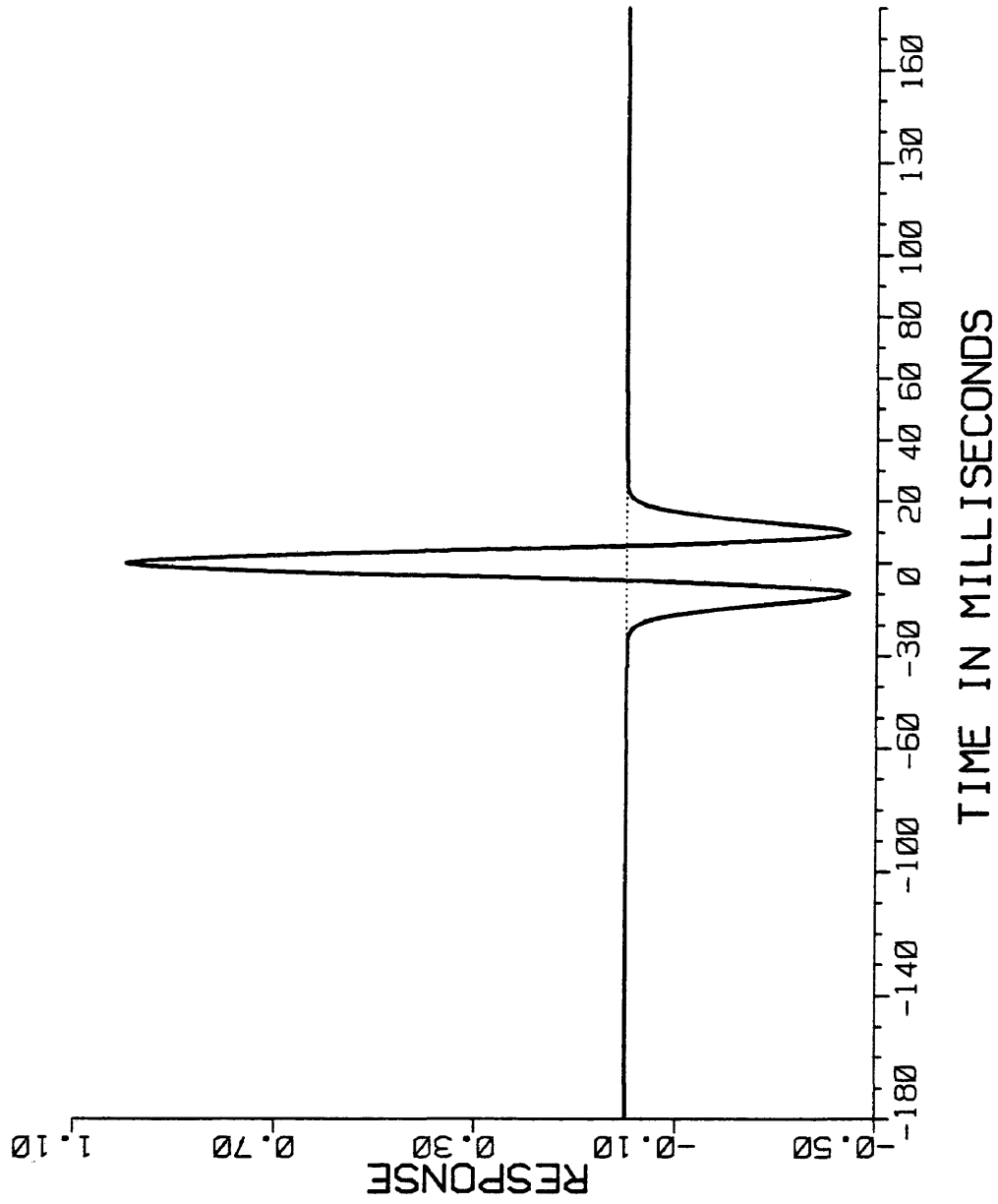


FIGURE 3-1:RICKER WAVELET

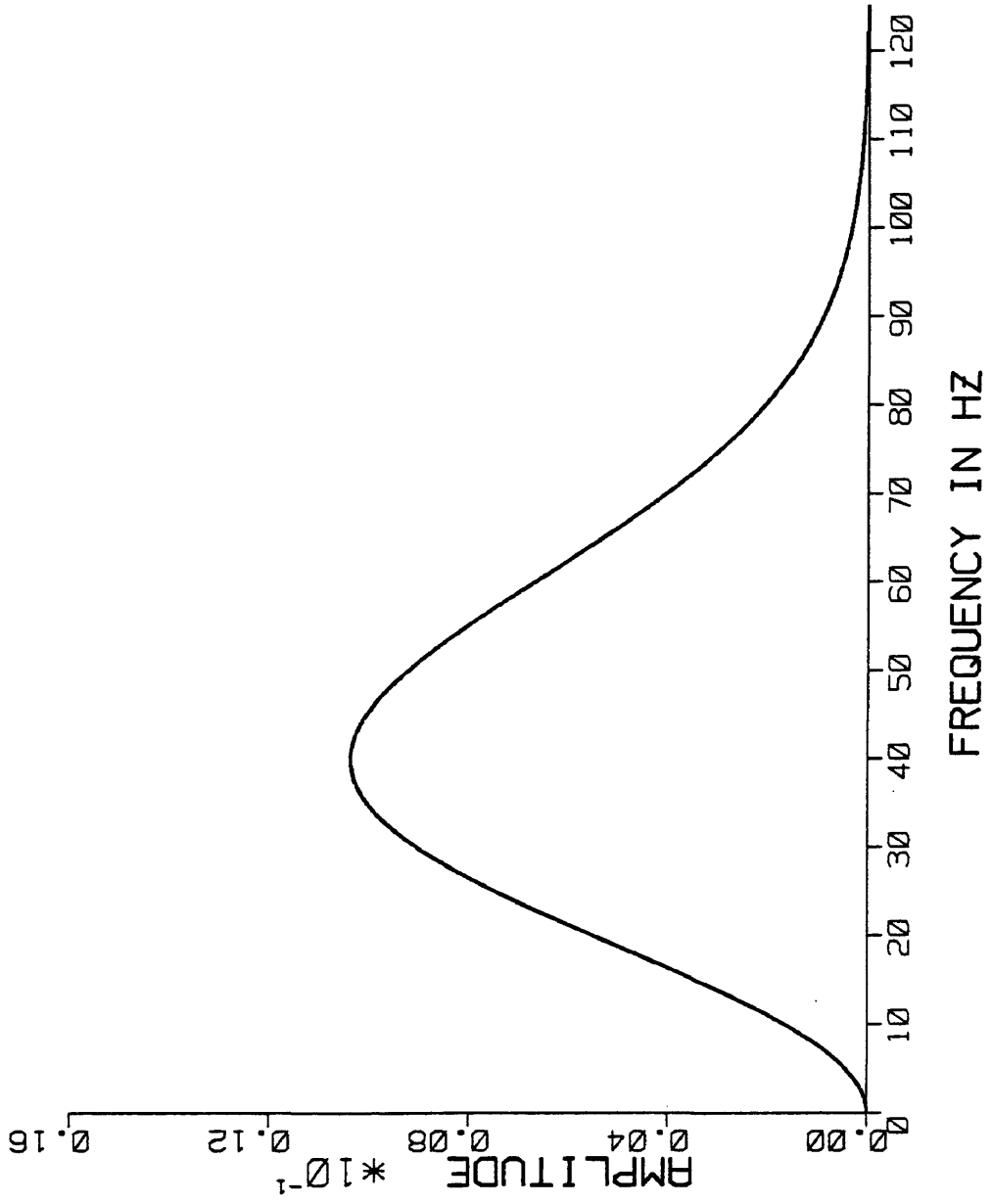


FIGURE 3-2:RICKER WAVELET SPECTRUM

$$F(t) = (1 - 2\pi^2 v_m^2 t^2) e^{-\pi^2 v_m^2 t^2} \quad (3-1)$$

in the time domain, and

$$\bar{F}(v) = \frac{2}{\sqrt{\pi}} \frac{v^2}{v_m^3} e^{-v^2/v_m^2} \quad (3-2)$$

in the frequency domain. Here v_m is the peak frequency in the wavelet, which we fixed at around 40 Hz for our calculations.

We implemented a variety of options in our program package which permits calculations of the time and frequency domain representations of all desired quantities of interest. We also allowed for user specified time sampling rates and used a standard FFT subroutine and multiplications of spectra rather than discrete time convolution. A complete program listing appears in the appendix B.

Another task for the program is to find the reflection response of the same three and four-layer model based upon the conventional reflectivity model. Starting with the given velocity function

$$v(z) = v_0 + \beta(z-z_0) , \quad (3-3)$$

we calculate the travel time as a function of depth to be

$$\begin{aligned}
 t(z) &\equiv t_0 + \int_{z_0}^z \frac{dz}{v(z)} \\
 &= t_0 + \frac{1}{\beta} \ln \left| 1 + \frac{\beta}{v_0} (z-z_0) \right| .
 \end{aligned} \tag{3-4}$$

After some algebra, we find the velocity as a function of time as

$$v(t) = v_0 e^{\beta(t-t_0)} . \tag{3-5}$$

This yields the one-way time width for the transition zone as

$$T = \frac{1}{\beta} \ln \frac{v_f}{v_s} \tag{3-6}$$

in terms of the velocity gradient β in the transition zone and the ratio of the final and the starting velocities v_s and v_f in the zone.

As is well known, Peterson et al (1955), the convolutional model reflectivity for constant ρ

$$R(t) = \frac{1}{2} \frac{d}{dt} \ln v(t) . \tag{3-7}$$

Substituting (3-5) in (3-7) we obtain the time domain reflectivity function for a transition zone to be

$$R(t) = \frac{\beta}{2} \quad t_s < t < t_f, \quad (3-8)$$

which is simply a time domain box car function for the zone. As we shall see in the following, the actual wave-theoretic reflection response in the time domain response is, in principle, quite different even for this simple linear velocity variation.

4. NUMERICAL RESULTS

The numerical results presented and discussed in this chapter were calculated in the frequency domain. All time responses were calculated through a discrete fast Fourier transform after experimenting with suitable time sampling rates and record lengths as appropriate for the four models considered here. These include a theoretical model, a realistic practical model, and two models derived from offshore Arabian Gulf velocity logs, one of which represents a soft sea floor and the other a hard sea floor. Analytical results given in previous chapters are directly applicable and form the basis for these numerical results. The conventional responses of the transition zones are scaled to the number of samples in the zones.

A Theoretical Model

For the purpose of a deeper analytical study, we start with the presentation of the numerical results for an exaggerated theoretical model. While being aware that this model would be of no practical use in actual seismic modeling, it has been designed for analytical purposes of

demonstrating the reflection and transmission functions clearly. Therefore we consider a three layer case which includes a linearly varying velocity layer between two constant velocity half spaces. In the transition layer the velocity gradient is 31.73 ft/sec/ft which is quite reasonable practically, but the ratio of the final velocity to the starting velocity is 5712.4 which is impractical. The upper half space constant (water) velocity is 5000 ft/sec to the top of the transition layer and the lower half space constant velocity is, therefore, 2.856×10^7 ft/sec reached linearly at the bottom of the transition layer. This data set and all others in the following start with table 4-1 which lists all of the particular model and calculation parameters in a simple format.

The reflection impulse response from the top and the bottom of this exaggerated linearly varying velocity layer is shown in figure 4-1. The reflection Ricker-wavelet response is shown in figure 4-2. The wave-theoretic reflection impulse response is superimposed on the conventional response in figure 4-3. The wave-theoretic reflection Ricker response of a transition layer is compared to the conventional reflection Ricker response, as shown in figure 4-4. Recalling the conventional manner of defining the reflectivity function, equation (3-7) and (3-8), the

reflectivity is a step function at the onset of the transition zones and a step function of equal amplitude and opposite polarity at the base of the transition zone. This produces a rectangular reflectivity function. The transmission impulse and Ricker responses into the lower half space through the transition layer are shown in figures 4-5 and 4-6. The conventional reflectivity model transmission responses would simply be the incident impulse or Ricker without change.

We next show our wave theoretic reflection and transmission functions R_{12} , R_{23} , T_{12} , T_{23} from an alternative approach. Before we do that, let us review briefly the principles of this alternative approach along a line of reasoning similar to the one just described for the conventional reflectivity modeling.

We analyze the problem, however, by using basic wave theoretic principles. First we define the reflection and the transmission functions between a constant velocity half space and the start of an infinite transition half space as R_{12} and T_{12} . Then we define similar reflection and transmission functions between the termination of an infinite transition zone and a constant velocity half space as R_{23} and T_{23} .

Comparison of equations obtained by the two approaches suggested in Chapter 2 of this thesis, namely equation (2-14) with (2-19), (2-30) with (2-35), (2-15) with (2-20) and (2-31) with (2-36) suggests the following definitions

$$R_{12} = \frac{k_1 - k_{2s}}{k_1 + k_{2s}}, \quad R_{21} = \frac{\tilde{k}_{2s} - k_1}{k_{2s} + k_1},$$

$$R_{23} = \frac{\tilde{k}_{2f} - k_3}{k_{2f} + k_3}, \quad R_{32} = \frac{k_3 - k_{2f}}{k_3 + k_{2f}}$$

for the possible reflection functions and

$$T_{12} = \frac{\tilde{k}_{2s} + k_{2s}}{k_1 + k_{2s}}, \quad T_{21} = \frac{2k_1}{k_1 + k_{2s}},$$

$$T_{23} = \frac{2k_3}{k_{2f} + k_3}, \quad T_{32} = \frac{\tilde{k}_{2f} + k_{2f}}{k_{2f} + k_3}$$

for the possible transmission functions. Recall that these are all frequency domain representations for our definitions from which we generated time responses. We first show time domain representation for direct comparison with the conventional reflectivity modeling results. Our reflection function R_{12} is shown in figure 4-7 compared with the conventional reflectivity step response (the amplitude of the

step is not to scale). Similarly figure 4-8 shows our reflection function R_{23} compared with the conventional reflectivity negative step response. These figures show clearly the fundamentally incorrect and asymptotically (for large times) absurd behavior of the conventional reflectivity modeling scheme in comparison to the actual wave theoretic responses R_{12} and R_{23} for such cases. While this will be discussed further later on, for the present we continue with figures 4-9 and 4-10 which show our transmission functions T_{12} and T_{23} time-domain representations for similar times. We remark here that the conventional reflectivity modeling transmission responses in these cases would again be just the incident impulses without any change. The actual wave theoretic responses show significant detail as the incident impulse propagates through the transition zone. We conclude this discussion of the numerical results for the exaggerated theoretical model with figures 4-11 through 4-18 which show the frequency domain amplitude and phase spectra pairs for each of the just discussed four functions R_{12} , R_{23} , T_{12} , and T_{23} in that order. These are all piece-wise continuous bounded functions of the frequency with characteristic individual initial and asymptotic behaviors.

Table 4-1

A Theoretic Model For Basic Analytical Results

Region 1: Upper Half Space	Constant Velocity	5000 fps
	Bottom Depth	100 ft
Region 2: Transition Layer	Starting Velocity	5000 fps
	Ending Velocity	28562000 fps
	Bottom Depth	900100 ft
	Layer Thickness	900000 ft
	Velocity Gradient	31.73 fpspf
	Velocity Ratio	5712.40
Region 3: Reflector Layer	Constant Velocity	28562000 fps
	Bottom Depth	900100 ft
	Layer Thickness	0 ft
Region 4: Lower Half Space	Constant Velocity	28562000 fps
Time Sampling	: 4 ms;	Frequency Sampling : 0.244 Hz
Record Length	: 4092 ms;	Nyquist Frequency : 125 Hz
z0=0	- - - - Datum Upper Half Space - - - - - - - - - - - - - - - -	
	Constant Velocity	= 5000
	Datum to Bottom	= 100 ft; 40 ms
z1=100	- - - Starting Velocity = 5000 - - - - - - - - - - -	
	Layer Thickness	= 900000 ft; 545 ms
z2=900100	- Ending Velocity = 28562000 - - - - - - - - - - -	
	Constant Velocity	= 28562000
	Layer Thickness	= 0
z3=900100	- Start of Lower Half Space - - - - - - - - - - -	
	Constant Velocity	= 28562000

THEORETICAL MODEL

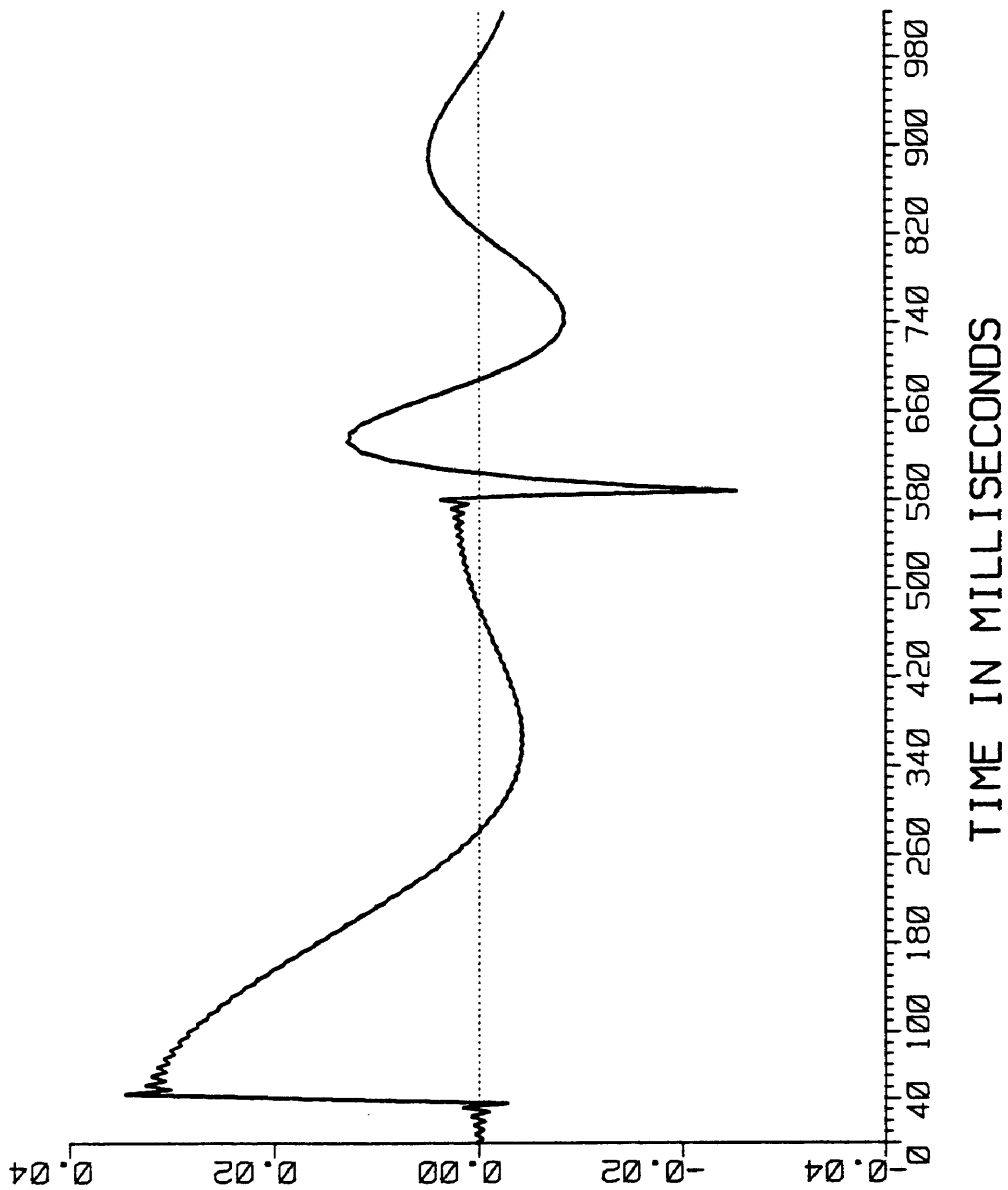
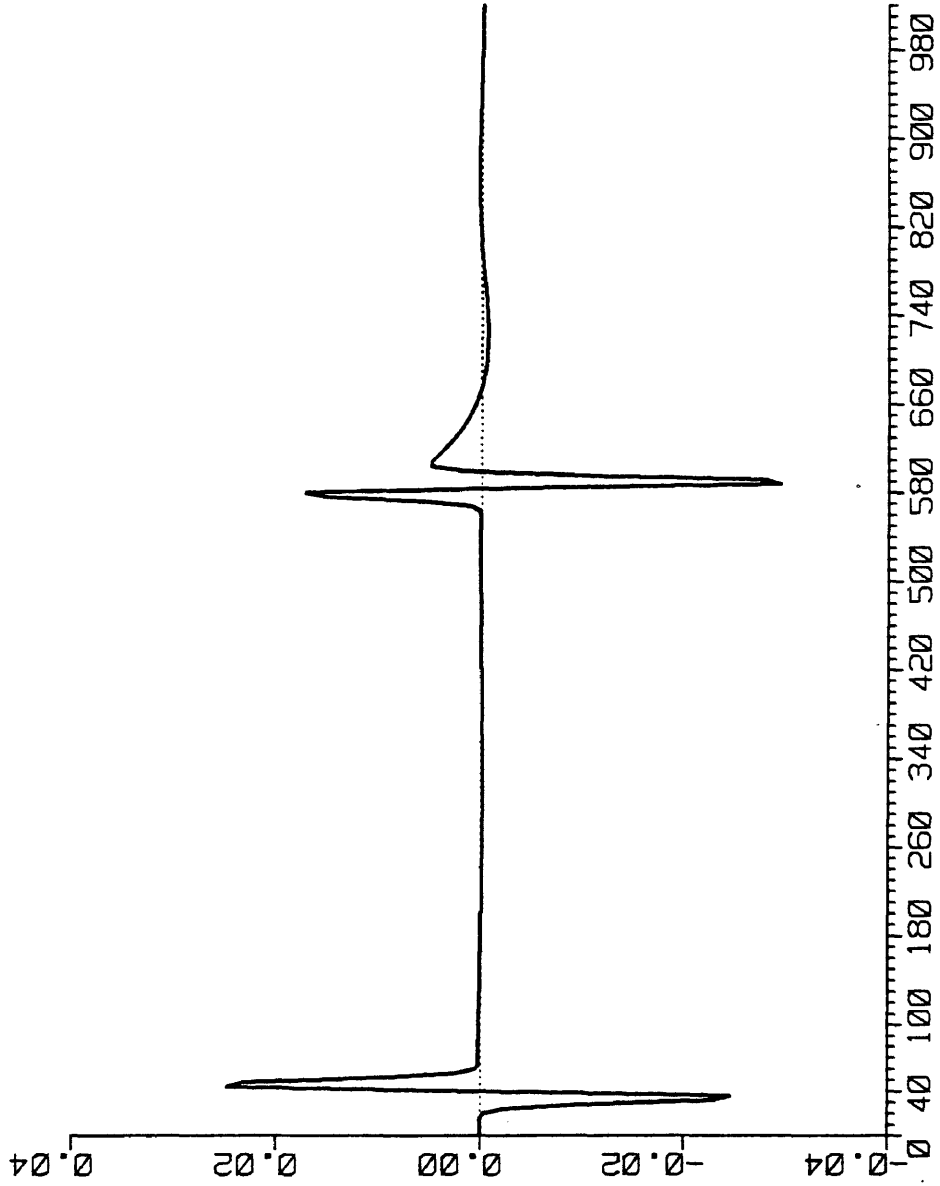


FIGURE 4-1: REFLECTION IMPULSE RESPONSE

THEORETICAL MODEL



TIME IN MILLISECONDS

FIGURE 4-2: REFLECTION RICKER RESPONSE

THEORETICAL MODEL

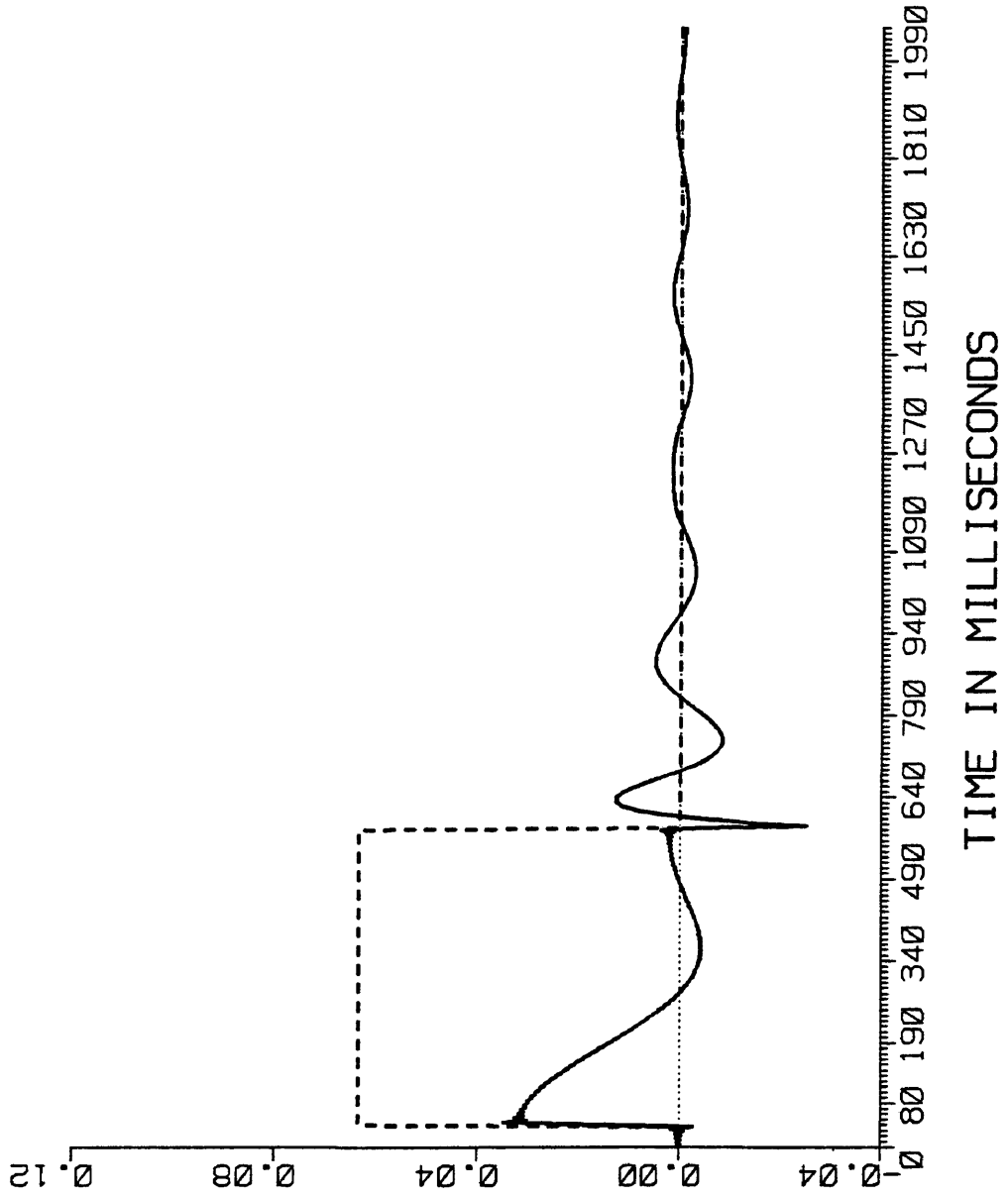


FIGURE 4-3: REFLECTION IMPULSE RESPONSE
WAVE THEORETIC (SOLID) VS. CONVENTIONAL REFLECTIVITY (DASHED)

THEORETICAL MODEL

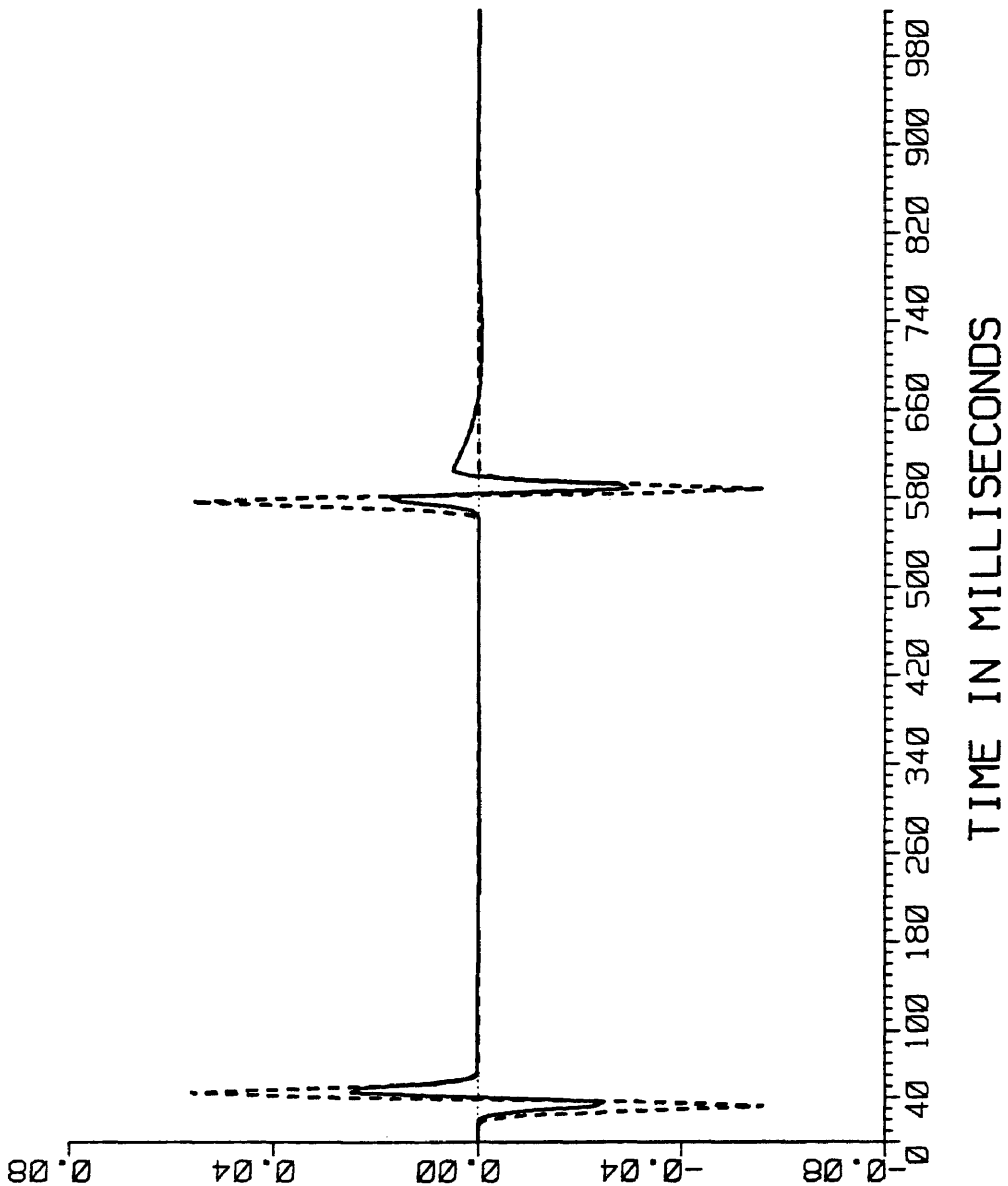


FIGURE 4-4: REFLECTION RICKER RESPONSES
WAVE THEORETIC (SOLID) VS. CONVENTIONAL REFLECTIVITY (DSHED)

THEORETICAL MODEL

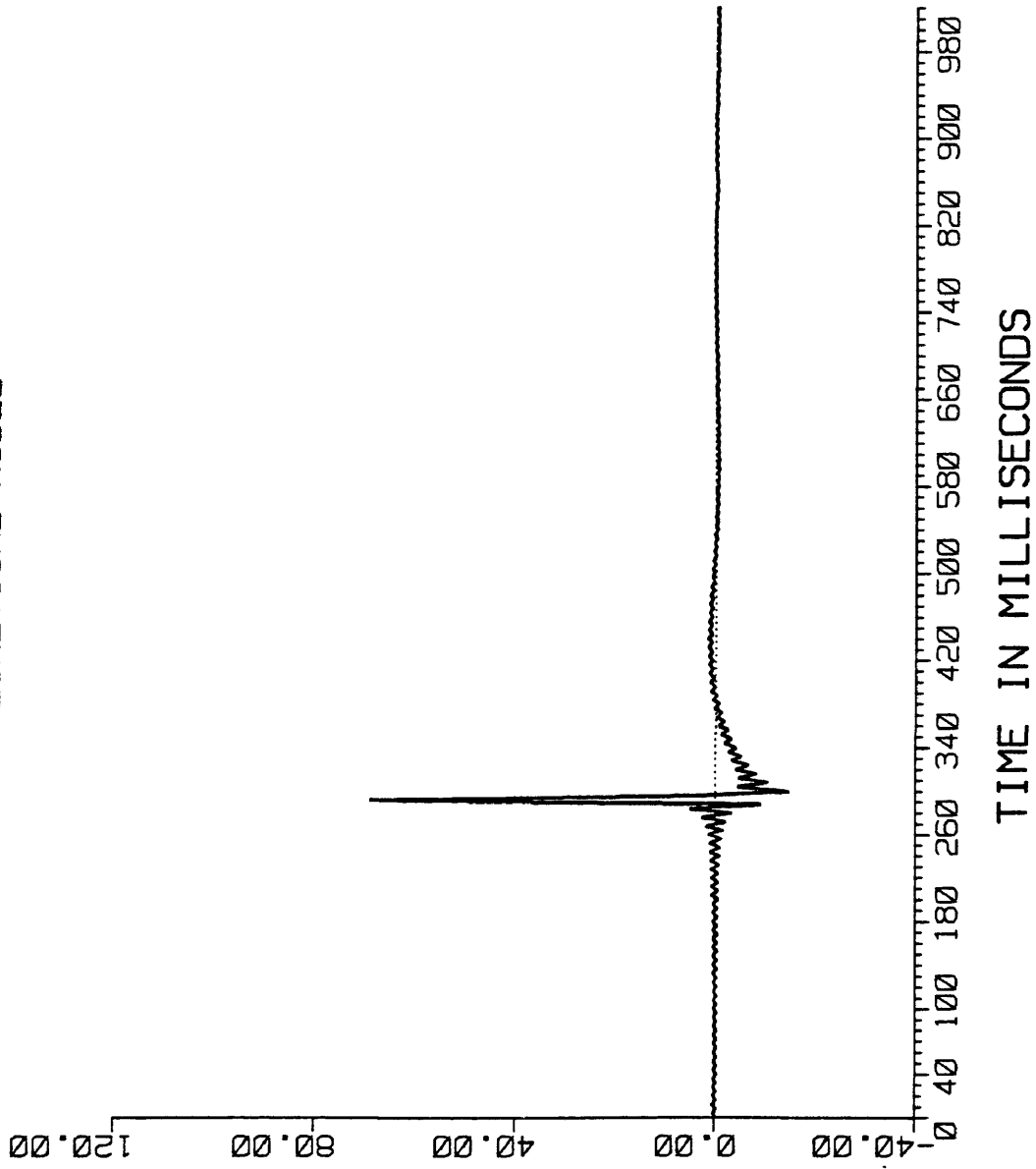


FIGURE 4-5: TRANSMISSION IMPULSE RESPONSE

THEORETICAL MODEL

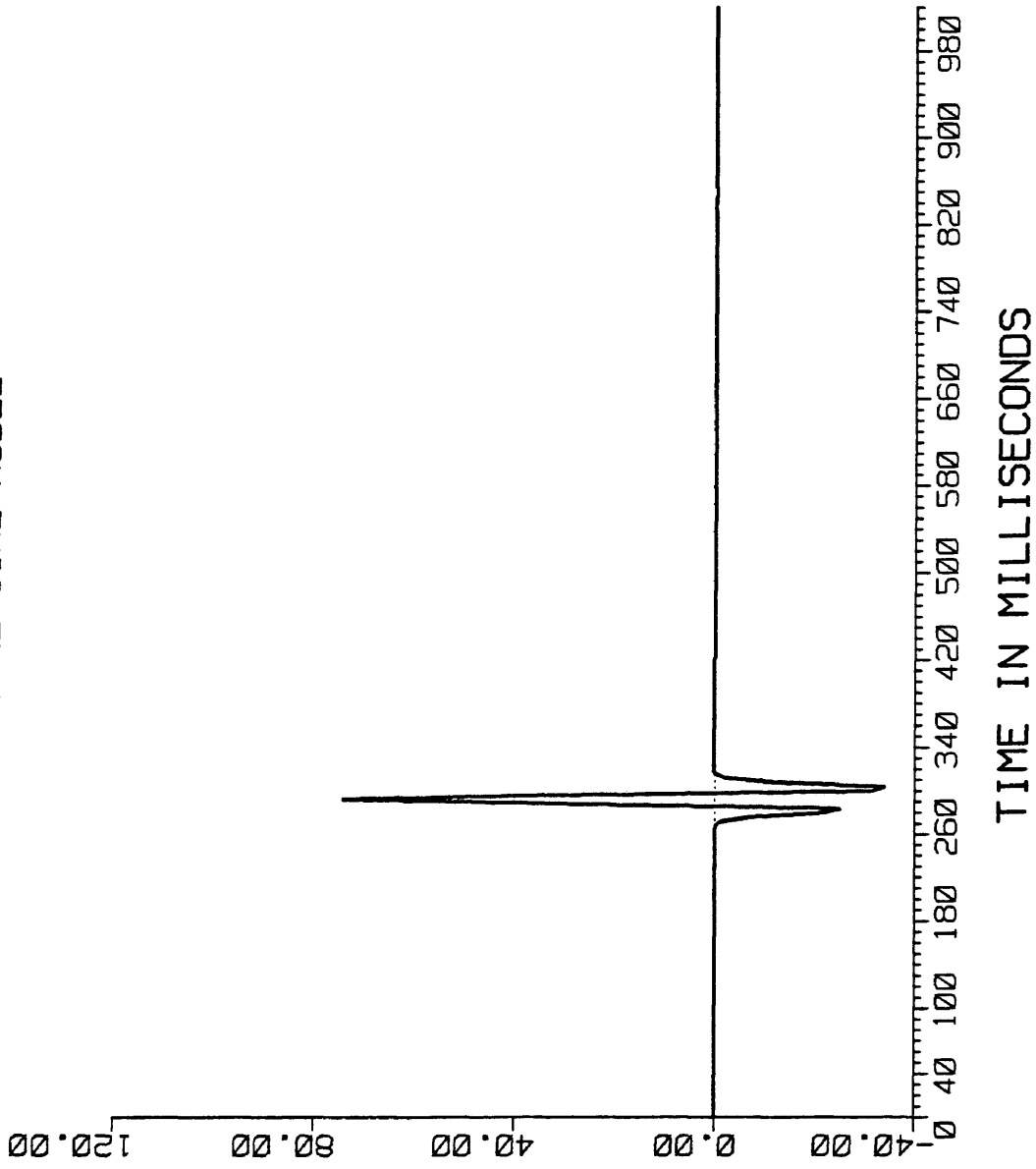


FIGURE 4-6: TRANSMISSION RICKER RESPONSE

THEORETICAL MODEL

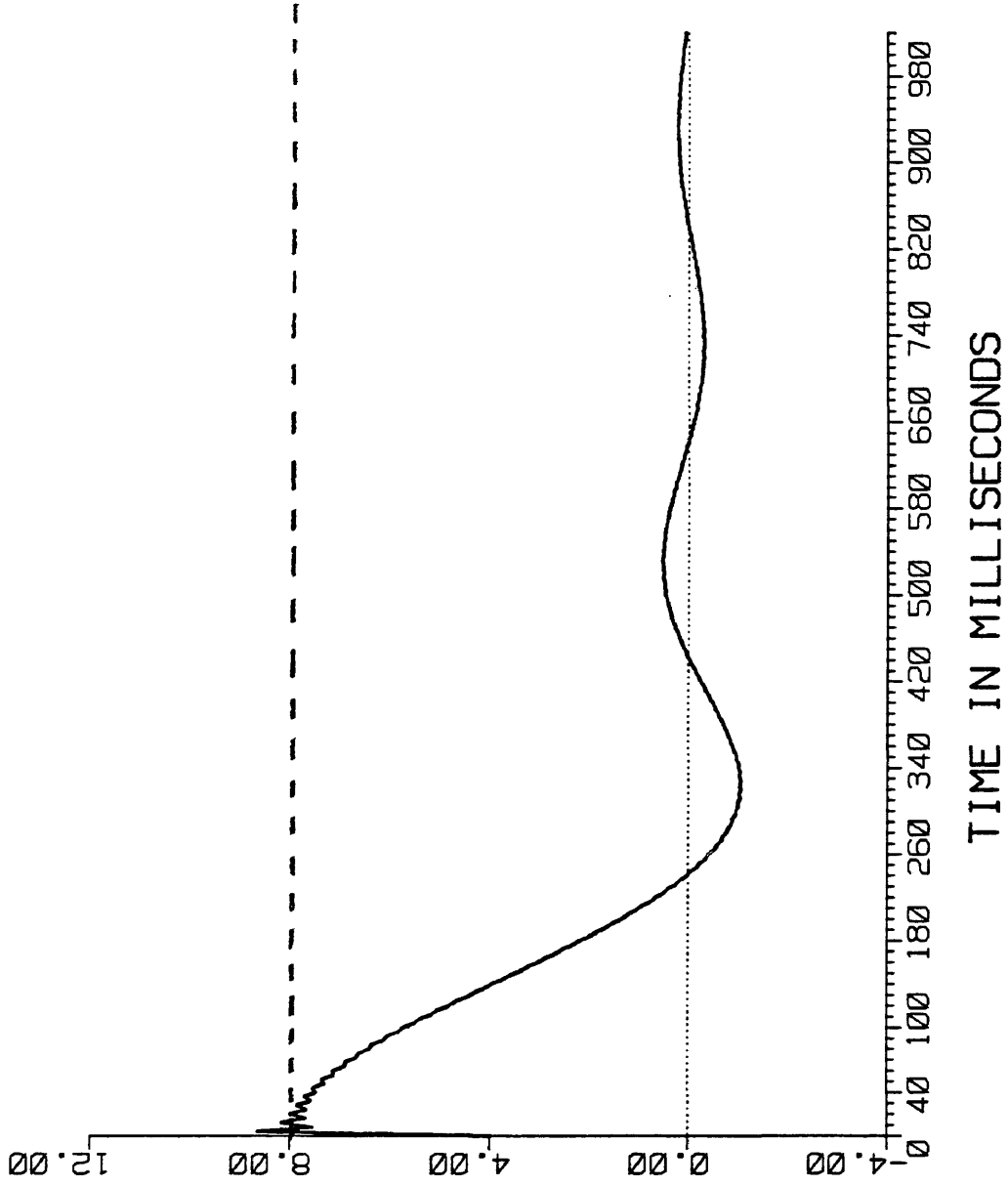


FIGURE 4-7: REFLECTION FUNCTION R12
WAVE THEORETIC (SOLID) VS. CONVENTIONAL REFLECTIVITY (DASHED)

THEORETICAL MODEL

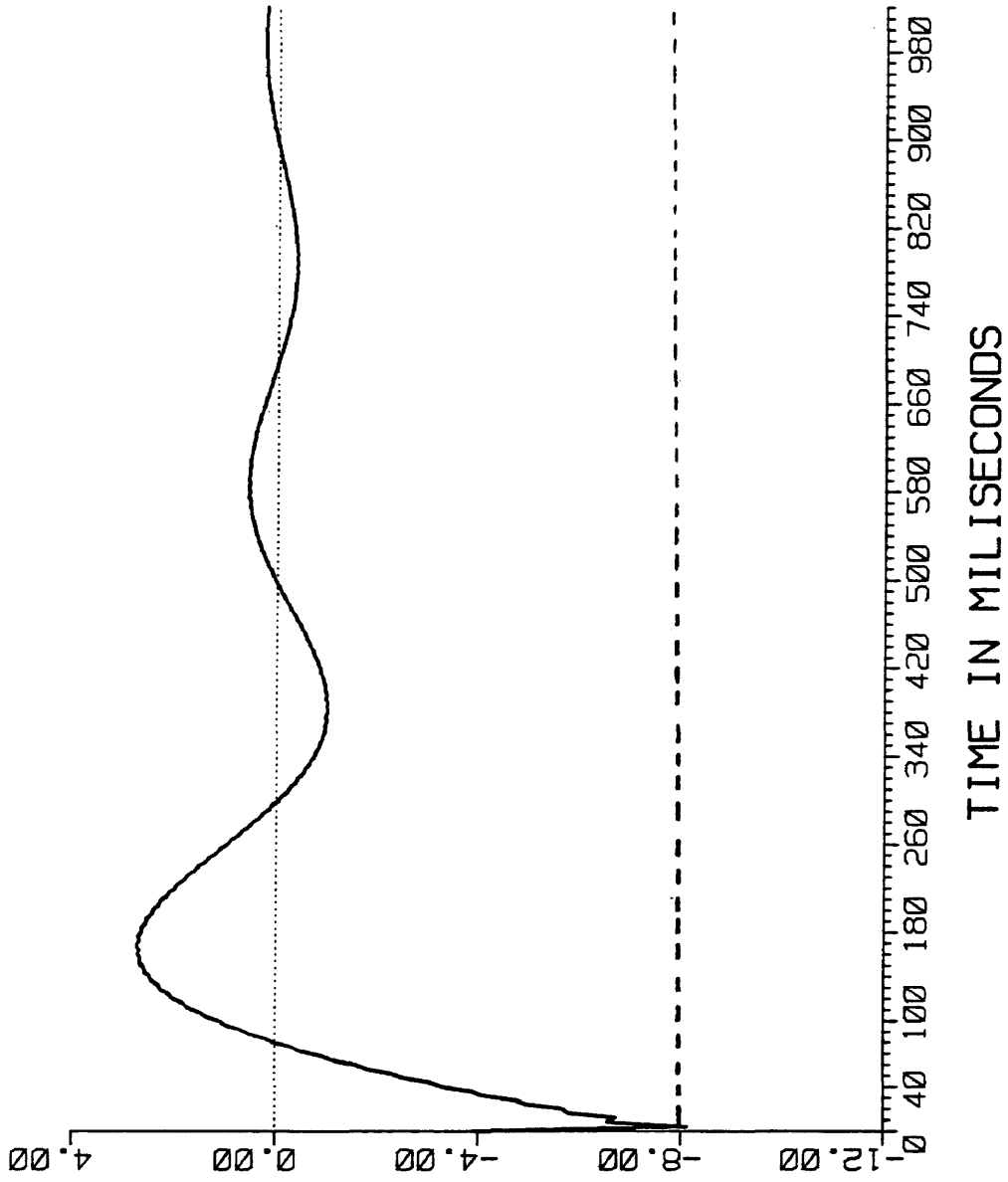


FIGURE 4-8: REFLECTION FUNCTION R23
WAVE THEORETIC (SOLID) VS. CONVENTIONAL REFLECTIVITY (DASHED)

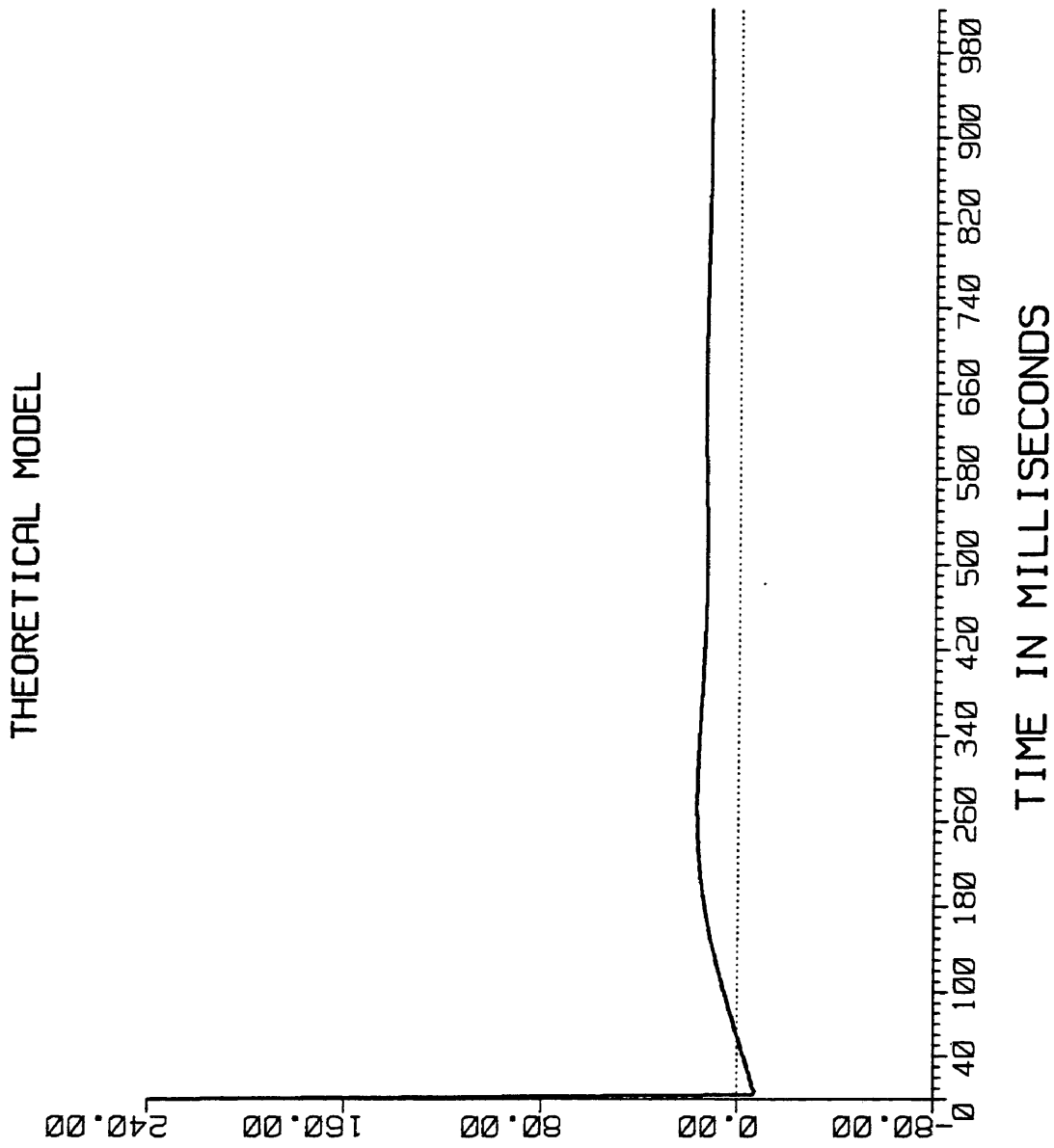


FIGURE 4-9: TRANSMISSION FUNCTION T12

THEORETICAL MODEL

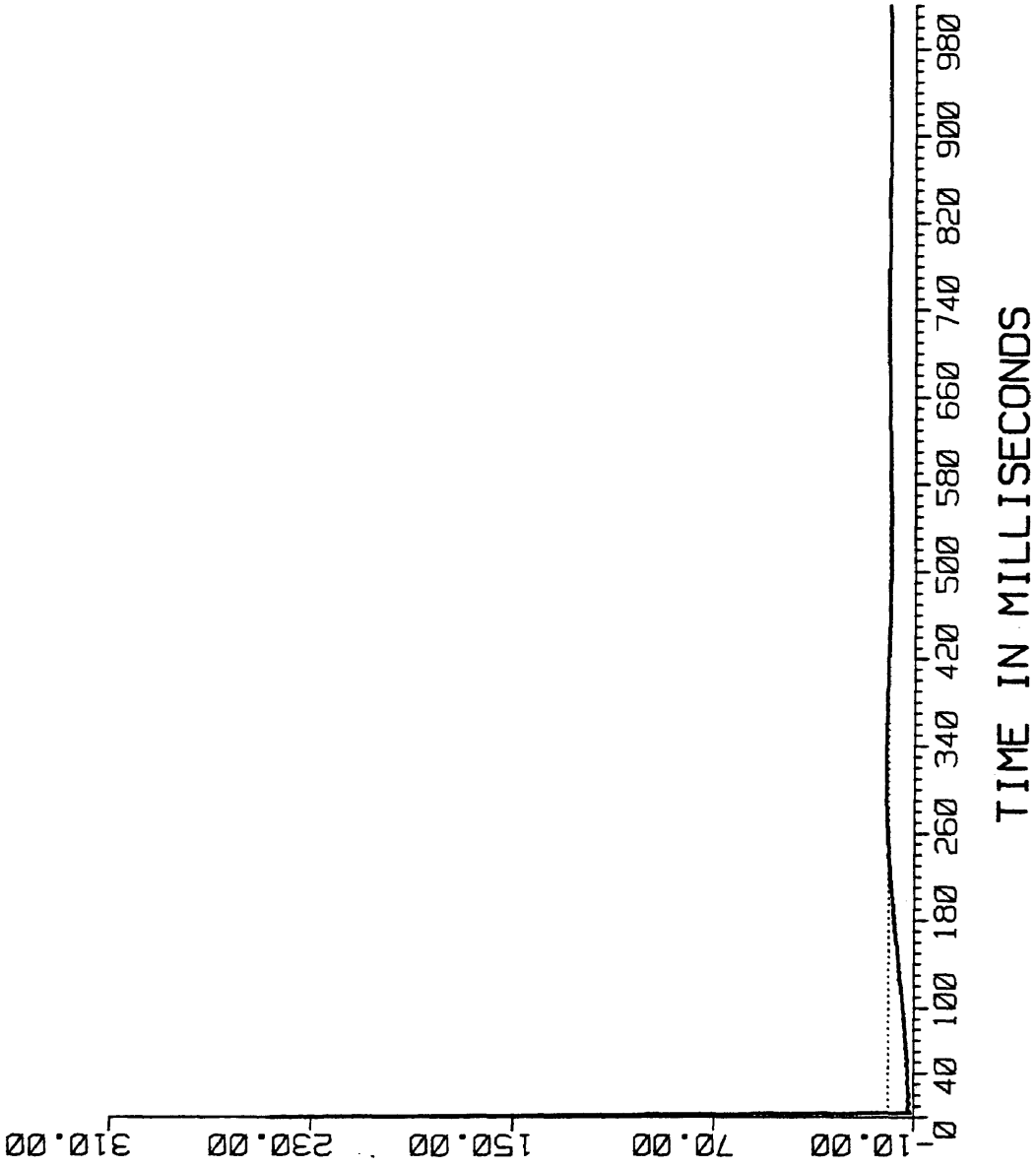


FIGURE 4-10: TRANSMISSION FUNCTION T23

THEORETICAL MODEL

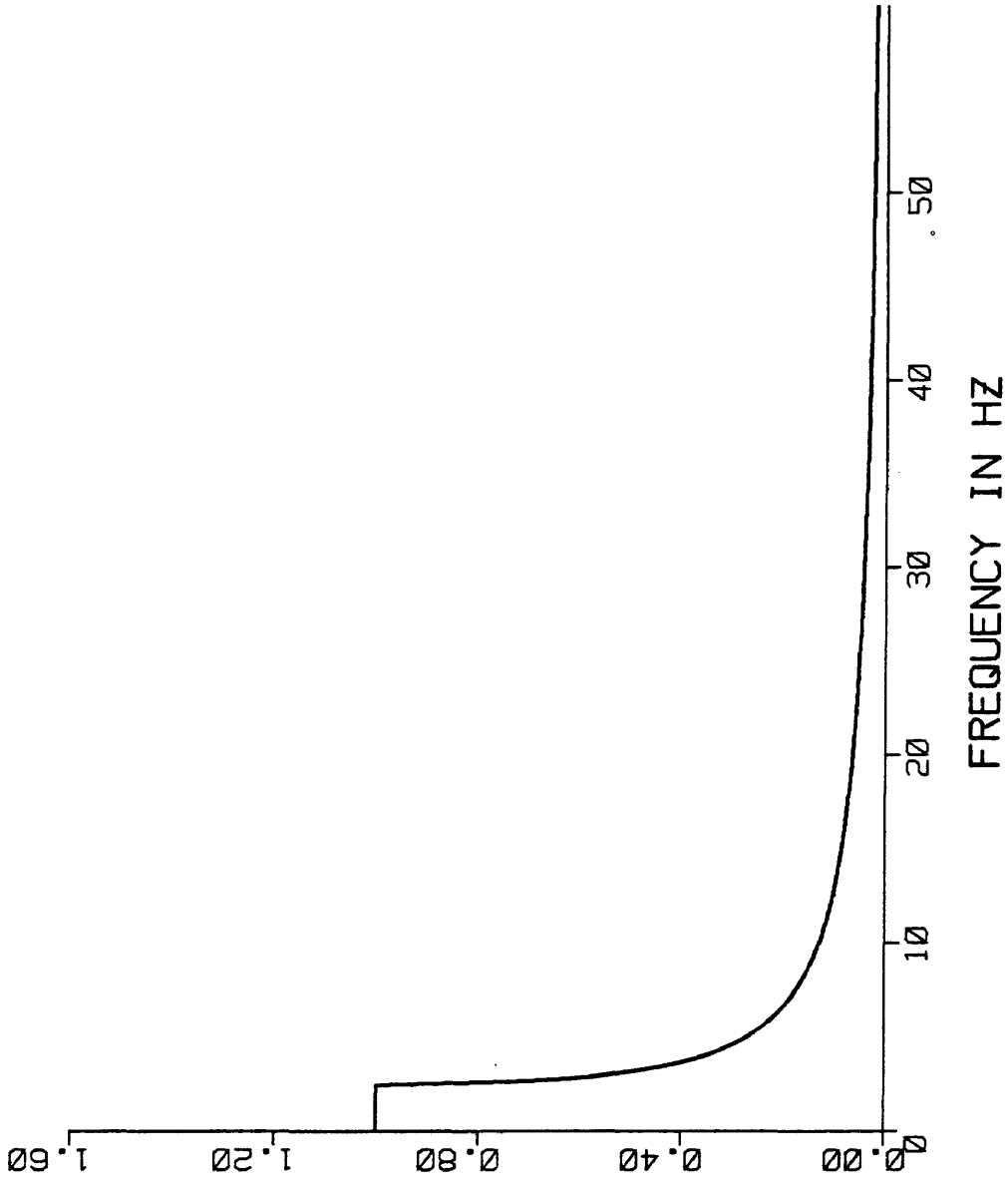


FIGURE 4-11: AMPLITUDE SPECTRUM OF REFLECTION FUNCTION R12

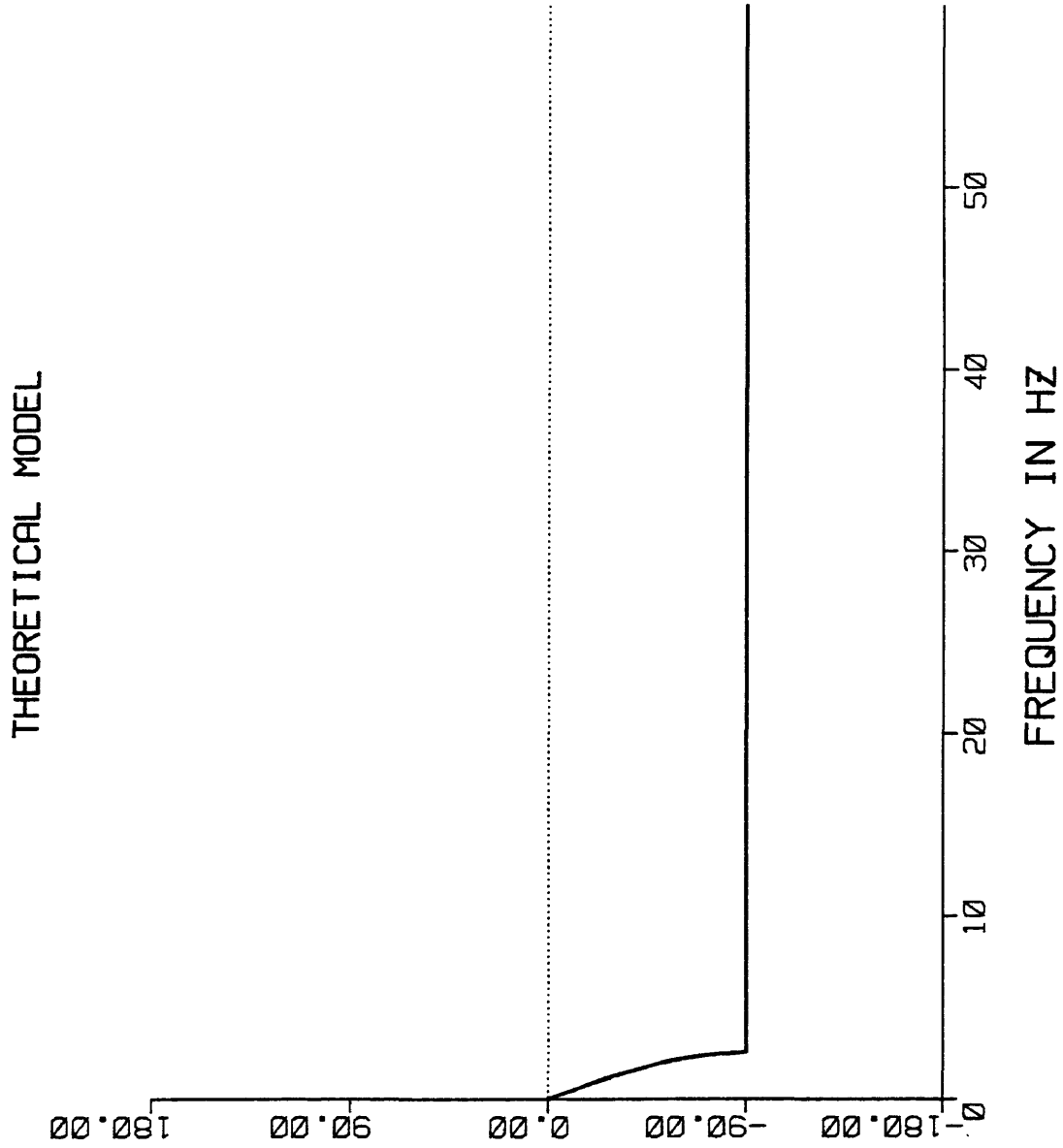


FIGURE 4-12: PHASE SPECTRUM OF REFLECTION FUNCTION R12

THEORETICAL MODEL

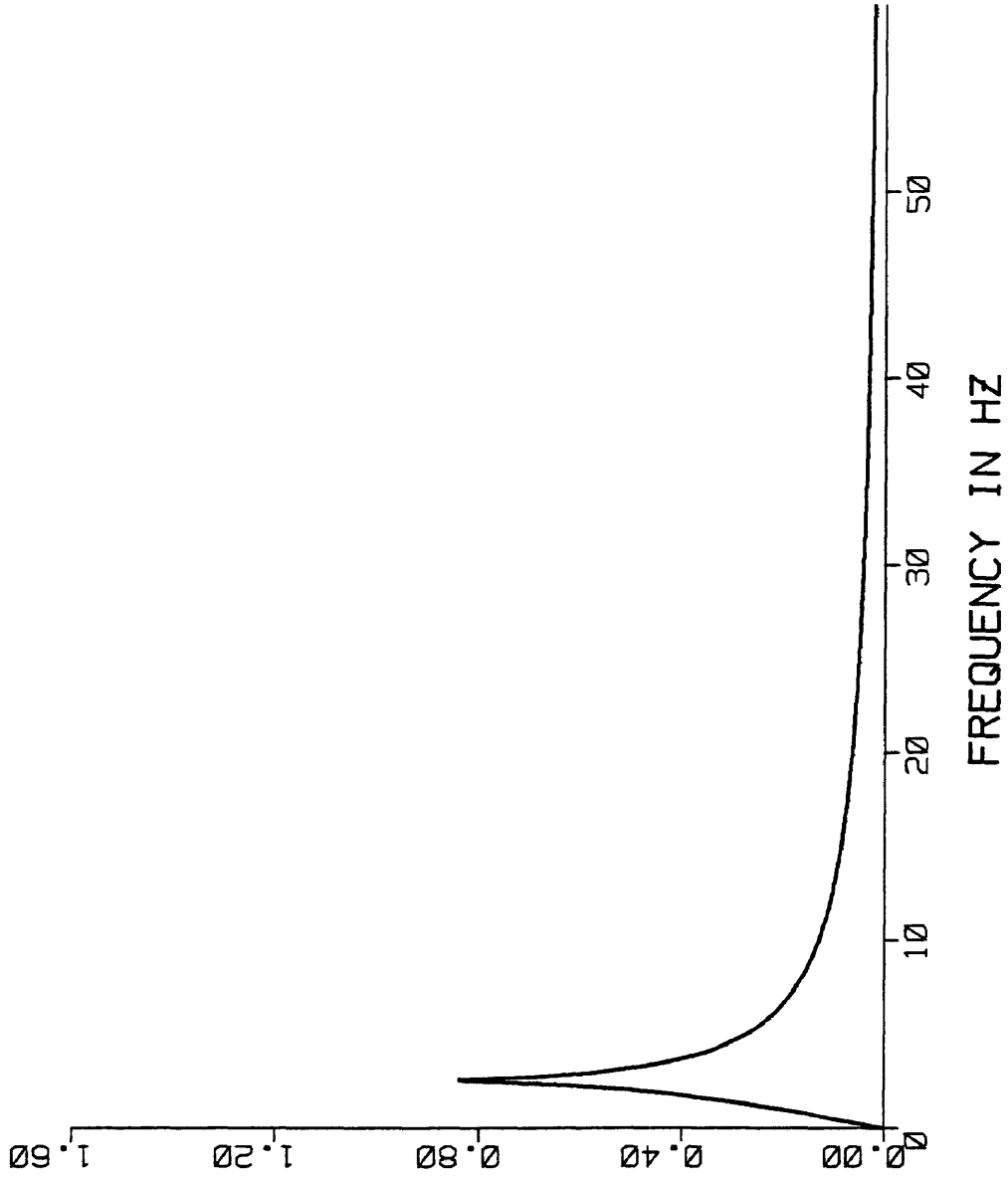


FIGURE 4-13: AMPLITUDE SPECTRUM OF REFLECTION FUNCTION R23

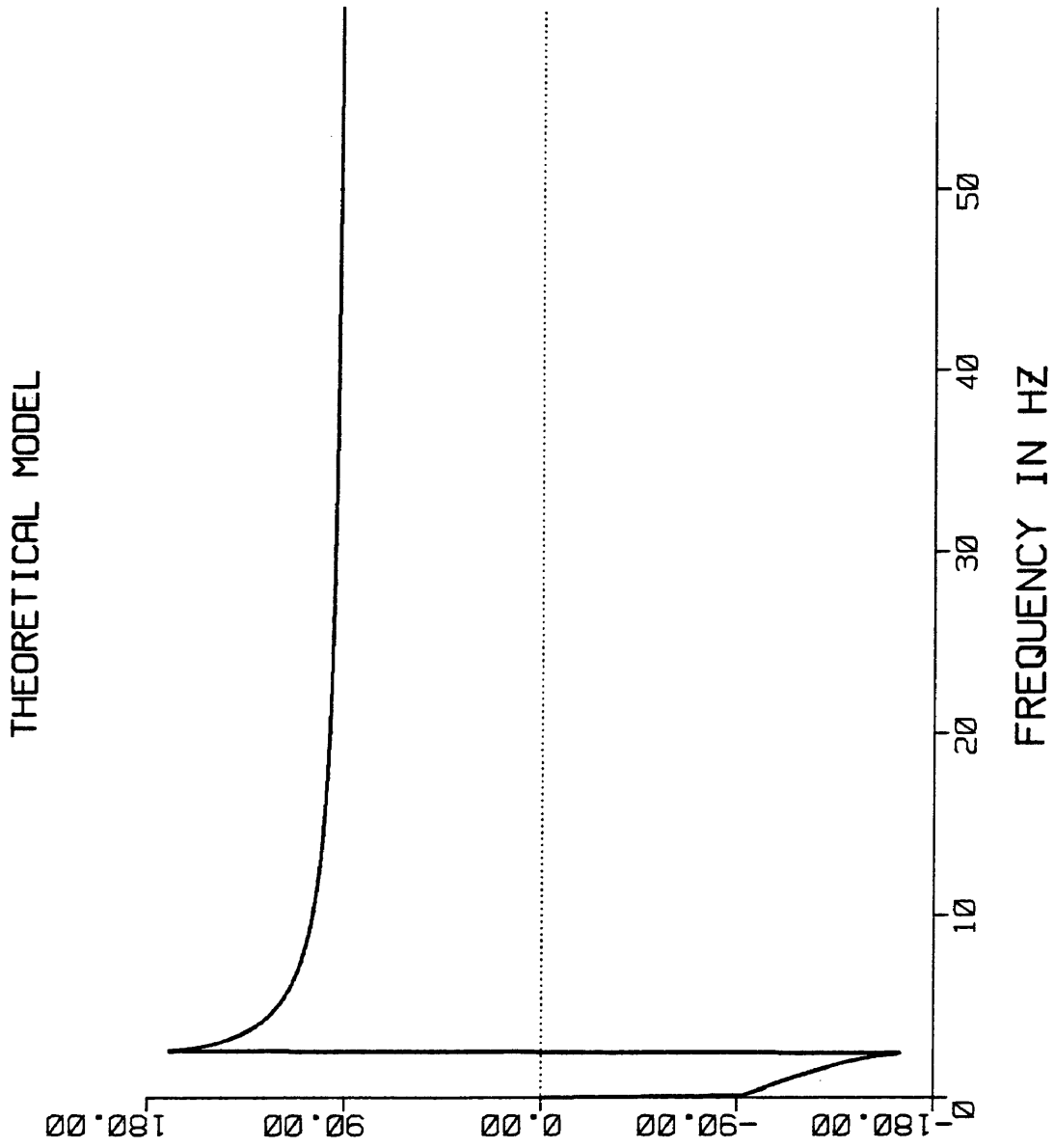


FIGURE 4-14: PHASE SPECTRUM OF REFLECTION FUNCTION R23

THEORETICAL MODEL

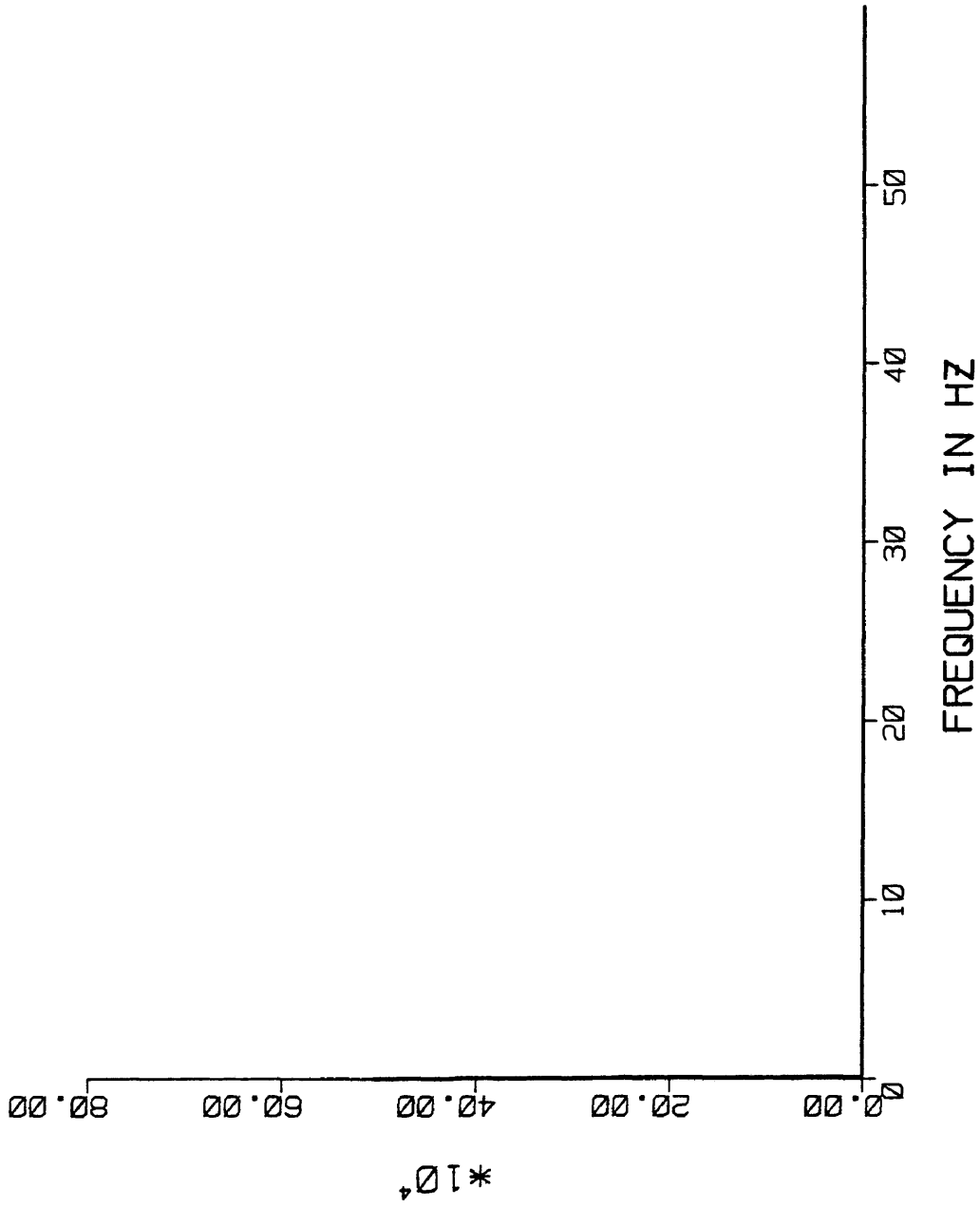


FIGURE 4-15: AMPLITUDE SPECTRUM OF TRANSMISSION FUNCTION T12

THEORETICAL MODEL

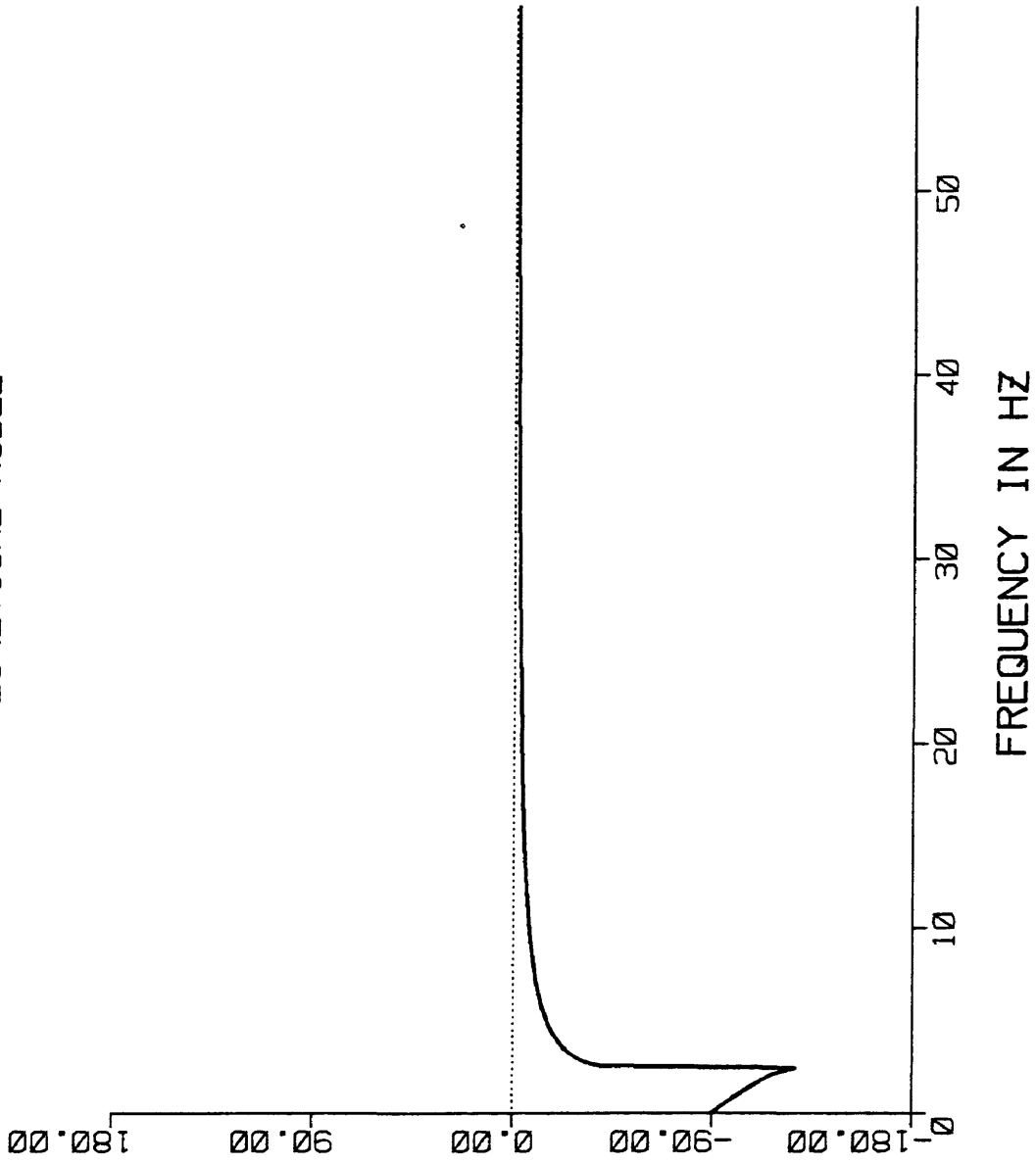


FIGURE 4-16: PHASE SPECTRUM OF TRANSMISSION FUNCTION T12

THEORETICAL MODEL

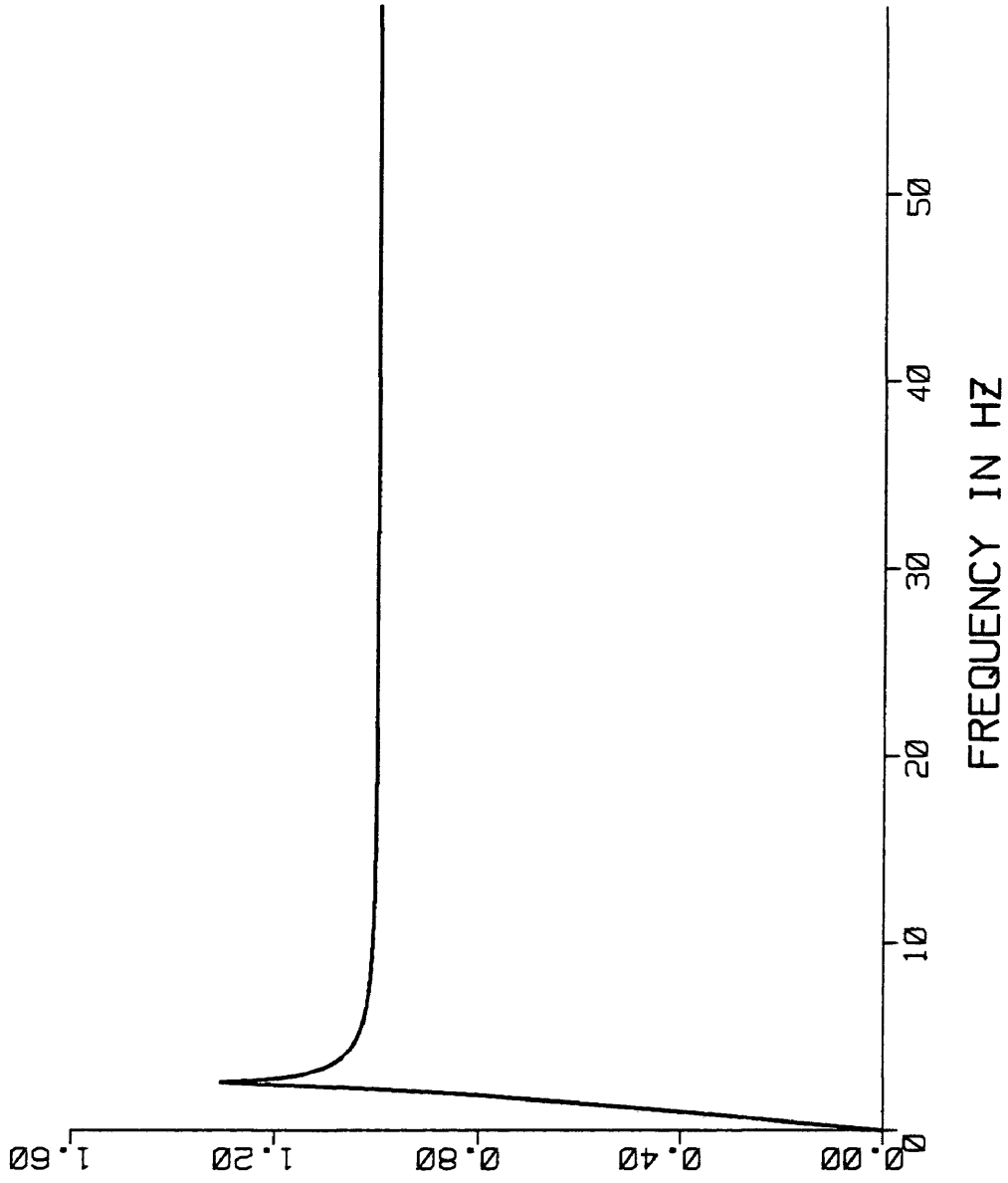


FIGURE 4-17: AMPLITUDE SPECTRUM OF TRANSMISSION FUNCTION T23

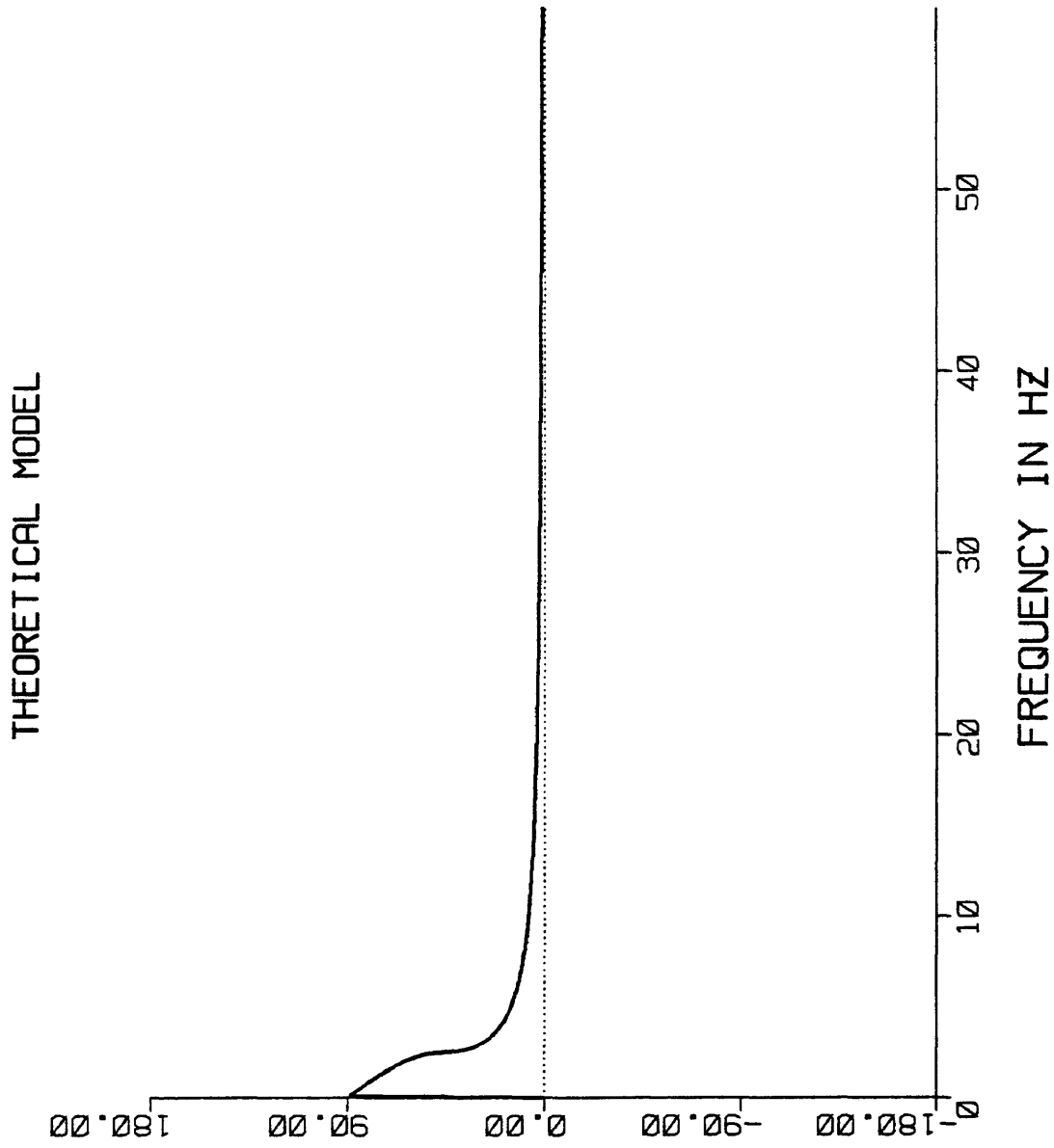


FIGURE 4-18: PHASE SPECTRUM OF TRANSMISSION FUNCTION T23

A Realistic Model

A realistic model is chosen here from real field data built into a four layer model. It contains a linearly varying velocity transition zone between a constant velocity half space at the top and a constant velocity layer at the bottom which, in turn, is followed by a constant velocity half space. The velocity of the first region top half space (water) is 5000 ft/sec which also starts the second region transition zone with a velocity gradient of 12.27 ft/sec/ft with a ratio of 1.4. The zone ends with the final velocity of 7000 ft/sec which continuous into the third region constant velocity layer. The fourth region bottom half space has a constant velocity of 7552 ft/sec. This data set and the calculation parameters are shown below in the Table 4-2.

The reflection impulse response from this model is shown in figure 4-19 which is followed by the reflection Ricker response of the system is shown compared with the wave theoretic reflection Ricker response in figure 4-21. In this realistic case, although there are meaningful differences in detail, the reflection responses compare quite favorably principally because of the particular band width of

the chosen Ricker wavelet. However, it appears that the convolutional results would be misleading in an engineering study. The transmission impulse and Ricker responses into the lower half space through the transition (second) region and the constant velocity (third) region are shown in figures 4-22 and 4-23. The time domain reflection functions R_{12} and R_{23} which control the reflection responses are shown in figures 4-24 and 4-25.

Table 4-2

A Realistic Model For Basic Analytical Results

Region 1: Upper Half Space	Constant Velocity	5000 fps
	Bottom Depth	31 ft
Region 2: Transition Layer	Starting Velocity	5000 fps
	Ending Velocity	7000 fps
	Bottom Depth	194 ft
	Layer Thickness	163 ft
	Velocity Gradient	12.27 fpspf
	Velocity Ratio	1.40
Region 3: Reflector Layer	Constant Velocity	7000 fps
	Bottom Depth	406 ft
	Layer Thickness	212 ft
Region 4: Lower Half Space	Constant Velocity	7552 fps
Time Sampling	: 1 ms;	Frequency Sampling : 0.488 Hz
Record Length	: 2047 ms;	Nyquist Frequency : 500 Hz
z0=0 - - - - Datum Upper Half Space - - - - - - - - - - - - - - - -		
	Constant Velocity	= 5000
	Datum to Bottom	= 31 ft; 12.4 ms
z1=31 - - - Starting Velocity = 5000 - - - - - - - - - - -		
	Layer Thickness	= 163 ft; 55 ms
z2=194 - - - Ending Velocity = 7000 - - - - - - - - - - -		
	Constant Velocity	= 7000
	Layer Thickness	= 212 ft; 60.6 ms
z3=406 - - - Start of Lower Half Space - - - - - - - - - - -		
	Constant Velocity	= 7552

REALISTIC MODEL

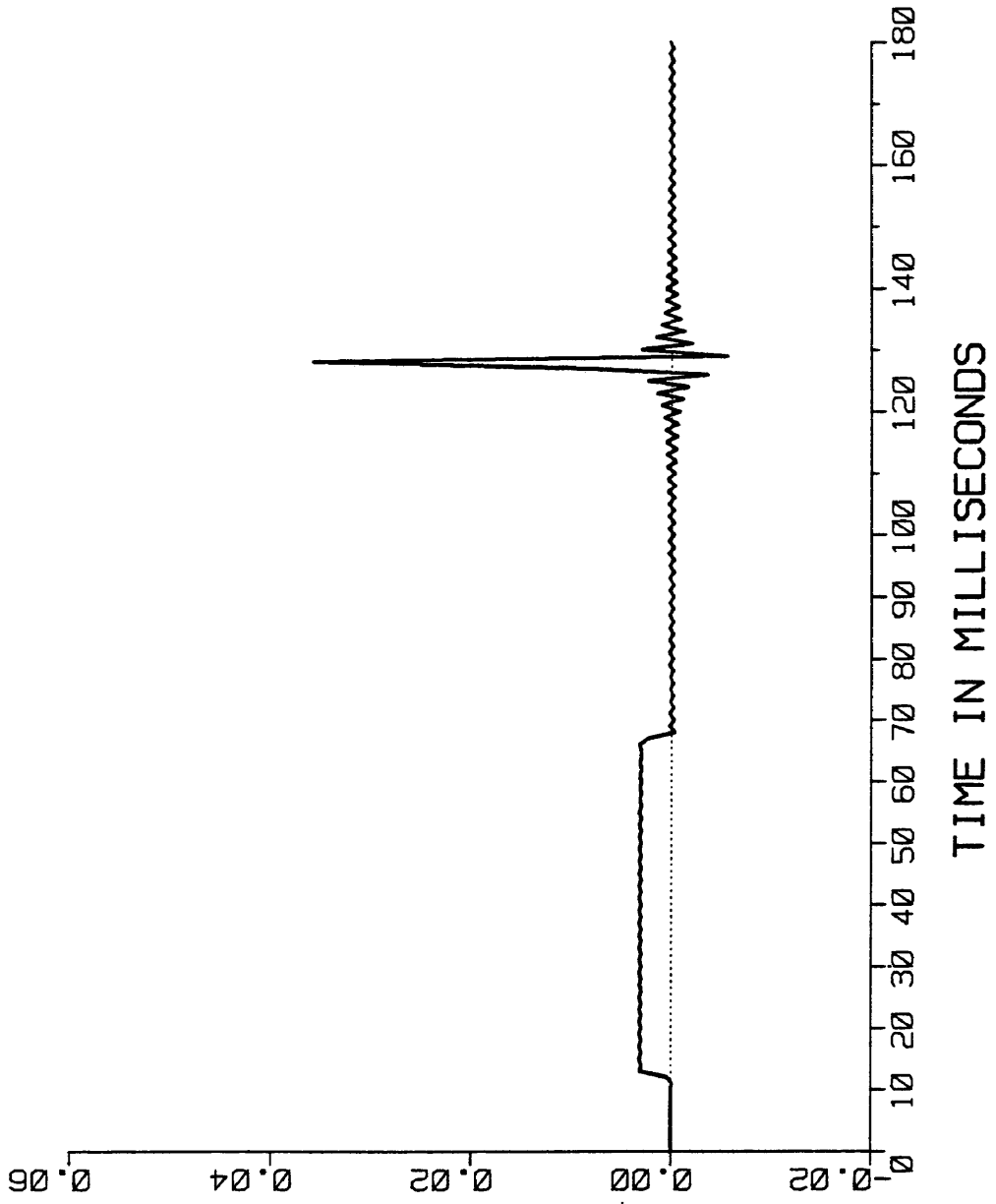


FIGURE 4-19: REFLECTION IMPULSE RESPONSE

REALISTIC MODEL

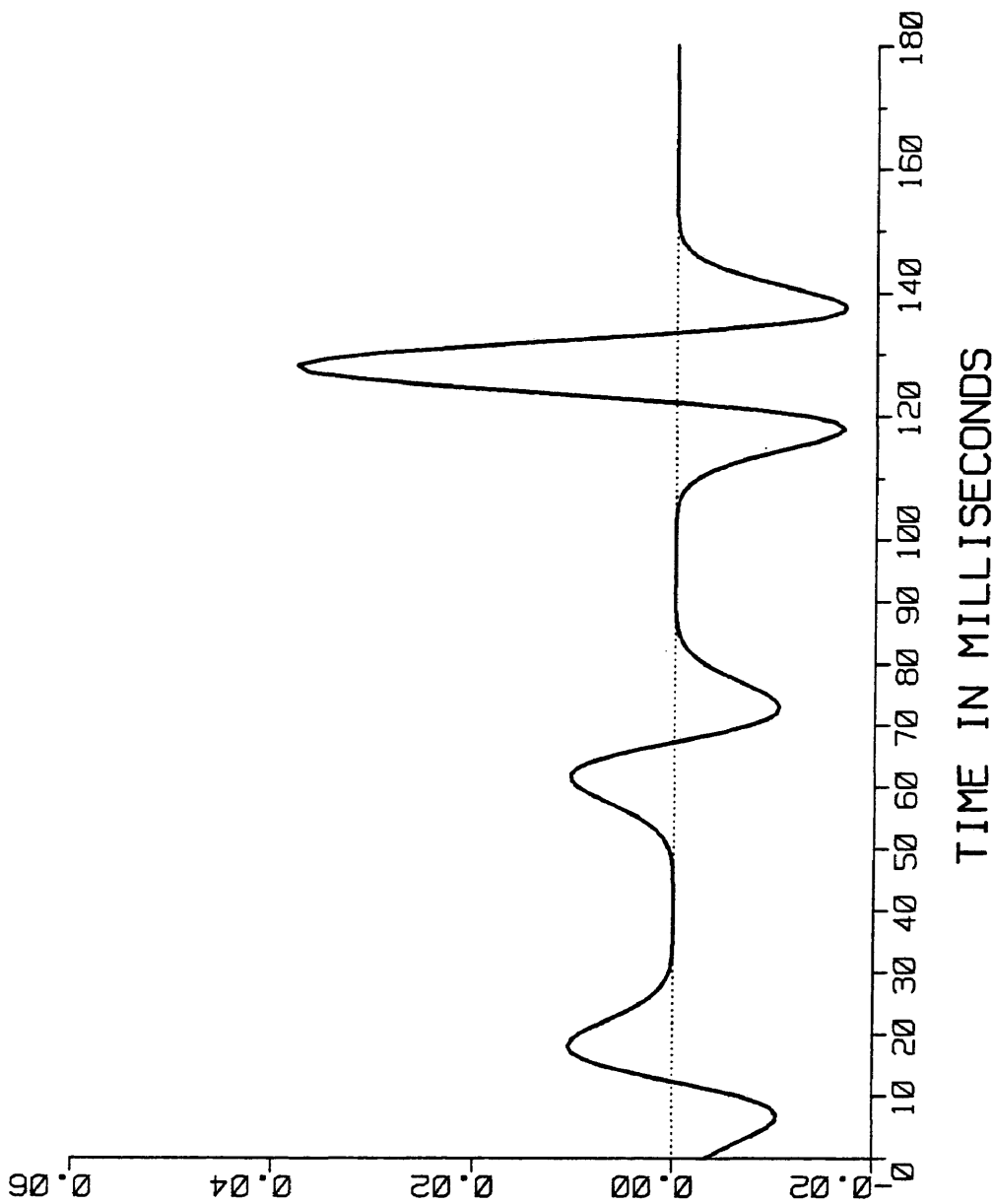


FIGURE 4-20: REFLECTION RICKER RESPONSE

REALISTIC MODEL

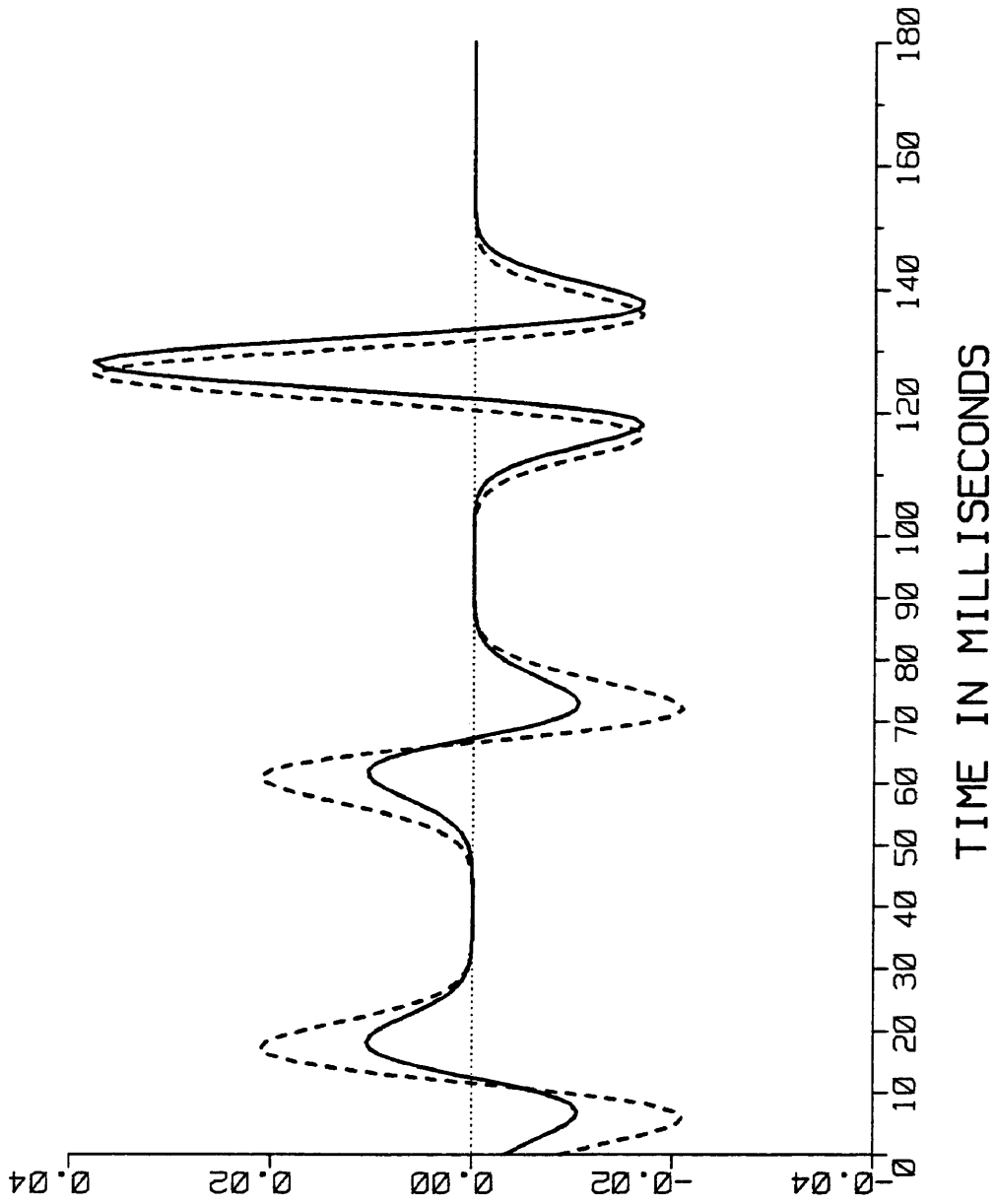


FIGURE 4-21: REFLECTION RICKER RESPONSES
WAVE THEORETIC (SOLID) VS. CONVENTIONAL REFLECTIVITY (DSHED)

REALISTIC MODEL

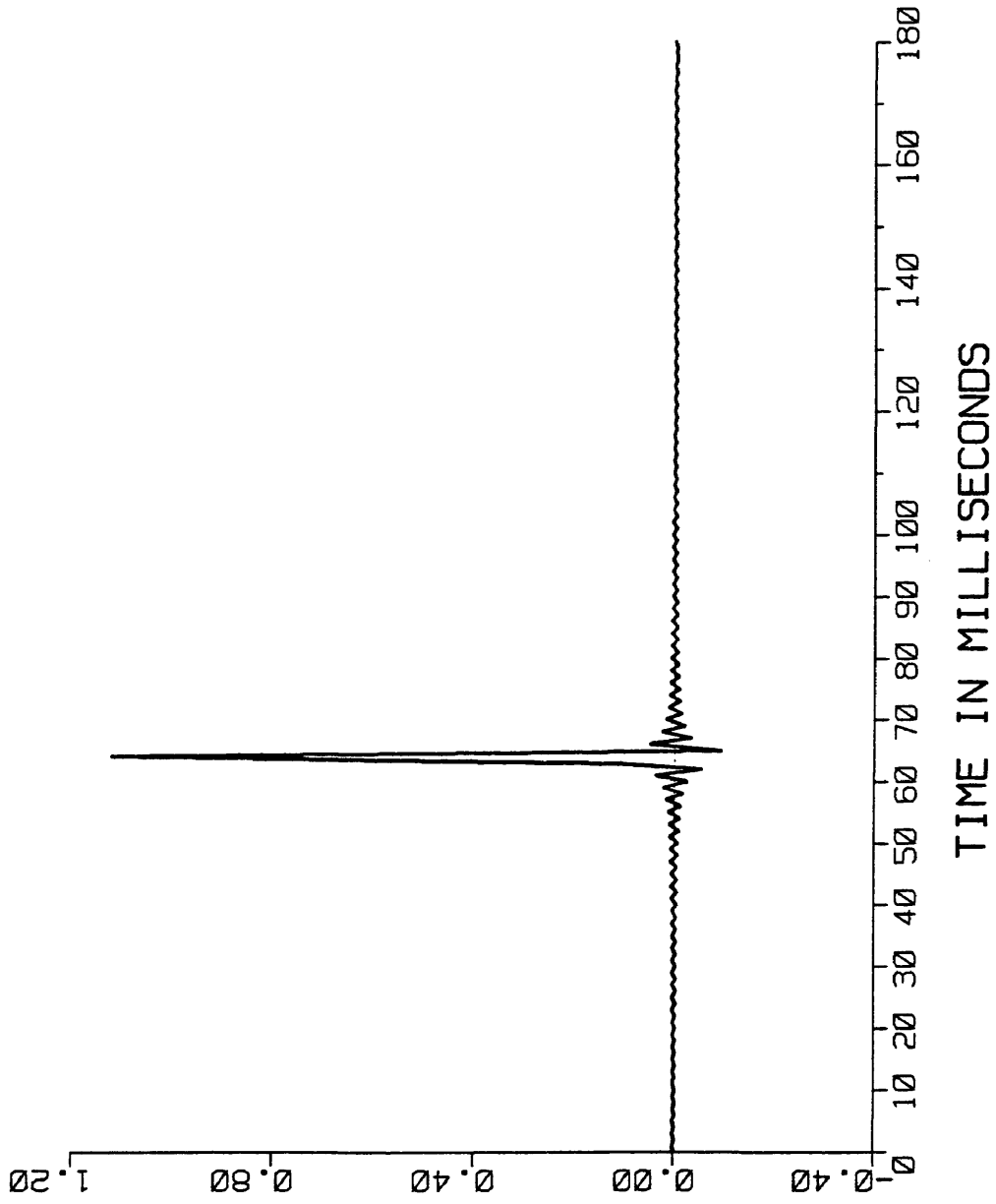


FIGURE 4-22: TRANSMISSION IMPULSE RESPONSE

REALISTIC MODEL

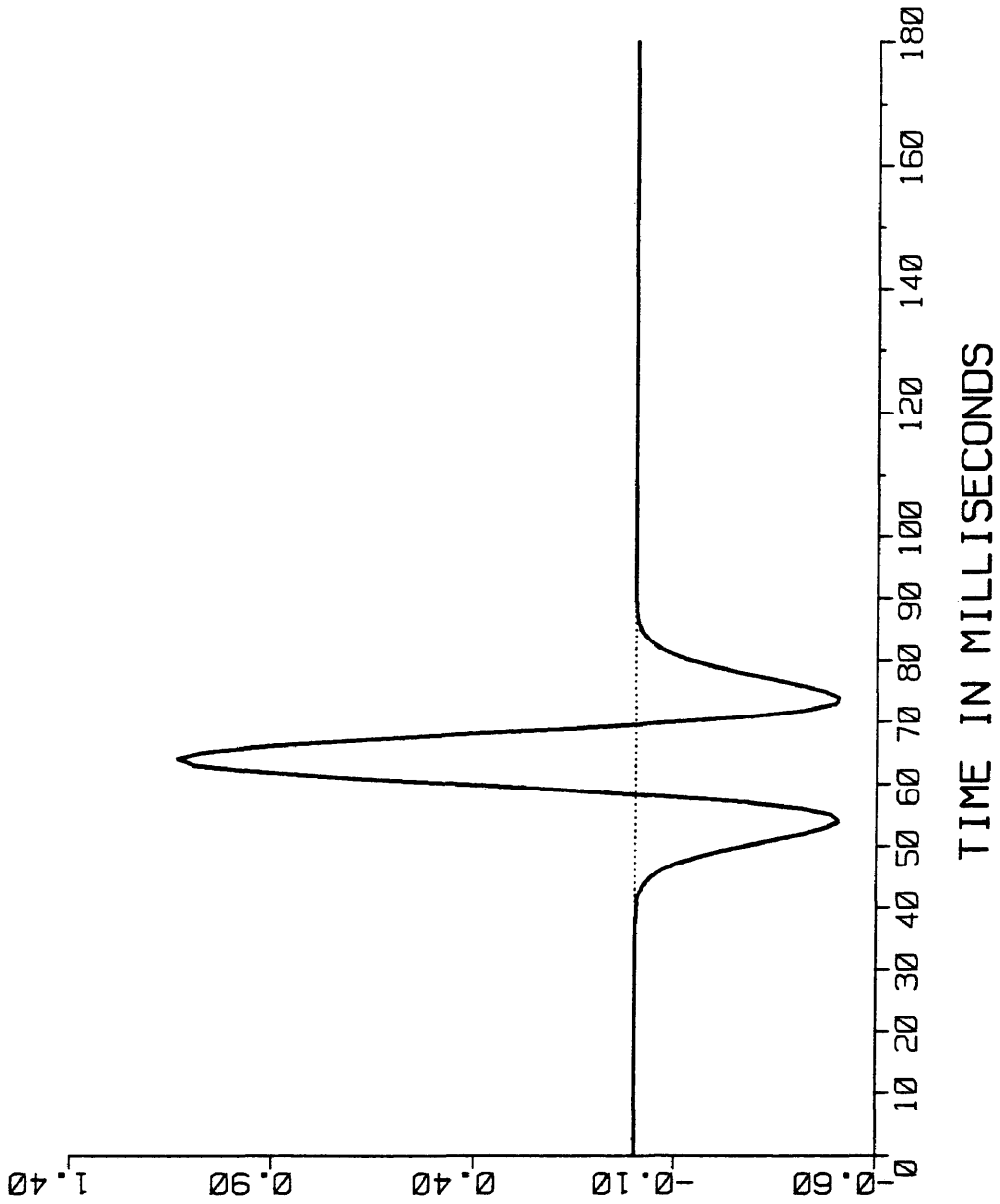


FIGURE 4-23: TRANSMISSION RICKER RESPONSE

REALISTIC MODEL

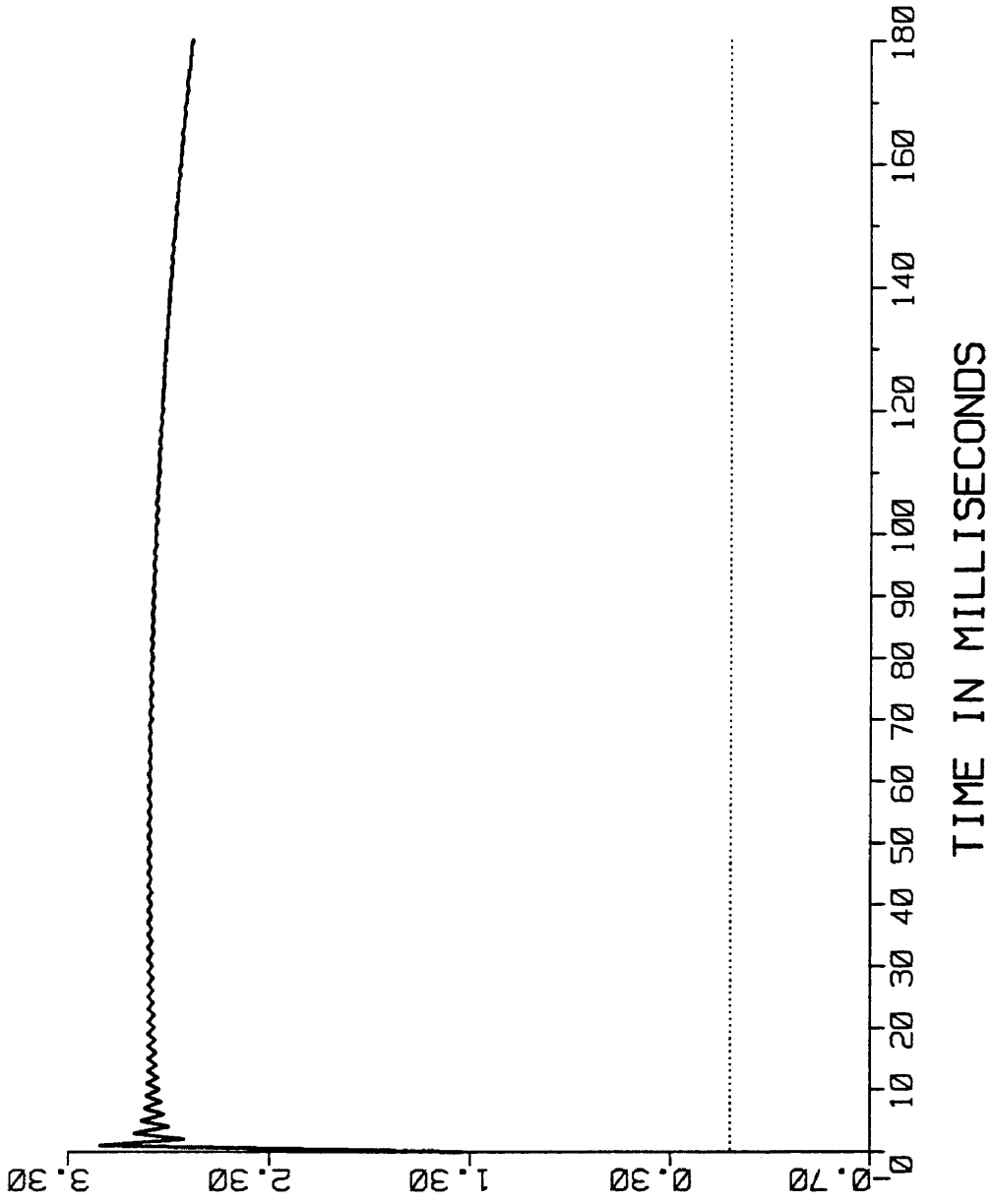


FIGURE 4-24: REFLECTION FUNCTION R12

REALISTIC MODEL

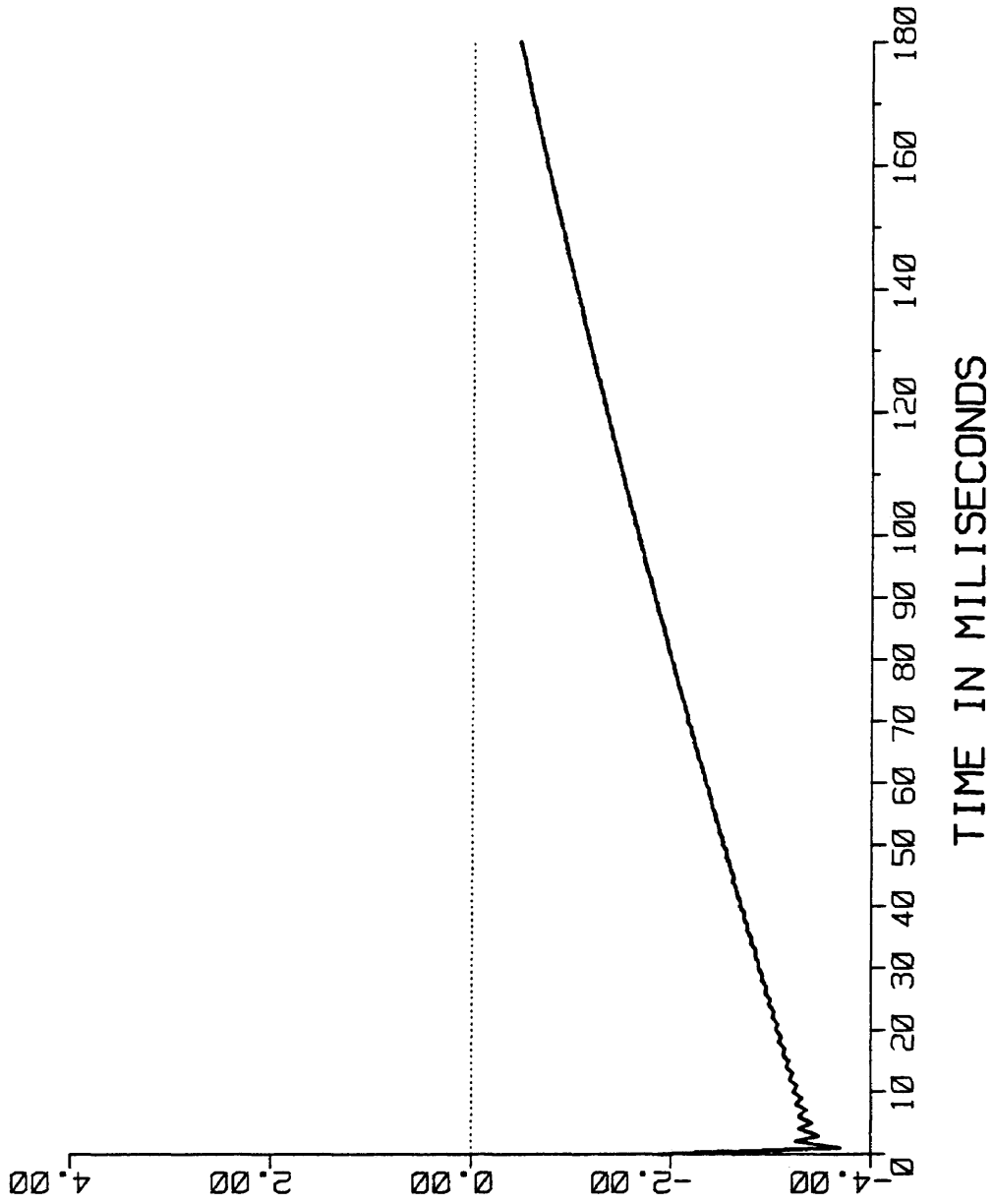


FIGURE 4-25: REFLECTION FUNCTION R23

Soft Sea Floor Model

This soft sea floor model was chosen from a field well log from offshore Saudi Arabia in the Arabian Gulf. This model forms a four layer system with a constant velocity half space of water at a velocity of 5000 ft/sec as the first region in the model. Below the water there exists a transition zone through the soft sea floor showing a starting velocity of 6200 ft/sec at the top and a positive constant velocity gradient of 3.07 ft/sec/ft. The ratio of the velocity between the bottom and the top of the sea floor transition is 1.08 to make the final velocity of the second region transition zone as 6700 ft/sec. There is an unconformity between the bottom of the sea floor zone and the PNU formation layer below, the third region, with a constant velocity of 7000 ft/sec. The fourth region, the RUS formation, is assumed to be the bottom half space with a constant velocity of 7552 ft/sec. This data and the needed parameters are shown in Table 4-3.

The reflection impulse response from the soft sea floor model is shown in figure 4-26 followed by the reflection Ricker wavelet response in figure 4-27. The reflection Ricker wavelet responses of the system from the theoretical

wave approach compared with that from the conventional reflectivity modeling is shown in figure 4-28. Transmission responses from the wave theoretic approach into the lower half space are shown for the impulse and Ricker wavelet incidences in figures 4-29 and 4-30. Finally, the time domain reflection functions R_{12} and R_{23} for this soft sea floor model are shown in figures 4-31 and 4-32. Again due to the particular Ricker wavelet band width we do not see much difference between the Ricker incidence wave theoretic and conventional reflectivity results in this model.

Table 4-3

Soft Sea Floor Model For Basic Analytical Results

Region 1: Upper Half Space	Constant Velocity	5000 fps
	Bottom Depth	31 ft
Region 2: Transition Layer	Starting Velocity	6200 fps
	Ending Velocity	6700 fps
	Bottom Depth	194 ft
	Layer Thickness	163 ft
	Velocity Gradient	3.07 fpspf
	Velocity Ratio	1.08
Region 3: Reflector Layer	Constant Velocity	7000 fps
	Bottom Depth	406 ft
	Layer Thickness	212 ft
Region 4: Lower Half Space	Constant Velocity	7552 fps
Time Sampling	: 1 ms;	Frequency Sampling : 0.488 Hz
Record Length	: 2047 ms;	Nyquist Frequency : 500 Hz
z0=0	- - - Datum Upper Half Space	- - - - -
	Constant Velocity =	5000
	Datum to Bottom =	31 ft; 12.4 ms
z1=31	- - - Starting Velocity =	6200 - - - - -
	Layer Thickness =	163 ft; 50 ms
z2=194	- - - Ending Velocity =	6700 - - - - -
	Constant Velocity =	7000
	Layer Thickness =	212 ft; 60.6 ms
z3=406	- - - Start of Lower Half Space	- - - - -
	Constant Velocity =	7552

SOFT SEA FLOOR MODEL

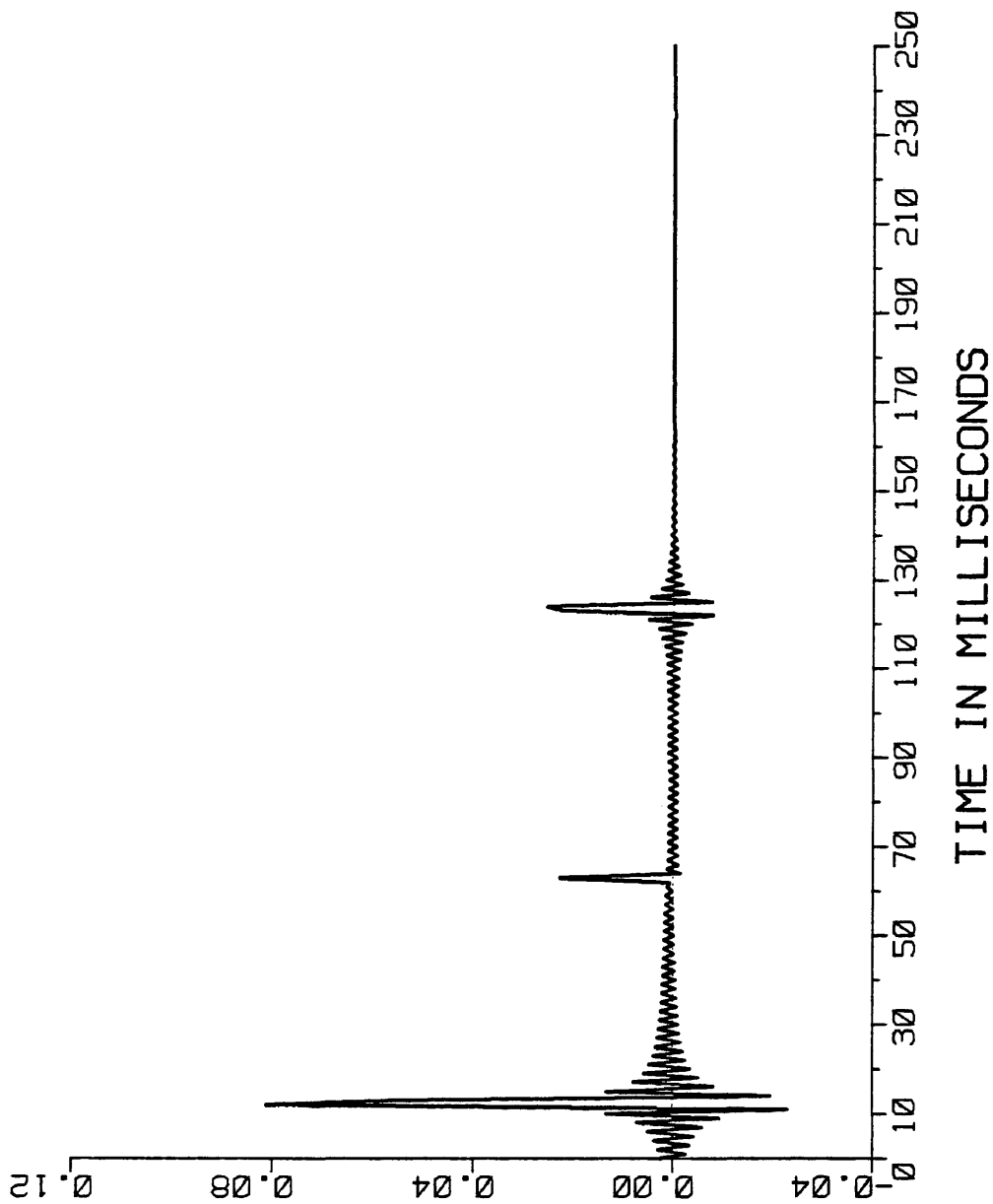


FIGURE 4-26: REFLECTION IMPULSE RESPONSE

SOFT SEA FLOOR MODEL

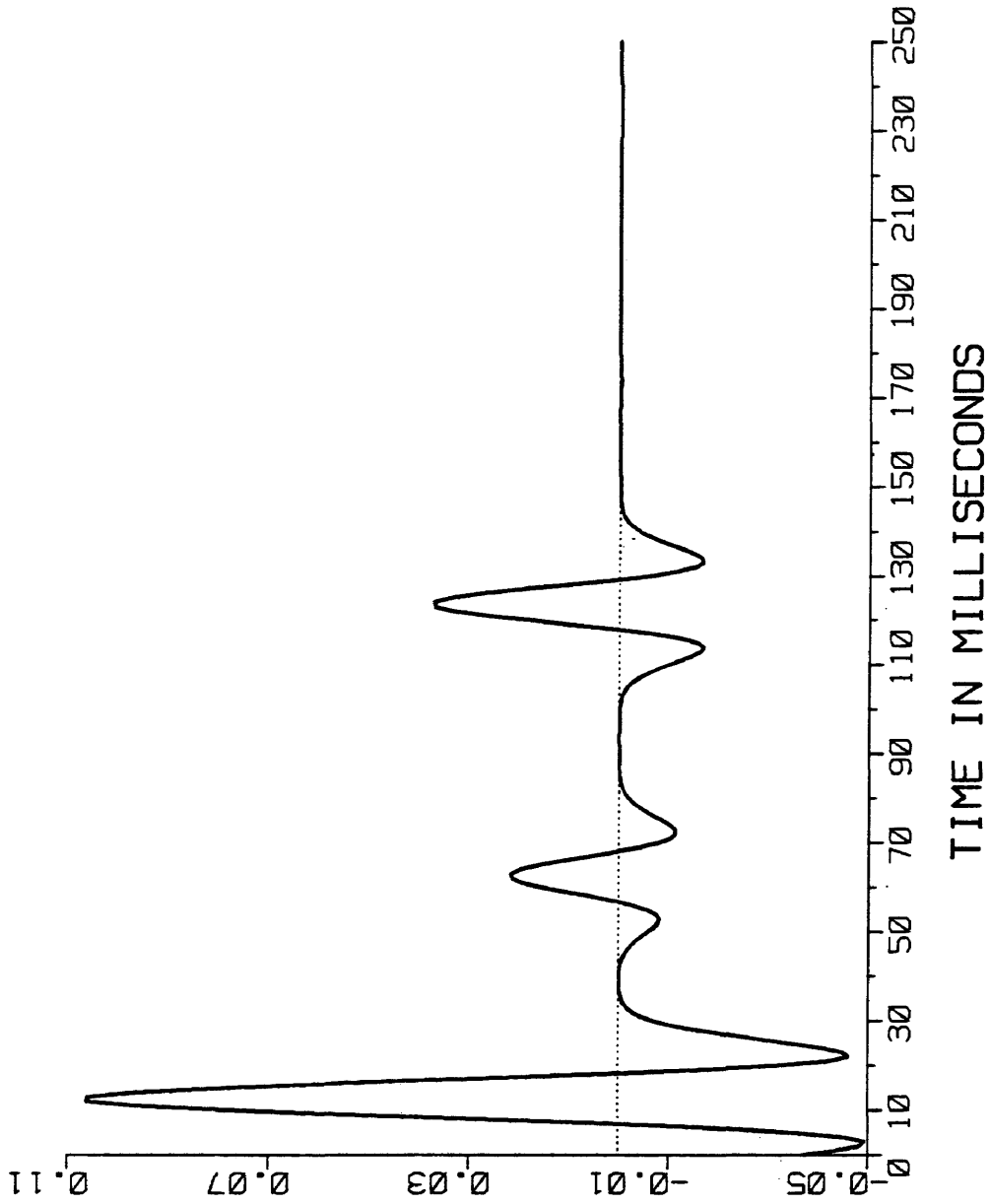


FIGURE 4-27: REFLECTION RICKER RESPONSE

SOFT SEA FLOOR MODEL

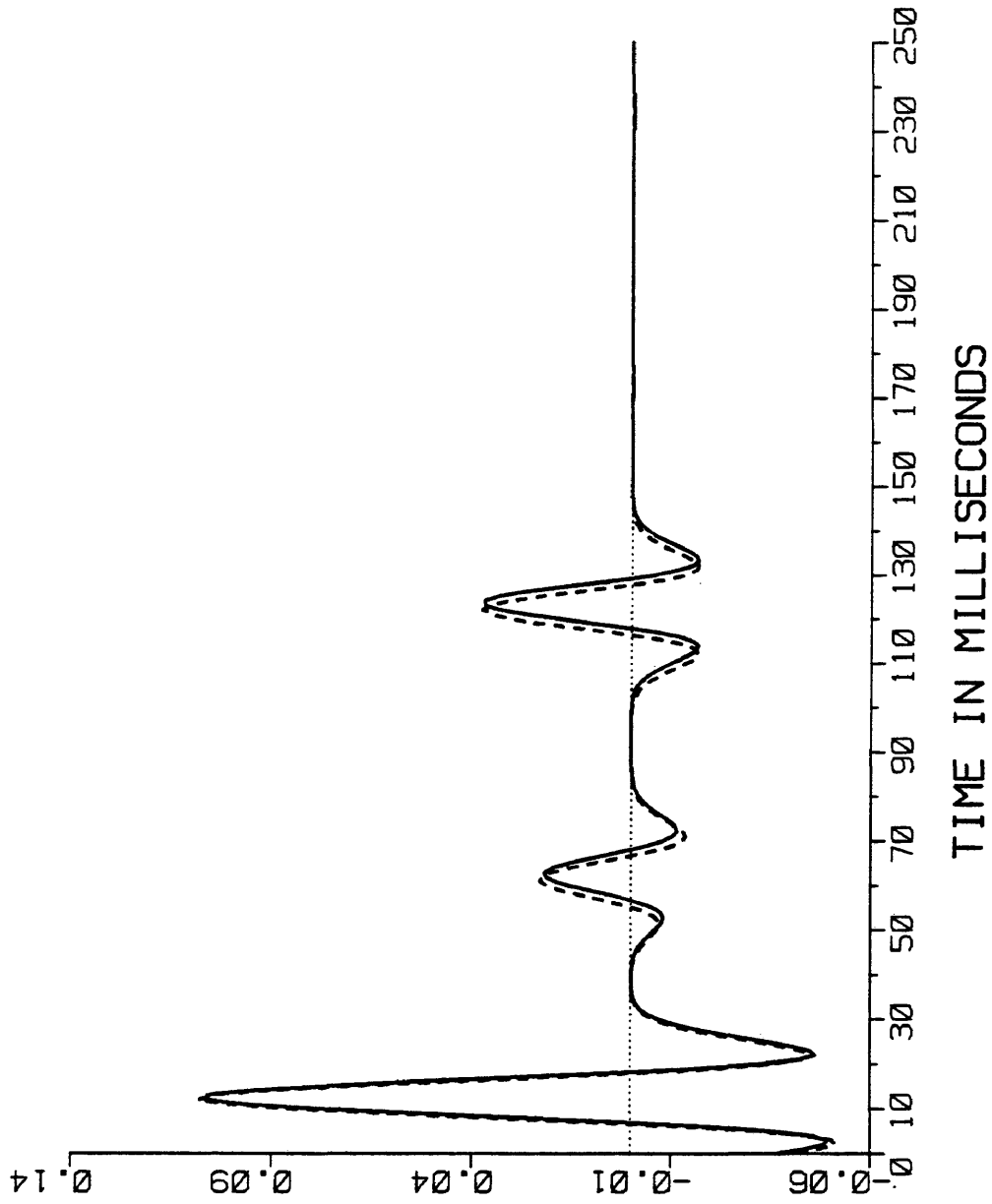


FIGURE 4-28: REFLECTION RICKER RESPONSES
WAVE THEORETIC (SOLID) VS. CONVENTIONAL REFLECTIVITY (DSHED)

SOFT SEA FLOOR MODEL

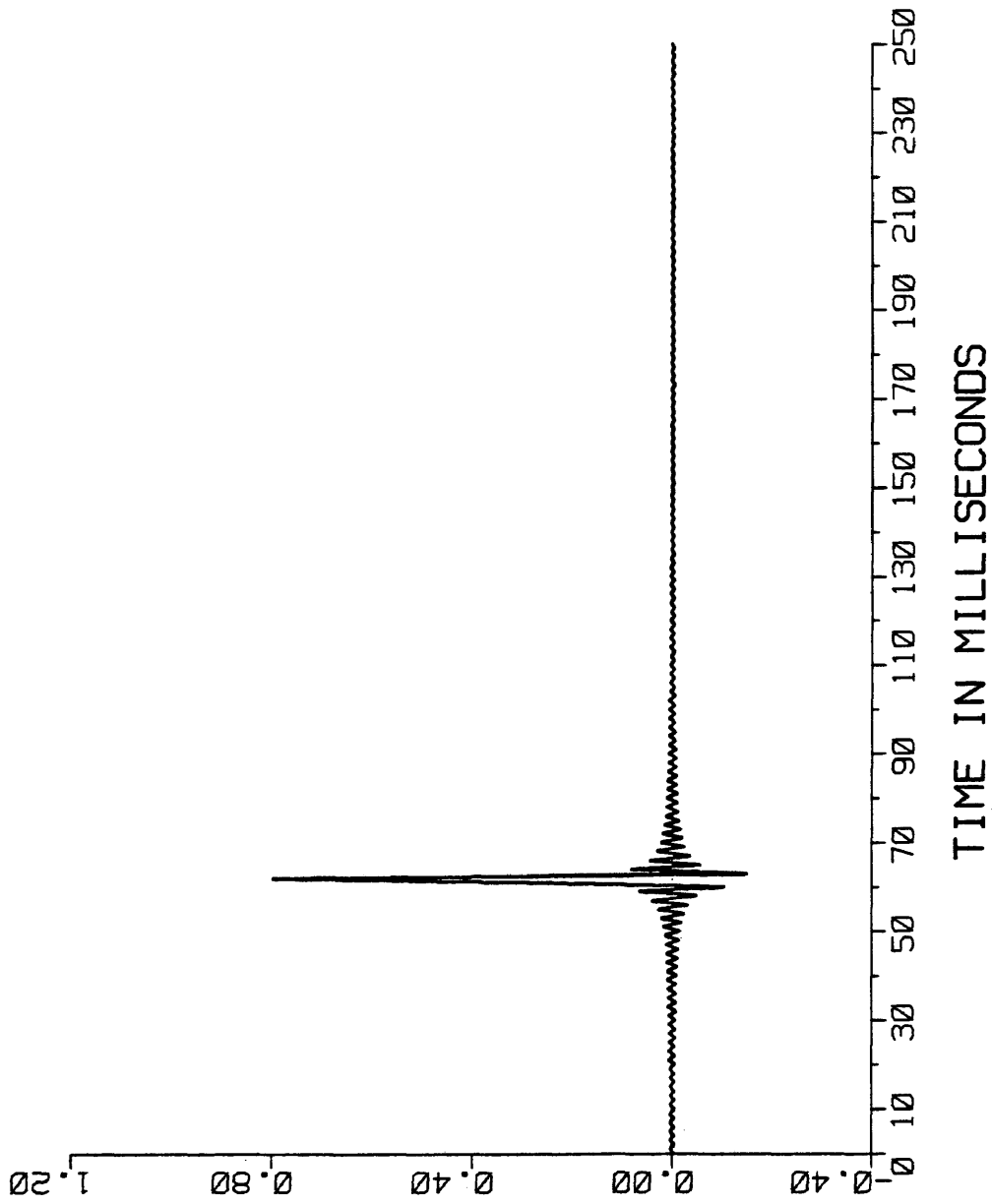


FIGURE 4-29: TRANSMISSION IMPULSE RESPONSE

SOFT SEA FLOOR MODEL

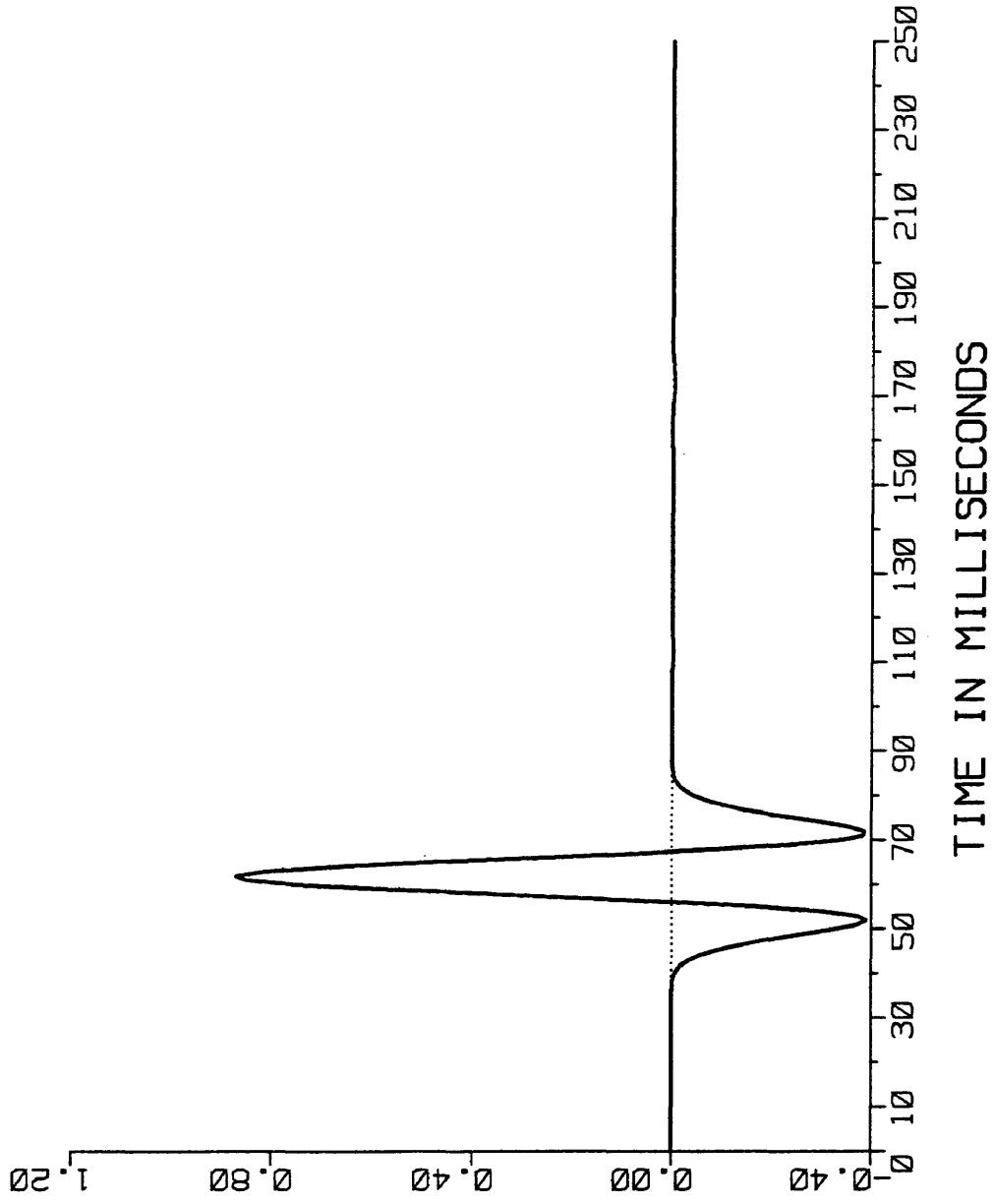


FIGURE 4-30: TRANSMISSION RICKER RESPONSE

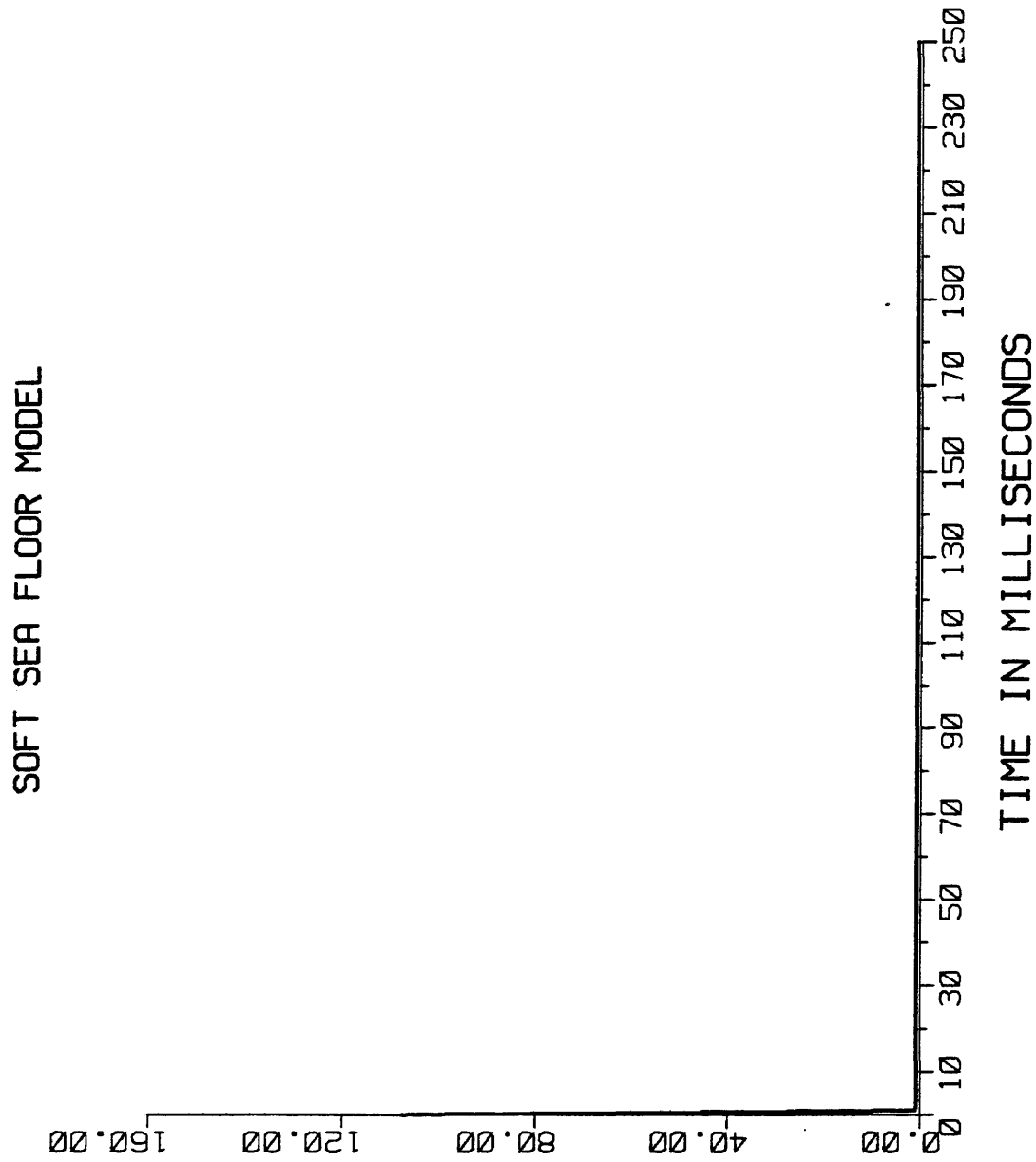


FIGURE 4-31: REFLECTION FUNCTION R12

SOFT SEA FLOOR MODEL

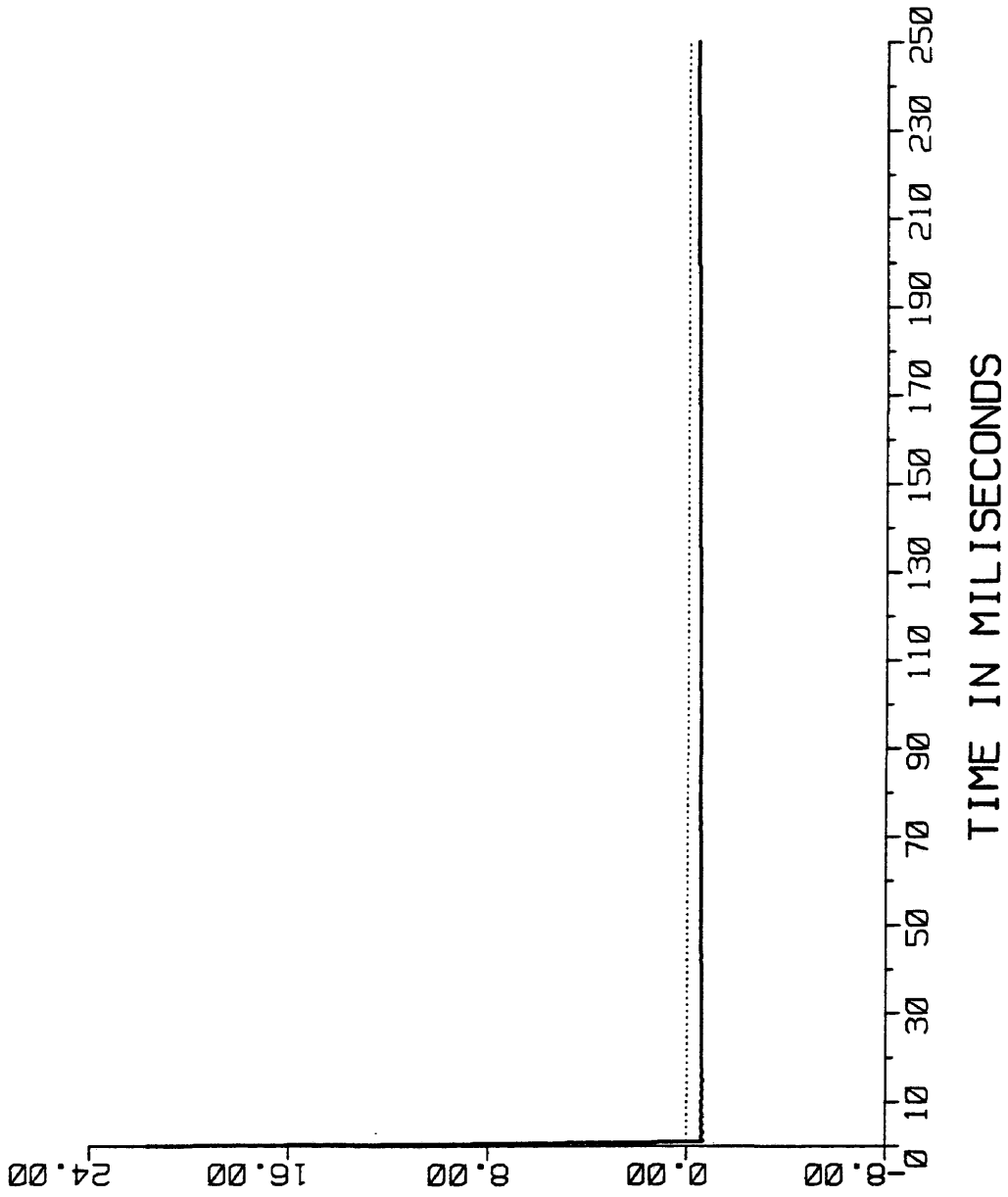


FIGURE 4-32: REFLECTION FUNCTION R23

Hard Sea Floor Model

This hard sea floor model is also chosen from a real well log from Saudi Arabia offshore field in the Arabian Gulf. It shows the behavior of a transition zone in the presence of a negative velocity gradient with depth. This model also contains four regions. The first region is a constant velocity half space of water with a velocity of 5000 ft/sec. The second region is a sea floor transition zone with a negative gradient of -171.2 ft/sec/ft and a velocity ratio of 0.658. The velocity is continuous across the lower boundary of the transition zone. The fourth region is again a half space with a constant velocity of 7000 ft/sec. In this model we have a realistic velocity inversion. The data and the parameters required are shown in Table 4-4.

The results are shown here in the same order as the previous models. The reflection impulse response is shown in figure 4-33 followed by the reflection Ricker wavelet response in figure 4-34. Then we show the comparison of the reflection responses for Ricker incidence for the wave theoretic approach and the conventional reflectivity approach in figure 4-35. Here we see some differences due to

presence of velocity inversion. Transmission Ricker wavelet and impulse response into the fourth region are shown in figures 4-36 and 4-37. Last two figures 4-38 and 4-39 in this set show the time domain reflection functions R_{12} and R_{23} from the top and the bottom of the sea floor transition zone, respectively, as before.

Table 4-4

Hard Sea Floor Model For Basic Analytical Results

Region 1: Upper Half Space	Constant Velocity	5000 fps
	Bottom Depth	31 ft
Region 2: Transition Layer	Starting Velocity	10000 fps
	Ending Velocity	6576 fps
	Bottom Depth	51 ft
	Layer Thickness	20 ft
	Velocity Gradient	-171.2 fpspf
	Velocity Ratio	.658
Region 3: Reflector Layer	Constant Velocity	6576 fps
	Bottom Depth	194 ft
	Layer Thickness	143 ft
Region 4: Lower Half Space	Constant Velocity	7000 fps
Time Sampling	: 1 ms;	Frequency Sampling : 0.977 Hz
Record Length	: 1023 ms;	Nyquist Frequency : 500 Hz
z0=0 - - - -	Datum Upper Half Space - - - - -	
	Constant Velocity =	5000
	Datum to Bottom =	31 ft; 12.4 ms
z1=31 - - -	Starting Velocity =	10000 - - - - -
	Layer Thickness =	20 ft; 2.4 ms
z2=51 - - -	Ending Velocity =	6576 - - - - -
	Constant Velocity =	6576
	Layer Thickness =	143 ft; 43.5 ms
z3=194 - - -	Start of Lower Half Space - - - - -	
	Constant Velocity =	7000

HARD SEA FLOOR MODEL

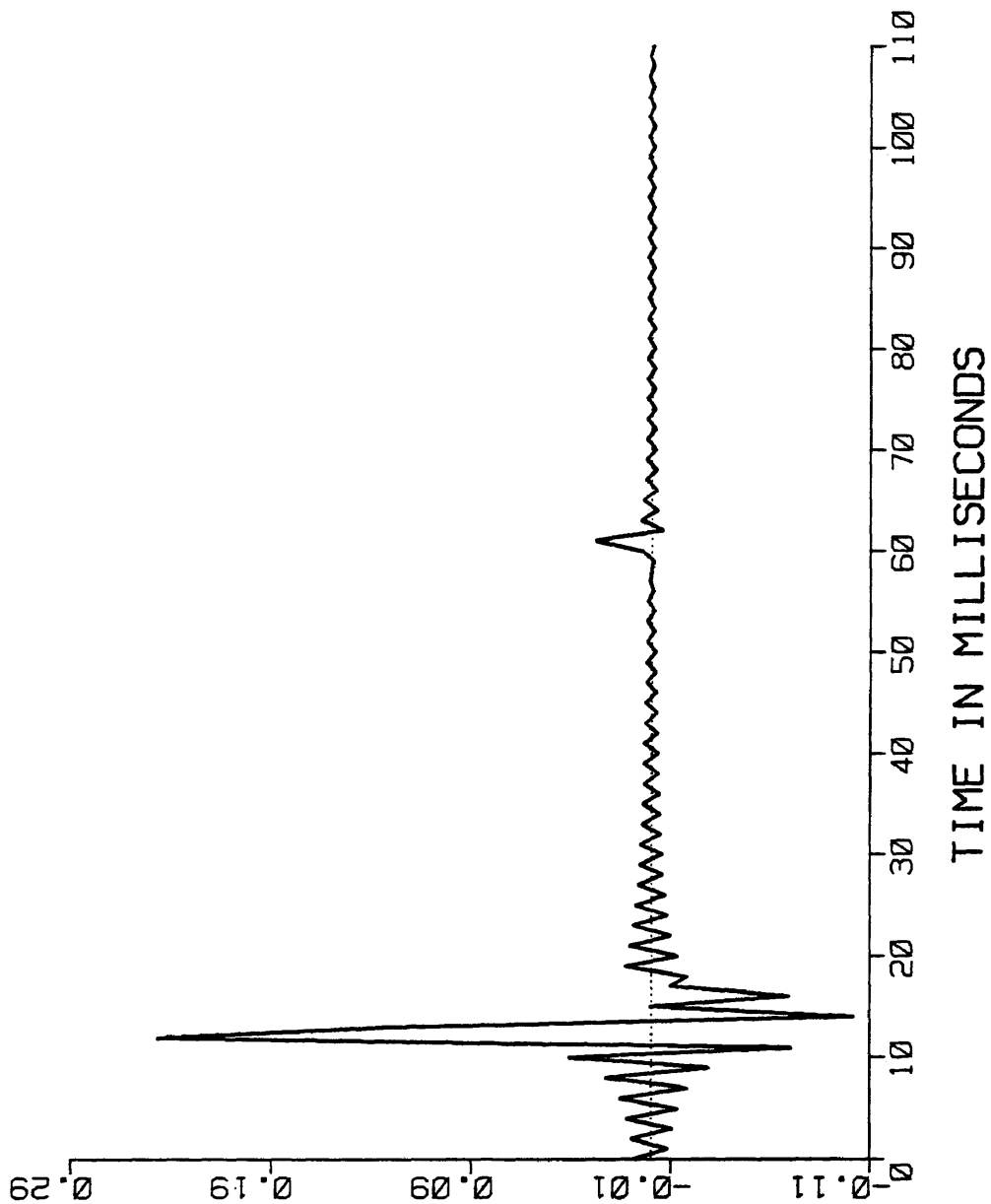


FIGURE 4-33: REFLECTION IMPULSE RESPONSE

HARD SEA FLOOR MODEL

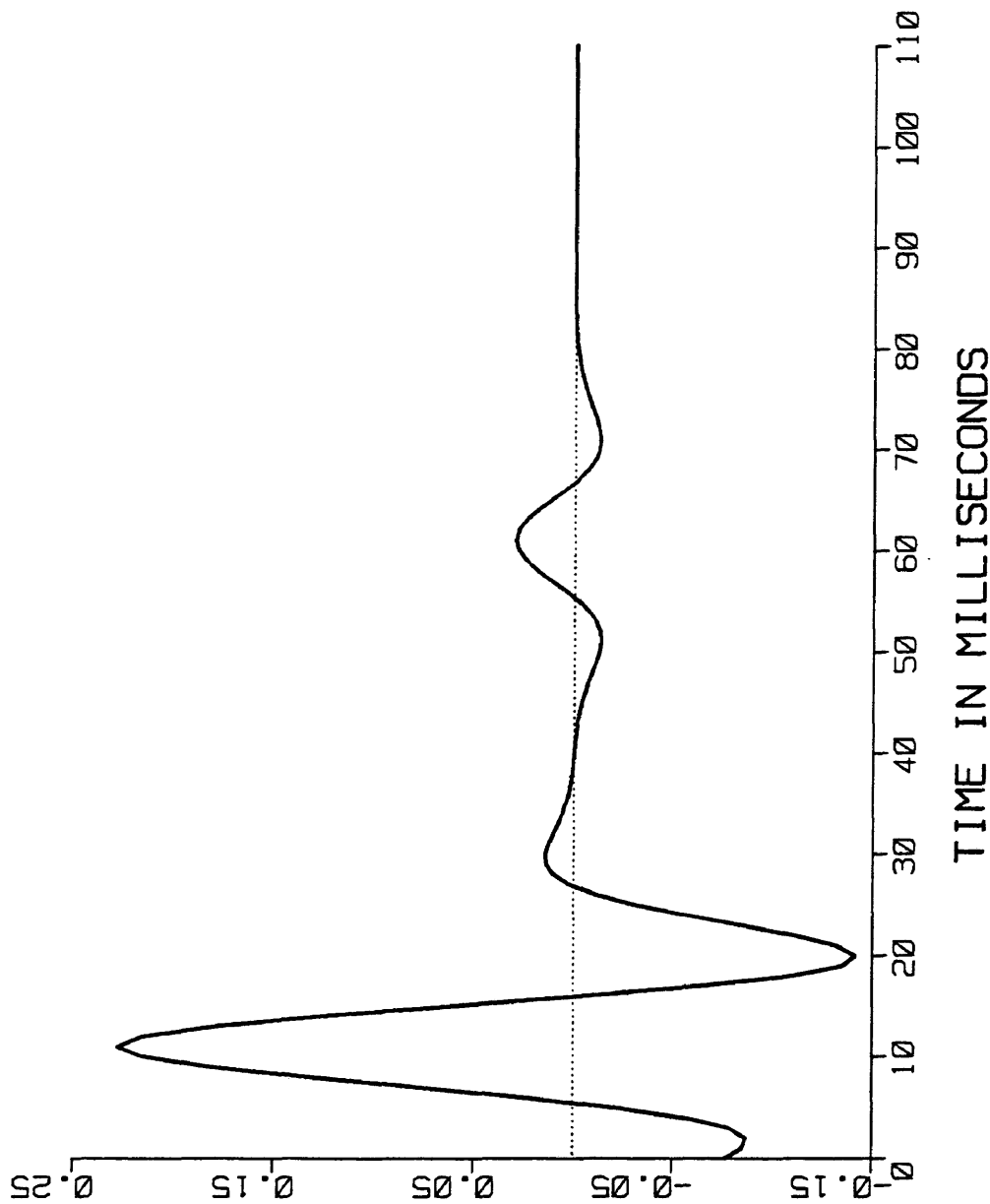


FIGURE 4-34: REFLECTION RICKER RESPONSE

HARD SEA FLOOR MODEL

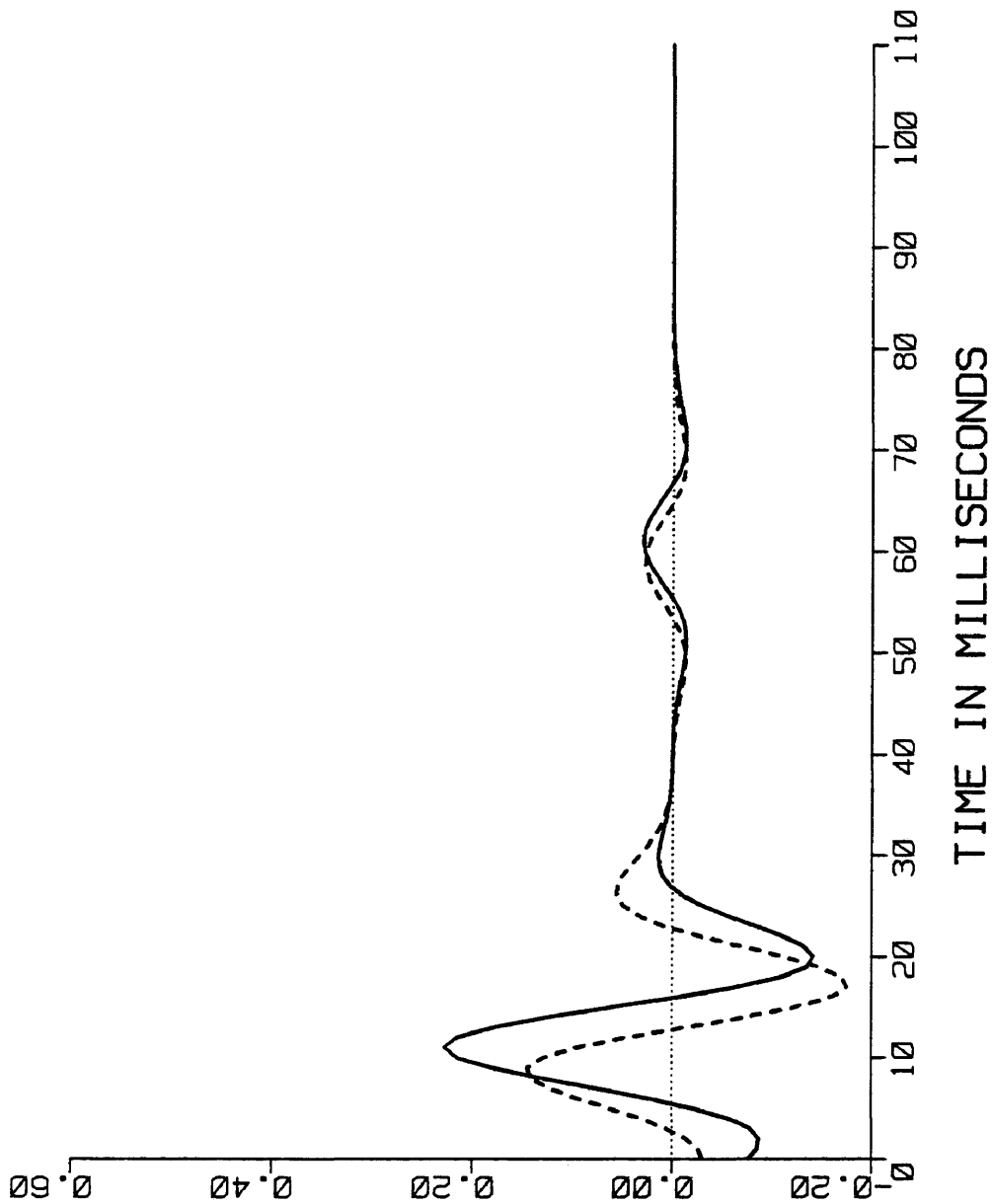


FIGURE 4-35: REFLECTION RICKER RESPONSES
WAVE THEORETIC (SOLID) VS. CONVENTIONAL REFLECTIVITY (DASHED)

HARD SEA FLOOR MODEL

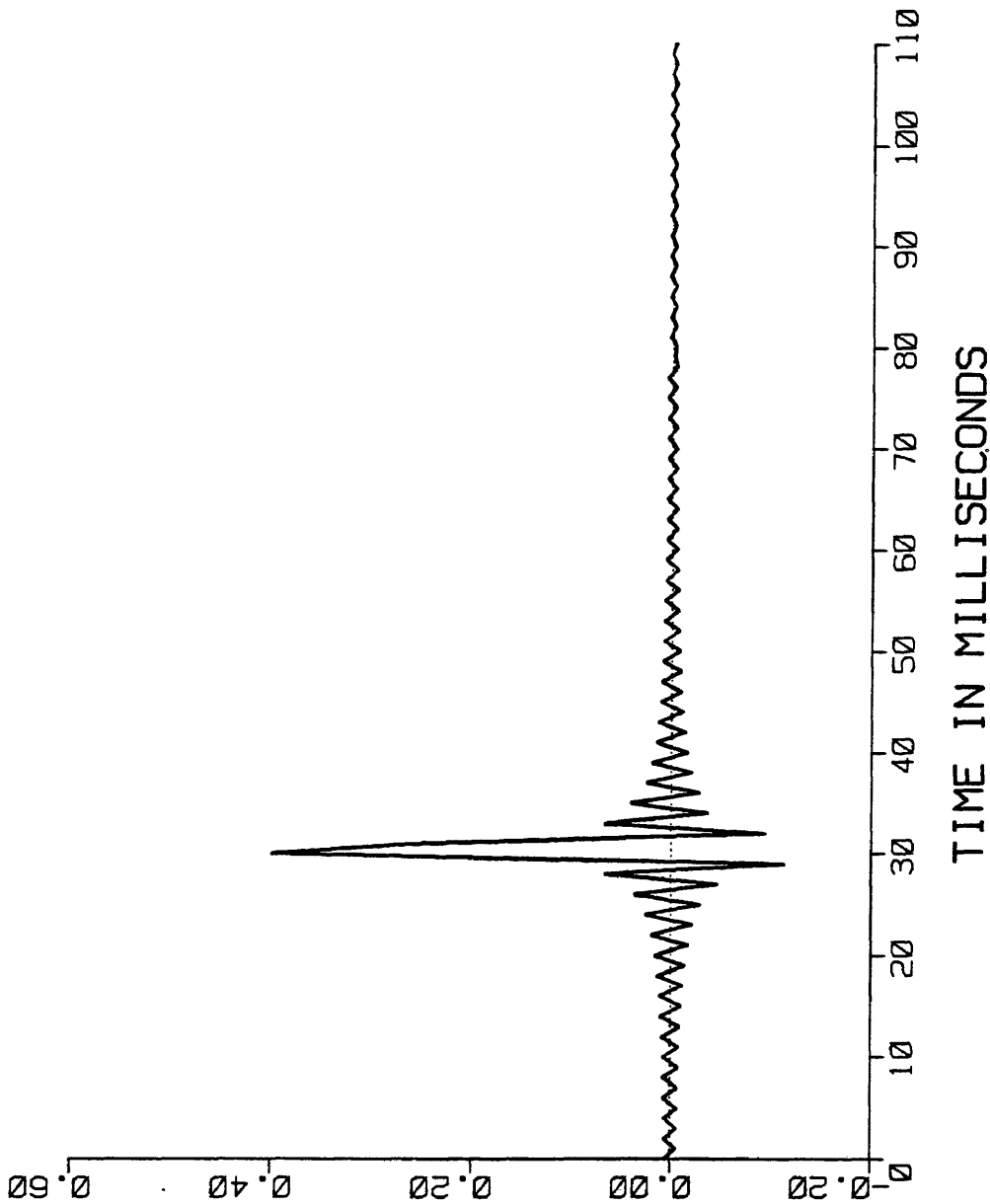


FIGURE 4-36: TRANSMISSION IMPULSE RESPONSE

HARD SEA FLOOR MODEL

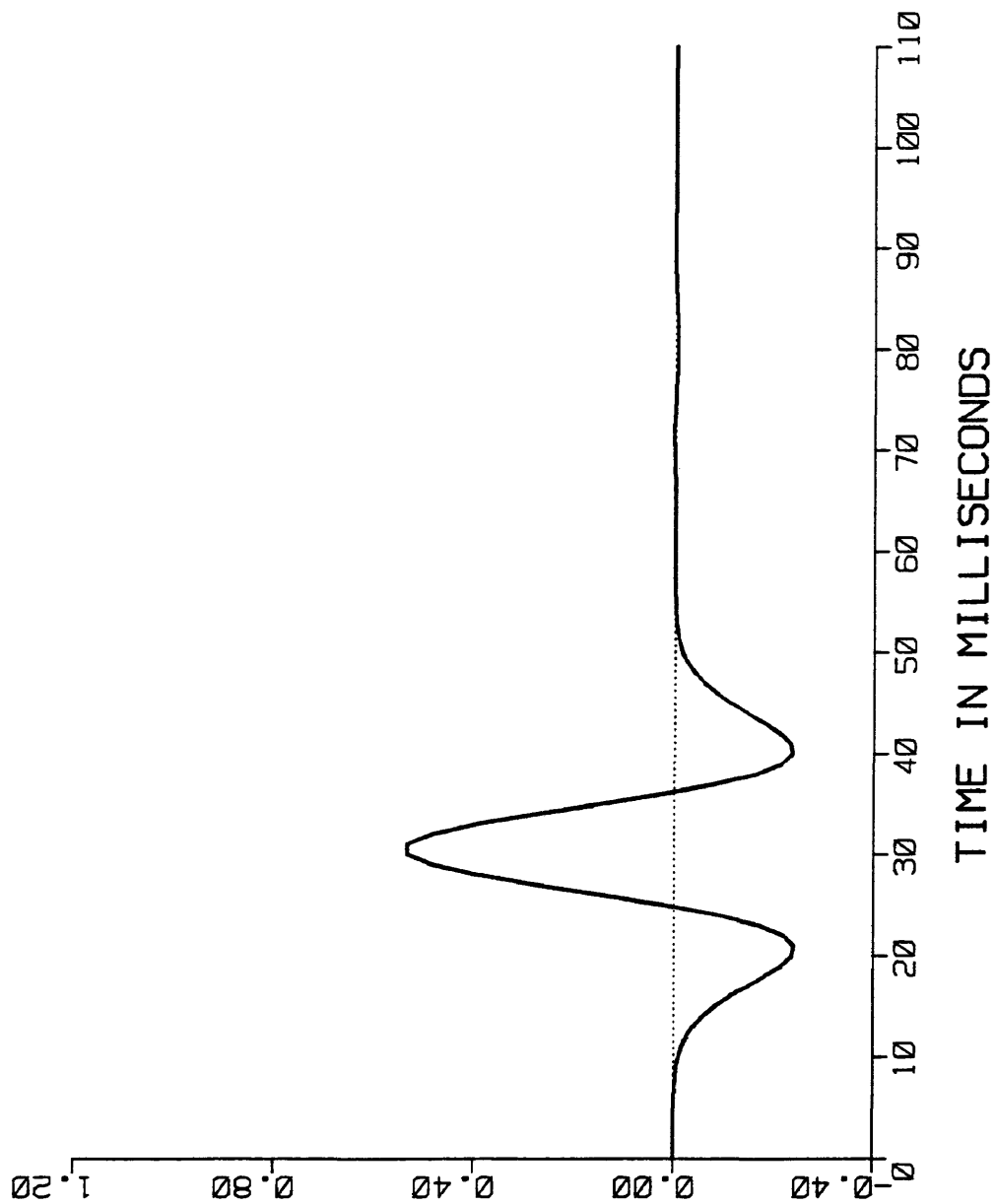


FIGURE 4-37: TRANSMISSION RICKER RESPONSE

HARD SEA FLOOR MODEL

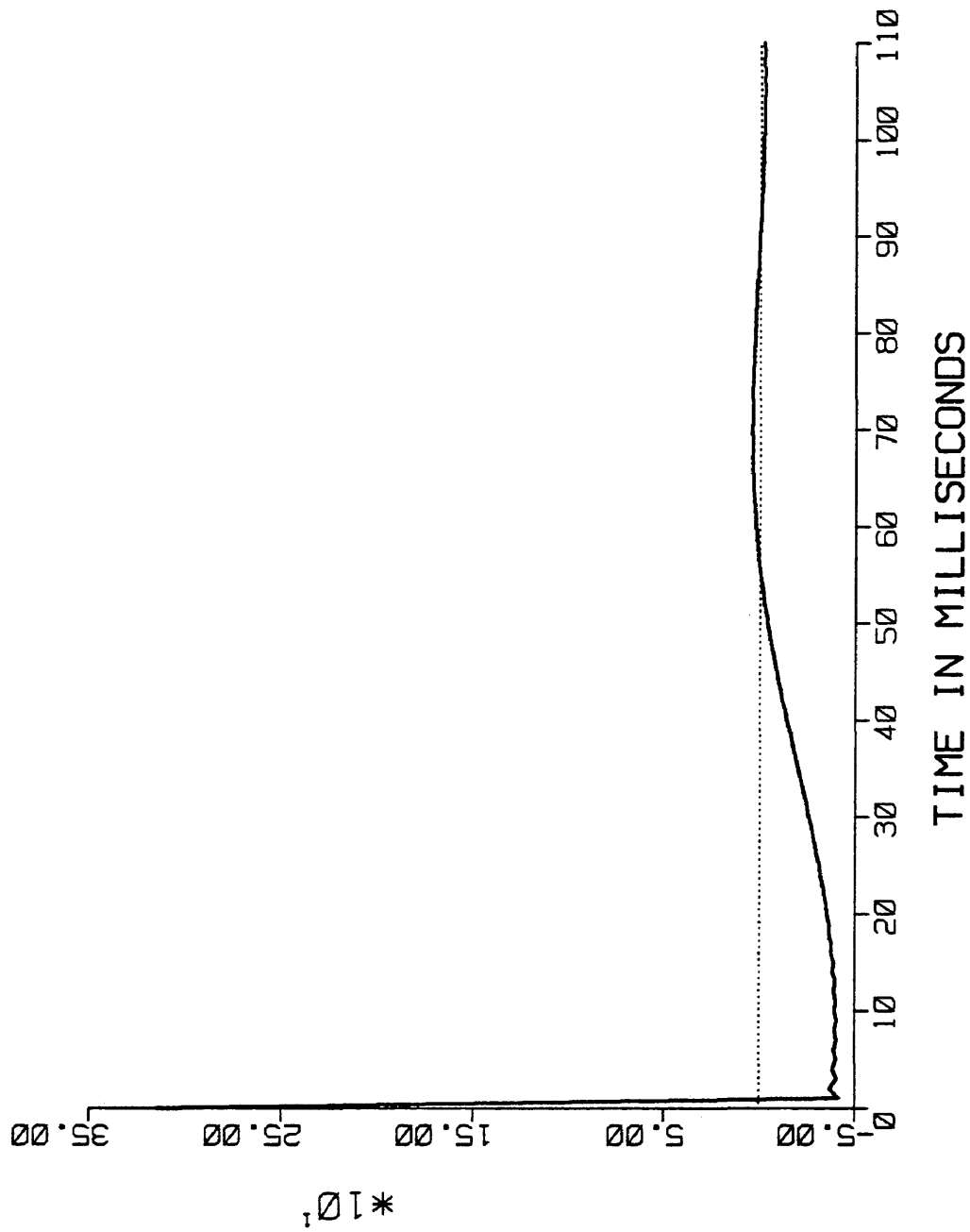


FIGURE 4-38: REFLECTION FUNCTION R12

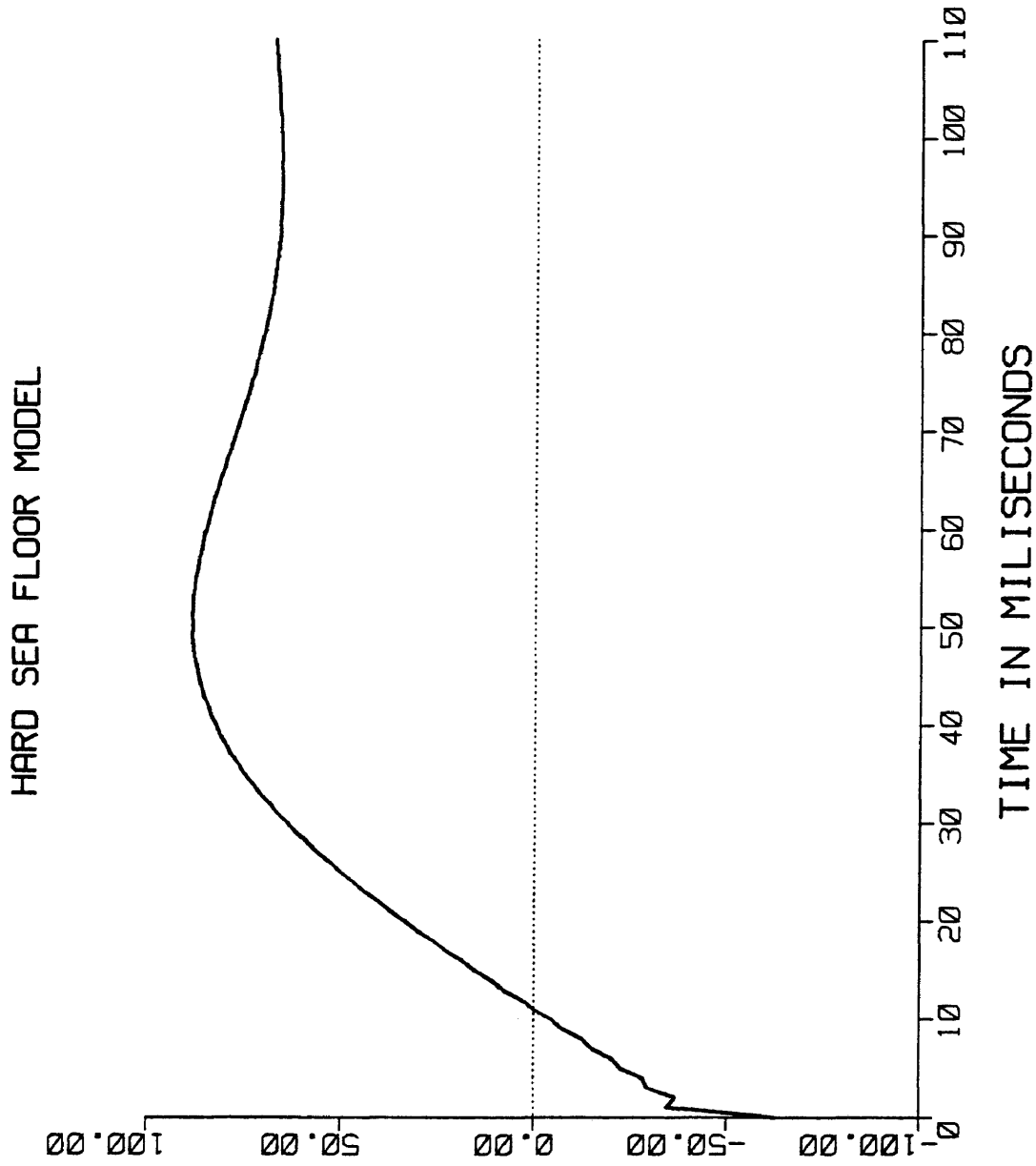


FIGURE 4-39: REFLECTION FUNCTION R23

General Discussion of the Results

We have shown four sets of model results in this chapter. In this section we will confine ourselves to a general discussion of the first, the theoretical, model only. This consists of just the transition layer between two constant velocity half spaces.

If the transition zone is unbounded, the reflection R_{12} function is clearly the impulse response. For a thick transition zone, the impulse response from the top will be equal to the reflection function at the top and the impulse response from the bottom will be equal to the reflection function at the bottom. The complete response from the transition zone is the superposition of the two functions, with the latter appropriately shifted by a time equal to the two-way time through the transition zone, as shown in figure 4-1. The idea is similar to superposition of reflections in the uniform velocity layer case. If we compare the conventional reflectivity response with the wave-theoretic response, figure 4-3, we note that for transition zones with large time thicknesses, the responses are completely different. Clearly the conventional procedure is a poor approximation in this case. However, the conventional

procedure is a fair approximation for practical cases as we have seen in the figures 4-10, 4-28, 4-35. The main reason is that the two-way time through practical thickness transition zones is a very small initial part, of the time domain reflection function.

The frequency domain $R_{12}(\omega)$ equation 2.22 is of a simple enough form to allow it to be transformed to time domain $R_{12}(t)$. The result is

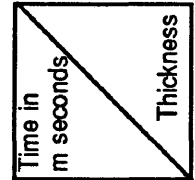
$$R_{12}(t) = \pi \frac{J_1\left(\frac{\beta t}{2}\right)}{t} \quad (4-1)$$

where J_1 is the ordinary Bessel function of the first kind of order one. It has proved difficult to obtain similar explicit formulas for the other functions of interest here, namely, R_{23} , T_{12} , and T_{23} .

We relate the argument of the Bessel function in $R_{12}(t)$, the zeroes of the Bessel function, the velocity gradient and the velocity ratio to build table 4-5 as follows: The first five zeroes of the Bessel function occur for the argument values

$$\frac{\beta t_0}{2} = 3.83, 7.02, 10.17, 13.32, 16.47 \quad (4-2)$$

Bessel function argument	velocity ratio	$\beta = .1$	$\beta = .5$	$\beta = 1$	$\beta = 5$	$\beta = 10$	$\beta = 50$	$\beta = 100$	zeros
.0953	1.1	953	191	95.3	19.1	9.5	1.9	.95	
		1.0	.2	.1	.02	.01	.002	.001	
.4045	1.5	4045	811	405	81.1	40.5	8.1	4.0	
		5.0	1.0	.5	.1	.05	.01	.005	
.6931	2.0	6931	1386	693	138	69.3	13.8	6.9	
		10.0	2.0	1.0	.2	.1	.02	.01	
1.6094	5.0	16094	3218	1609	321	160	32.1	16.0	
		40	8.0	4.0	.8	.4	.08	.04	



Thickness normalized to v_s

Table 4-5

Bessel function argument	velocity ratio	$\beta = .1$	$\beta = .5$	$\beta = 1$	$\beta = 5$	$\beta = 10$	$\beta = 50$	$\beta = 100$	zeros
2.3025	10.0	23025 90	4605 18	2302 9.0	460 1.8	230 .9	46.0 .18	23.0 .09	
3.83	46.06	38300 460	7700 92	3830 46	776 9.2	383 4.6	77 .92	38.3 .46	First zero
7.02	1118.79	70200 1180	14040 236	7020 118	1404 23.6	702 11.8	140 2.36	70.2 1.18	Second zero
10.17	26108.7	101700 261000	20340 52200	10170 26100	2034 5220	1017 2610	203 522	102 261	Third zero

Continuation of Table 4-5

From equation 3-6 we equate the argument of the Bessel function to the natural logarithm of the ratio of top to bottom velocity of the transition zone

$$\frac{\beta t_0}{2} = \ln \frac{v_{2f}}{v_{2s}} \quad (4-3)$$

for the condition that t_0 be exactly equal to the two way travel time through the zone. This relationship then gives the entries shown in table 4-5. We make the following observations from this table:

1. Given the velocity gradient and the velocity ratio, we can determine the transition zone travel time.
2. Given the velocity gradient and the velocity ratio, we can determine the zone thickness normalized to the starting velocity v_s .
3. The zeroes of the Bessel function, which are the zeroes of the reflection function R_{12} , depend only on the velocity ratio. The first zero occurs for velocity ratio equal to 46.06, as shown in the table.

The table and the observations explain why we do not see a drastic difference between wave theoretic and conventional reflectivity results in wave shape for practical cases. For a fixed velocity gradient β , if we consider a velocity-ratio range from 1.1 to 5, we find the two-way time through the

transition zone is much smaller than the time of the first zero in the Bessel function. When this occurs, the wave-theoretic form can be approximated by a straight line which makes the conventional and wave-theoretic responses similar in shape. For example, for $\beta = 100$ ft/sec/ft and velocity ratio 5, table 4-5 gives the one-way time as 16 ms. The first zero of the Bessel function occurs at 38.3. Similar remarks can be made about the behavior R_{23} . Although we have not been able to obtain its time-domain inverse analytically, numerical results suggest that it is close to a Bessel function of the second kind or the Neumann function of order one.

The conventional reflectivity modeling gives the reflection impulse response from the top of the transition zone as a step function, and the negative of that step function is the reflection impulse response from the bottom. The reflectivity is a rectangle, so its amplitude spectrum is the absolute value of a sinc function. The conventional reflectivity is a good approximation to the wave-theoretic reflectivity in the time domain if the travel time through the transition zone is small. However, significant differences exist in the frequency domain (See figures 4-11 through 4-15). In order to get a more correct delineation of a linearly varying velocity transition zone, better

approximations are needed for R_{12} , R_{21} , R_{23} , R_{32} , T_{12} , T_{21} , T_{23} , and T_{32} . We reiterate that the conventional reflectivity responses are only a fair approximation for small times and are rather absurd approximations globally. How these might be significantly improved will be discussed in the conclusions.

5. CONCLUSIONS AND RECOMMENDATIONS

We have shown that the response from a finite transition zone is the sum of the response of the top R_{12} and the response of the bottom R_{23} , with R_{23} shifted by time equal to the two-way time through the transition zone.

We have shown that the wave-theoretic impulse response differs significantly from the impulse response of the conventional model. We have found that the reflectivity function R_{12} from the interface between a uniform zone and a transition zone is proportional to a Bessel function of the first order divided by t . The reflectivity function R_{23} at the interface between the base of a transition zone and a uniform zone appears to be related to a Bessel-Neumann function.

The work in this thesis shows that there are no significant multiples due to the presence of a linearly varying velocity zone. It is quite possible that the tail of the reflection function R_{23} is usually mistaken for multiples. We have deduced the exact frequency-domain reflection and transmission functions from a transition zone imbedded between uniform half-spaces.

The work in this thesis suggests that it is possible to provide certain corrections to the conventional reflectivity

modeling. We have found that the conventional reflectivity response is a good approximation if the travel time through the transition zone is small. For transition zones with large time thicknesses, the conventional reflectivity response is a poor approximation to the wave theory results.

It is shown from the plots of the responses that the relative amplitudes of transition zone reflection response is low and can be easily masked by the other reflections.

As a continuation of this work, we recommend finding the analytical functions for the reflection and transmission functions. We also recommend studying oblique incidence responses to simulate offset dependence for a better correlation with the field data.

BIBLIOGRAPHY

- Bortfeld, R., 1960, Seismic waves in transition layers: Geophysical Prospecting, volume VIII, page 178-217.
- Berryman, L.H., Goupillaud, P. L. and Waters, K. H., 1958, Reflection from multiple transition layers; Part I -theoretical results, geophysics, volume XXIII, page 223-243.
- Berryman, L. H., Goupillaud, P. L. and Waters, K. H., 1958, Reflection from multiple transition layers; Part II -experimental investigation, geophysics, volume XXIII, page 244-252.
- Endtz, J., 1959, Change of shape of seismic pulses, Geophysical Prospecting, volume VII, page 10.
- Foster, M., 1975, Transmission effects in the continuous one-dimensional seismic model, Geophysics. J. R. Astr. soc. volume XXXII, page 519-527.
- Gray, S. H., 1984, A problem of discrete approximations to an arbitrary varying one - dimensional seismic model: Geophys. J.R. Astr. Soc., volume 78, page 431-437.
- Gupta, N. R., 1965, Reflection of plane waves from a linear transition layer in liquid media: Geophysics, volume XXX, page 122-132.
- Hauser, W., 1966, Introduction to the principles of mechanics, Addison-Wesley series in physics.
- Justice, J. H. and Zuba, C., May 1986, Transition zone reflection and permafrost analysis, Geophysics, volume XXXXI, page 1075-1086.
- Menzel, H. Rosenbach, O., 1957, Theoretische untersuchungen über den einfluss der verwitterungsschicht auf das spectrum elastischer wellen in der reflexionsseismik: Geophysical Prospecting, volume V, page 328-348.
- Menzel, H. and Rosenbach, O., 1958a, the influence of a layer complying with a linear Velocity law on the shape of seismic pulses, Geophysical Prospecting, volume VI, page 408-432.

Peterson, R. A., Fillipone, W. R., and Coker, F. B., 1955,
The synthesis of seismograms from well log data:
Geophysics, volume XX, page 516-538.

Sengbush, R. L., Lawrence P. L., McDonal F. J., May 1961,
Interpretation of synthetic seismograms: Geophysics,
volume XXVI, page 138-157.

Wuenschel, P. C., 1960, Seismogram synthesis including
multiples and transmission coefficients: Geophysics,
volume XXV, page 106-129.

Wolf, A., 1940, The time delay of a wave group in the
weathered layer: Geophysics, volume V, page 367-372.

Wolf, A., 1937, The reflection of elastic wave from
transition layers of variable velocity: Geophysics,
volume II, page 357-363.

APPENDIX A

Three Uniform Layers

For three uniform layers, the reflected pulse amplitude is given by

$$B e^{i k_1 z_1} = \left[\frac{k_1 - k_2}{k_1 + k_2} + \frac{\left(\frac{k_2 - k_3}{k_2 + k_3} \right) \left(\frac{2k_1}{k_1 + k_2} \right) \left(\frac{2k_2}{k_1 + k_2} \right)}{e^{+i 2 k_2 (z_2 - z_1)} - \left(\frac{k_2 - k_3}{k_2 + k_3} \right) \left(\frac{k_2 - k_1}{k_1 + k_2} \right)} \right] \times A e^{-i k_1 z_1} ,$$

or by

$$B e^{i k_1 z_1} = \left[R_{12} + \frac{R_{23} T_{21} T_{12}}{e^{i 2 k_2 (z_2 - z_1)} - R_{23} R_{21}} \right] A e^{-i k_1 z_1}$$

$$= [R_{12} + R_{23} T_{21} T_{12} e^{-i 2 k_2 (z_1 - z_1)} \{1 + R_{23} R_{21} e^{-i 2 k_2 (z_2 - z_1)} + (R_{23} R_{21})^2 e^{-i 4 k_2 (z_2 - z_1)} + \dots\}] A e^{-i k_1 z_1}$$

which will give the primaries and the multiples by using z-transform. These equations for uniform layers are related to equations 2-14 and 2-19 for the case of transition zones.

We can follow the same procedure to find the transmitted pulse amplitude $E e^{i k_1 z_1}$. The corresponding equations for the case of transition zones are 2-15 and 2-21.

APPENDIX B
Program Listings

*THIS PGM WILL FIND RESPONSE OF THE REFLECTIVITY OF
 * 4 _ LAYER CASE FOR THE IMPULSE WAVELET & RICKER WAVELET
 * SOURCE & TIME RESPONSE USING FAST FOURIER TRANSFORM.
 * USING THEORETIC WAVE APPROACH AND CONVENTIONAL PROCEDURE.
 ** WRITTEN BY JAAFAR MUHAMMAD ALNEMER, T-3291, CSM

```

    IMPLICIT NONE
    INTEGER M
    PARAMETER (M=16384)
    COMPLEX R12,R23,R34,R21,R32
    COMPLEX RR12(M),RR23(M)
    COMPLEX TT12(M),TT23(M)
    COMPLEX T12,T23,T34,T21,T32
    COMPLEX CMLX,PHASE2,PHASE3,PHASE4,PHASE1
    COMPLEX GI(M),GR(M),PHASET,PF,PHT
    COMPLEX BI(M),BR(M)
    COMPLEX K2S,K2F,K#2S,K#2F,AIMAG,TTT,DD
    REAL G,B,V2S,V2F,FREQ,K1,K2,K3,K4,PH
    REAL V0,V1,V2,V3,V4,Z1,Z2,Z3,T
    REAL VM,THICK2,THICK3,PI,F0
    REAL TIMETHICK1,TIMETHICK2,TIMETHICK3
    REAL SAMF,SAMT,SAMTC
    REAL TIMESAM,TIME,SOURCE_NORM,AF_SOURCE
    REAL CO(0:M),CON(0:M),CON_SOURCE(0:M),PP
    REAL TL1,TL2,TTL,XAXIS,XZERO
    INTEGER I,NUMSAM,NYQ,MM,NNEW,N,NOLD
    INTEGER N1,N2,N3,J
    CHARACTER*4 MODE
    EXTERNAL FORK,PHASE,CIRCON
    WRITE(6,1)
1   FORMAT(1X,' THIS IS FREQUENCY RESPONSE OF FOUR_LAYER
1   CASE & TIME RESPONSE USING FORK')
    WRITE(6,2)
2   FORMAT(1X,' ENTER V1, V2, V3, V4, VM(≠0), Z1, Z2,Z3
1   SAMT(TIME SAMPLING ms) ,MODE')
    READ(5,*)V1,V2S,V2,V2F,V3,V4,VM,Z1,Z2,Z3 ,SAMT,MODE
*
    WRITE(6,*) ' PARAMETERS FOR 4-LAYER RESPONSE USING '
1   MODE, ' MODE'
    WRITE(66,*) ' PARAMETERS FOR 4-LAYER RESPONSE USING '
1   MODE, ' MODE'
    WRITE(6,*)' VELOCITY IN REGION 1           '.V1
    WRITE(66,*)' VELOCITY IN REGION 1           '.V1
    WRITE(6,*)' STARTING VELOCITY IN REGION 2 '.V2S
    WRITE(66,*)' STARTING VELOCITY IN REGION 2 '.V2S
    WRITE(6,*)' VELOCITY IN REGION 2           '.V2
    WRITE(66,*)' VELOCITY IN REGION 2           '.V2
    WRITE(6,*)' ENDING VELOCITY IN REGION 2   '.V2F
    WRITE(66,*)' ENDING VELOCITY IN REGION 2   '.V2F
    WRITE(6,*)' VELOCITY IN REGION 3           '.V3
    WRITE(66,*)' VELOCITY IN REGION 3           '.V3

```

```

WRITE(6,*) VELOCITY IN REGION 4          '.V4
WRITE(66,*) VELOCITY IN REGION 4        '.V4
WRITE(6,*) PEAK FREQUENCY IN RICKER     '.VM
WRITE(66,*) PEAK FREQUENCY IN RICKER     '.VM
WRITE(6,*) DEPTH OF THE TOP 2nd LAYER    '.Z1
WRITE(66,*) DEPTH OF THE TOP 2nd LAYER   '.Z1
WRITE(6,*) DEPTH OF THE BOTTOM 2nd LAYER '.Z2
WRITE(66,*) DEPTH OF THE BOTTOM 2nd LAYER '.Z2
WRITE(6,*) DEPTH OF THE BOTTOM 3rd LAYER '.Z3
WRITE(66,*) DEPTH OF THE BOTTOM 3rd LAYER '.Z3
*

THICK2 = Z2-Z1
THICK3 = Z3-Z2
*

TIMETHICK1 = Z1*1000./V1
IF(MODE .EQ. 'TRAN' )THEN
  B = (V2F - V2S)/THICK2
  IF(ABS(B) .GT. 0.0)THEN
    TIMETHICK2 = ALOG(V2F/V2S)/B*1000.
  ELSE
    TIMETHICK2 = THICK2/((V2S+V2F)/2.)*1000.
ENDIF
ENDIF
IF (MODE .EQ. 'DISC')THEN
  TIMETHICK2=THICK2/V2*1000.
ENDIF
TIMETHICK3 = THICK3*1000./V3
*

T = 10.*(2.*(TIMETHICK1+TIMETHICK2+TIMETHICK3))
*

WRITE(6,*) SUGGESTED RECORD LENGTH      '.T. ' mS'
WRITE(66,*) SUGGESTED RECORD LENGTH     '.T. ' mS'
WRITE(6,*) MODE OF THE PROGRAM          '.MODE
WRITE(66,*) MODE OF THE PROGRAM         '.MODE
*

NOLD = T/SAMT
MM = ALOG(REAL(NOLD))/ALOG(2.)+.99999999999
NNEW = 2**(MM)
*

PI = 3.141592653589793
F0 = 1000./(2.*SAMT)
SAMF=1000./(REAL(NNEW)*SAMT)
V0 = 1.0
*

N=NNEW
NYQ =N/2+1
WRITE(6,*)  £ OF SAMPLED POINTS        ', N
WRITE(66,*)  £ OF SAMPLED POINTS       ', N
WRITE(6,*)  NYQUIST CHOSEN TO BE       '.F0,'Hz AT SAMPLE £ '.NYQ
WRITE(66,*)  NYQUIST CHOSEN TO BE      '.F0,'Hz AT SAMPLE £ '.NYQ

```

```

WRITE(6,*)' FREQUENCY SAMPLING RATE '.SAMF.' Hz'
WRITE(66,*)' FREQUENCY SAMPLING RATE '.SAMF.' Hz'
WRITE(6,*)' TIME SAMPLING           '.SAMT.' mS'
WRITE(66,*)' TIME SAMPLING           '.SAMT.' mS'
WRITE(6,*)' RECORD LENGTH           '.SAMT*(N-1).' mS'
WRITE(66,*)' RECORD LENGTH           '.SAMT*(N-1).' mS'
WRITE(6,*)' VELOCITY GRADIANT       '.B.' OVER THICKNESS '.THICK2
WRITE(66,*)' VELOCITY GRADIANT       '.B.' OVER THICKNESS '.THICK2
WRITE(6,*)' THICKNESS OF THE THIED LAYER      '.THICK3
WRITE(66,*)' THICKNESS OF THE THIED LAYER      '.THICK3
WRITE(6,*)' FIRST LAYER & LAST LAYER ARE HALF SPACE '
WRITE(66,*)' FIRST LAYER & LAST LAYER ARE HALF SPACE '

```

*

```

WRITE(6,*)
WRITE(66,*)
WRITE(6,*)
WRITE(66,*)
WRITE(6,*)
WRITE(66,*)
WRITE(6,*)
WRITE(66,*)
WRITE(6,*)'Z-----DATUM-----'
WRITE(66,*)'Z-----DATUM-----'
WRITE(6,*)'DEPTH'
WRITE(66,*)'DEPTH'
WRITE(6,*)
WRITE(66,*)
WRITE(6,*)'          V1= '.V1
WRITE(66,*)'          V1= '.V1
WRITE(6,*)'          THICK1 = '.TIMETHICK1.'mS'
WRITE(66,*)'          THICK1 = '.TIMETHICK1.'mS'
WRITE(6,*)
WRITE(66,*)
IF(MODE .EQ. 'TRAN')THEN
WRITE(6,*)'Z1-----V2S= '.V2S.'-----'
WRITE(66,*)'Z1-----V2S= '.V2S.'-----'
ENDIF
IF(MODE .EQ. 'DISC')THEN
WRITE(6,*)'Z1-----V2S= '.V2.'-----'
WRITE(66,*)'Z1-----V2S= '.V2.'-----'
ENDIF
WRITE(6,*)Z1
WRITE(66,*)Z1
WRITE(6,*)
WRITE(66,*)
IF(MODE .EQ. 'TRAN')THEN
WRITE(6,*)'          V2(AVE)= '.(V2S+V2F)/2..'GRADIANT= '.B
WRITE(66,*)'          V2(AVE)= '.(V2S+V2F)/2..'GRADIANT= '.B
ENDIF
IF(MODE .EQ. 'DISC')THEN

```

```

WRITE(6,*)'
WRITE(66,*)'
ENDIF
WRITE(6,*)'
WRITE(66,*)'
WRITE(6,*)'
WRITE(66,*)'
WRITE(6,*)
WRITE(66,*)
WRITE(6,*)
WRITE(66,*)
IF(MODE .EQ. 'TRAN')THEN
WRITE(6,*)'Z2-----V2F='V2F,'-----'
WRITE(66,*)'Z2-----V2F='V2F,'-----'
ENDIF
IF(MODE .EQ. 'DISC')THEN
WRITE(6,*)'Z2-----V2F='V2,'-----'
WRITE(66,*)'Z2-----V2F='V2,'-----'
ENDIF
WRITE(6,*)Z2
WRITE(66,*)Z2
WRITE(6,*)
WRITE(66,*)
WRITE(6,*)
WRITE(66,*)
WRITE(6,*)
WRITE(66,*)
WRITE(6,*)
WRITE(66,*)
IF (Z3 .EQ. Z2) GOTO 90
WRITE(6,*)'Z3-----'
WRITE(66,*)'Z3-----'
WRITE(6,*)Z3
WRITE(66,*)Z3
WRITE(6,*)
WRITE(66,*)
WRITE(6,*)
WRITE(66,*)
WRITE(6,*)
WRITE(66,*)
WRITE(6,*)
WRITE(66,*)
90
WRITE(66,*)
XAXIS=0.0
XZERO=0.0
SOURCE_NORM = 1.0
*TO NORMALIZE RICKER IN FREQUENCY DOMAIN
*
SOURCE_NORM = 2*EXP(-1.)/(SQRT(PI)*VM)
C
DO NUMSAM = 1,NYQ
FREQ = (NUMSAM-1)*SAMF

```

```

V2(AVE)= '.V2.'GRADIANT= '.B
V2(AVE)= '.V2.'GRADIANT= '.B

```

```

RATIO OF V2F/V2S = '.V2F/V2S
RATIO OF V2F/V2S = '.V2F/V2S
THICK2 = '.THICK2.'=='.TIMETHICK2.'mS'
THICK2 = '.THICK2.'=='.TIMETHICK2.'mS'

```

```

V3= '.V3
V3= '.V3
THICK3 = '.THICK3.'=='.TIMETHICK3.'mS'
THICK3 = '.THICK3.'=='.TIMETHICK3.'mS'

```

```

V4= '.V4
V4= '.V4

```

```

IN/2+1 NYQUIST

```

```

*IN CASE OF INTRODUCING Z1 WE USE PHASE1
  PHASE1 =CMPLX(0.,-FREQ*4.*PI/V1*Z1)
  IF (FREQ .LT. 1.0E-5) THEN
    FREQ = 1.0E-5
  END IF
*IN CASE OF IMPULSE RESPONSE AF_SOURCE = 1
  AF_SOURCE=1.0
*
  K1 = 2.*PI*FREQ/V1
  K3 = 2.*PI*FREQ/V3
  K4 = 2.*PI*FREQ/V4
  PHT=CMPLX(0.,-K1*Z1+K3*THICK3)
*
  IF (MODE .EQ. 'TRAN') THEN
    IF ((B**2.-(4.*PI*FREQ)**2.) .GT. 0.)THEN
      G = SQRT( B**2. - (4.*PI*FREQ)**2.)
      K2S = CMPLX(0.,(B-G))/(2.*V2S)
      K2F = CMPLX(0.,-(B+G))/(2.*V2F)
      K$2S= CMPLX(0.,-(B+G))/(2.*V2S)
      K$2F= CMPLX(0.,(B-G))/(2.*V2F)
      PHASE2 = 2.*G/B*ALOG(SQRT(V2F/V2S))
      PHASET = (1.+G/B)*ALOG(SQRT(V2F/V2S))+PHT
      PF =CEXP(PHASET)
    ELSE
      IF ((B**2.-(4.*PI*FREQ)**2.) .EQ. 0.) THEN
        G = ( 1.)
        K2S = CMPLX(0.,B/(2.*V2S))
        K2F = CMPLX(0.,-B*((1./(V2F*ALOG(V2F/V0)))+ 1./V2F))
        K$2S= CMPLX(0.,-B*((1./(V2S*ALOG(V2S/V0)))+ 1./V2S))
        K$2F= CMPLX(0.,B/(2.*V2F))
        PHASE2 =ALOG(ALOG(V2F/V0)/ALOG(V2S/V0))
        PF = SQRT(V2F/V2S)*CEXP(PHT+PHASE2)
      ELSE
        IF ((B**2.-(4.*PI*FREQ)**2.) .LT. 0.) THEN
          G = SQRT((4.*PI*FREQ)**2. - B**2.)
          K2S = CMPLX(G,B)/(2.*V2S)
          K2F = CMPLX(G,-B)/(2.*V2F)
          K$2S= CMPLX(G,-B)/(2.*V2S)
          K$2F= CMPLX(G,B)/(2.*V2F)
          IF (ABS(B) .LT. 1.0E-6)THEN
            PHASE2 = CMPLX(0.,4.*PI*FREQ*THICK2/V2S)
            PHASET = PHASE2/2.+ PHT
            GOTO 30
          END IF
          PHASE2=CMPLX (0.,2.*G/B*ALOG(SQRT(V2F/V2S)))
          PHASET= ALOG(SQRT(V2F/V2S))+PHASE2/2.+PHT
          PF = CEXP(PHASET)
        ENDIF
      ENDIF
    ENDIF
  END IF

```

30

```

*
R12 = (K1 - K2S)/(K1 + K2S)
R23 = (K$2F - K3)/(K2F + K3)
R34 = (K3 - K4)/(K3 + K4)
R21 = (K$2S - K1)/(K2S + K1)
R32 = (K3 - K2F)/(K3 + K2F)
T12 = (K$2S + K2S)/(K1 + K2S)
T21 = 2.*K1/(K1 + K2S)
T23 = 2.*K3/(K2F + K3)
T32 = (K$2F + K2F)/(K3 + K2F)
T34 = 2.*K4/(K3 + K4)
ELSE
  IF(MODE .EQ. 'DISC') THEN
    R12 = (V2-V1)/(V2+V1)
    R23 = (V3-V2)/(V3+V2)
    R34 = (V4-V3)/(V3+V4)
    R21 = -R12
    R32 = -R23
    T12 = 1.-R12
    T21 = 1.-R21
    T23 = 1. - R23
    T32 = 1. - R32
    T34 = 1. - R34

    PHASE2= CMPLX(0..4*PI*FREQ/V2*THICK2)
    PHASE3= CMPLX(0..4*PI*FREQ/V3*THICK3)
    PHASET= PHASE2/2.+2.*PI*FREQ*CMPLX(0..-Z1/V1)+PHASE3/2.
    PF     = CEXP(PHASET)
  ELSE
    WRITE(6,*)
    WRITE(6,*)'*** SORY *** SORY *** SORY ***'
    WRITE(6,*)'DISC OR TRAN IS NOT SPECIFIED '
    WRITE(6,*)'*****'
    WRITE(6,*)
    GOTO 1000
  END IF
ENDIF

C
PHASE3 = CMPLX(0..2.*K3*THICK3)
PHASE4 = (R23*CEXP(PHASE3) - R23*R34*R32 + T32*R34*T23)
DD= CEXP(PHASE3+PHASE2) - R34*R32*CEXP(PHASE2) - R21*PHASE4
BI(NUMSAM) = (R12 + T21*T12*PHASE4/
1 DD)*CEXP(PHASE1)*AF_SOURCE
BI(NYQ)=CMPLX(REAL(BI(NYQ)),0.)
BI(N-NUMSAM+2)=CMPLX(REAL(BI(NUMSAM)), -AIMAG(BI(NUMSAM)))
WRITE(11,*)FREQ.REAL(BI(NUMSAM))
WRITE(12,*)FREQ.AIMAG(BI(NUMSAM))
WRITE(13,*)FREQ.CABS(BI(NUMSAM)),BI(NUMSAM)
TTT = BI(NUMSAM)
CALL PHASE(TTT,PH)

```

```

        WRITE(14,*)FREQ,PH
        GI(NUMSAM) = T12*T23*T34/DD*PF*AF_SOURCE
        GI(NYQ)=CMPLX(REAL(GI(NYQ)),0.)
        GI(N-NUMSAM+2)=CMPLX(REAL(GI(NUMSAM)),.-AIMAG(GI(NUMSAM)))
        WRITE(15,*)FREQ,REAL(GI(NUMSAM))
        WRITE(16,*)FREQ,AIMAG(GI(NUMSAM))
        WRITE(17,*)FREQ,CABS(GI(NUMSAM)),GI(NUMSAM)
        TTT = GI(NUMSAM)
        CALL PHASE(TTT,PH)
        WRITE(18,*)FREQ,PH
*IN CASE OF RICKER WAVELELT WE HAVE
        AF_SOURCE= 2*FREQ**2*EXP(-FREQ**2/VM**2)/(SQRT(PI)*VM**3)/
1 SOURCE_NORM
        WRITE(1,*)FREQ,AF_SOURCE
        WRITE(3,*)(NUMSAM-N/2-1)*SAMT,XAXIS
        BR(NUMSAM) = BI(NUMSAM)*AF_SOURCE
        BR(N-NUMSAM+2)=CMPLX(REAL(BR(NUMSAM)),.-AIMAG(BR(NUMSAM)))
        WRITE(31,*)FREQ,REAL(BR(NUMSAM))
        WRITE(32,*)FREQ,AIMAG(BR(NUMSAM))
        WRITE(33,*)FREQ,CABS(BR(NUMSAM)),BR(NUMSAM)
        TTT = BR(NUMSAM)
        CALL PHASE(TTT,PH)
        WRITE(34,*)FREQ,PH
        GR(NUMSAM) = GI(NUMSAM)*AF_SOURCE
        GR(N-NUMSAM+2)=CMPLX(REAL(GR(NUMSAM)),.-AIMAG(GR(NUMSAM)))
        WRITE(35,*)FREQ,REAL(GR(NUMSAM))
        WRITE(36,*)FREQ,AIMAG(GR(NUMSAM))
        WRITE(37,*)FREQ,CABS(GR(NUMSAM)),GR(NUMSAM)
        TTT = GR(NUMSAM)
        CALL PHASE(TTT,PH)
        WRITE(38,*)FREQ,PH
*
        WRITE(51,*)FREQ,REAL(R12)
        WRITE(52,*)FREQ,AIMAG(R12)
        WRITE(53,*)FREQ,CABS(R12),R12
        CALL PHASE(R12,PH)
        WRITE(54,*)FREQ,PH
        RR12(NUMSAM) = R12
        RR12(NYQ)=CMPLX(REAL(RR12(NYQ)),0.)
        RR12(N-NUMSAM+2)=CMPLX(REAL(RR12(NUMSAM)),.-AIMAG(RR12(NUMSAM)))
        WRITE(71,*)FREQ,REAL(R23)
        WRITE(72,*)FREQ,AIMAG(R23)
        WRITE(73,*)FREQ,CABS(R23),R23
        CALL PHASE(R23,PH)
        WRITE(74,*)FREQ,PH
        RR23(NUMSAM) = R23
        RR23(NYQ)=CMPLX(REAL(RR23(NYQ)),0.)
        RR23(N-NUMSAM+2)=CMPLX(REAL(RR23(NUMSAM)),.-AIMAG(RR23(NUMSAM)))
*
        WRITE(56,*)FREQ,REAL(T12)

```

```

WRITE(57,*)FREQ,AIMAG(T12)
WRITE(58,*)FREQ,CABS(T12),T12
CALL PHASE(T12,PH)
WRITE(59,*)FREQ,PH
TT12(NUMSAM) = T12
TT12(NYQ)=CMPLX(REAL(TT12(NYQ)),0.)
TT12(N-NUMSAM+2)=CMPLX(REAL(TT12(NUMSAM)),-AIMAG(TT12(NUMSAM)))
WRITE(76,*)FREQ,REAL(T23)
WRITE(77,*)FREQ,AIMAG(T23)
WRITE(78,*)FREQ,CABS(T23),T23
CALL PHASE(T23,PH)
WRITE(79,*)FREQ,PH
TT23(NUMSAM) = T23
TT23(NYQ)=CMPLX(REAL(TT23(NYQ)),0.)
TT23(N-NUMSAM+2)=CMPLX(REAL(TT23(NUMSAM)),-AIMAG(TT23(NUMSAM)))
END DO
XAXIS=1.0
WRITE(3,*)XZERO,XAXIS
*
CALL FORK(N,RR12,+1.)
CALL FORK(N,RR23,+1.)
CALL FORK(N,TT12,+1.)
CALL FORK(N,TT23,+1.)
*
* USING FORK TO GET THE TIME RESPONSE OF THE REFLECTION & TRANSMISSION
* RESPONSE
CALL FORK(N,BR,+1.)
CALL FORK(N,BI,+1.)
CALL FORK(N,GI,+1.)
CALL FORK(N,GR,+1.)
N1 = 2.*TIMETHICK1/SAMT
N2 = 2.*TIMETHICK2/SAMT
N3 = 2.*TIMETHICK3/SAMT
DO J = 1,N
PP= (PI*VM*(J-N/2-1)*SAMT/1000.)**2.
CON_SOURCE(J-1) = (1.-2.*PP)*EXP(-PP)
*
WRITE(2,*)(J-N/2-1)*SAMT,CON_SOURCE(J-1)
CO(J-1) = 0.0
ENDDO
CLOSE(1)
CLOSE(2)
CLOSE(3)
CLOSE(11)
CLOSE(12)
CLOSE(13)
CLOSE(14)
CLOSE(15)
CLOSE(16)
CLOSE(17)

```

```

CLOSE(18)
CLOSE(31)
CLOSE(32)
CLOSE(33)
CLOSE(34)
CLOSE(35)
CLOSE(36)
CLOSE(37)
CLOSE(38)
CLOSE(51)
CLOSE(52)
CLOSE(53)
CLOSE(54)
CLOSE(56)
CLOSE(57)
CLOSE(58)
CLOSE(59)
CLOSE(71)
CLOSE(72)
CLOSE(73)
CLOSE(74)
CLOSE(76)
CLOSE(77)
CLOSE(78)
CLOSE(79)
SAMTC=SAMT                                I=1000.:
IF (MODE .EQ. 'DISC') THEN
  V2S = V2
  V2F = V2
ENDIF
  TL1=1.-((V2S-V1)/(V2S+V1))**2.
  TL2 = 1. - ((V3-V2F)/(V3+V2F))**2.
  TTL =TL1*TL2
  CO(N1) = (V2S-V1)/(V2S+V1) + (SAMTC*B/2000.)*TL1
  DO J = N1+1,N1+N2-1
    CO(J) = (SAMTC*B/2000.)*TL1
  ENDDO
  CO(N1+N2)=(V3-V2F)/(V3+V2F)*TL1 + SAMTC*B/2000.*TL1
  CO(N1+N2+N3) = (V4-V3)/(V4+V3)*TTL
  CALL CIRCON(N,CON_SOURCE,CO,CON)

  TIMESAM = SAMT
  TIME = 0.
  IF (ABS(B) .LT. 1.0E-6 ) SAMT=1000.
  DO I = 1 ,N
    RR12(I)=RR12(I)/(SQRT(REAL(N))*TIMESAM)*1000.
    WRITE(55,*)TIME,REAL(RR12(I)),RR12(I)
    RR23(I)=RR23(I)/(SQRT(REAL(N))*TIMESAM)*1000.
    WRITE(75,*)TIME,REAL(RR23(I)),RR23(I)
    TT12(I)=TT12(I)/(SQRT(REAL(N))*TIMESAM)*1000.

```

```
WRITE(60,*)TIME,REAL(TT12(I)),TT12(I)
TT23(I)=TT23(I)/(SQRT(REAL(N))*TIMESAM)*1000.
WRITE(80,*)TIME,REAL(TT23(I)),TT23(I)
BI(I) = BI(I)/SQRT(REAL(N))
WRITE(21,*)TIME,REAL(BI(I)),BI(I)
BR(I) = BR(I)/(SQRT(REAL(N))*TIMESAM)*1000.
WRITE(41,*)TIME,REAL(BR(I)),BR(I)
GI(I) = GI(I)/SQRT(REAL(N))
WRITE(25,*)TIME,REAL(GI(I)),GI(I)
GR(I) = GR(I)/(SQRT(REAL(N))*TIMESAM)*1000.
WRITE(45,*)TIME,REAL(GR(I)),GR(I)
WRITE(7,*)TIME,CO(I-1)
WRITE(8,*)TIME,CON(I+N/2-1)
TIME = TIME+TIMESAM
END DO
1000 STOP
END
```

```

*****
* SUBROUTINE FORK DOES FAST FOURIER TRANSFORM (AFTER CLAERBOUT)
* THIS IS A SYMETRICAL(BOTH SIDE IS DIVIDED BY SQRT(N))
* TO GET FORWARD TRANSFORM (-1.); MULTIPLY OUTPUT BY SQRT(N)
* TO GET INVERSE TRANSFORM (1.); MULTIPLY OUTPUT BY 1./SQRT(N)
SUBROUTINE FORK(LX,CX,SIGNI)
COMPLEX CX(LX),CARG,CEXP,CW,CTEMP
J=1
  SC =SQRT(1./ LX)
  DO I=1,LX
    IF(I .GT. J) GO TO 10
    CTEMP=CX(J)*SC
    CX(J)=CX(I)*SC
    CX(I)=CTEMP
10  M=LX/2
20  IF(J .LE. M) GO TO 30
    J=J-M
    M=M/2
    IF(M .GE. 1) GO TO 20
30  J = J+M
    END DO
    L=1
40  ISTEP=2*L
    DO M=1,L
      CARG=(0.,1.)*(3.14159265*SIGNI*(M-1))/L
      CW=CEXP(CARG)
      DO I=M,L,ISTEP
        CTEMP=CW*CX(I+L)
        CX(I+L)=CX(I)-CTEMP
        CX(I)=CX(I)+CTEMP
      END DO
    END DO
    L=ISTEP
    IF(L .LT. LX)GO TO 40
  RETURN
END

```

```
*****
****  CIRCON.FOR DOES CIRCULAR CONVOLUTION OF TWO
****  SEQUENCES OF M DATA.
****  WRITTEN BY JAAFAR MUHAMMAD ALNEMER T-3291
*****
      SUBROUTINE CIRCON(M,A,B,C)
      INTEGER M
      REAL A(0:M-1),B(0:M-1),C(0:M-1)
      DO I = 0,M-1
        N=M-1
        C(I) = 0.0
        DO J = 0,M-1
          T=B(ABS(I-J))
          IF (J .GE. I+1) THEN
            T=B(N)
            N=N-1
          ENDIF
          C(I)=C(I) + A(J)*T
        ENDDO
      ENDDO
      RETURN
      END
```

```

* THIS SUBROUTINE CALCULATES THE PHASE OF A SPECTRUM
* FROM GIVEN FOURIER TRANSFORM
* WRITTEN BY JAAFAR MUHAMMAD ALNEMER, T-3291
* CX = THE INPUT DATA
* PH = OUTPUT DATA
  SUBROUTINE PHASE(CX,PH)
  COMPLEX CX
  REAL PH
  PI = 3.141592653589793
  Y = AIMAG(CX)
  X = REAL(CX)
  IF( ABS(Y) .LE. 1.0E-5) THEN                                !MACHINE ZERO
    Y = 0.0
  ENDIF
  IF( ABS(X) .LE. 1.0E-5) THEN
    X = 0.0
  ENDIF
  IF( Y .EQ. 0.0 .AND. X .EQ. 0.0) THEN
    PH = 0.0
    GO TO 50
  ENDIF
  IF ( Y .GT. 0. .AND. X .EQ. 0.) THEN
    PH = 90.
    GO TO 50
  END IF
  IF ( Y .LT. 0. .AND. X .EQ. 0.) THEN
    PH = -90.
    GO TO 50
  END IF
  PH = ATAN(Y/X)*180./PI
  IF (Y .LT. 0. .AND. X .LT. 0.) THEN
    PH = PH - 180.
  END IF
  IF (Y .GE. 0. .AND. X .LT. 0.) THEN
    PH = PH + 180.
  END IF
50  RETURN
  END

```